Jupiter Orbiter Mission

Team 1: “Semele”

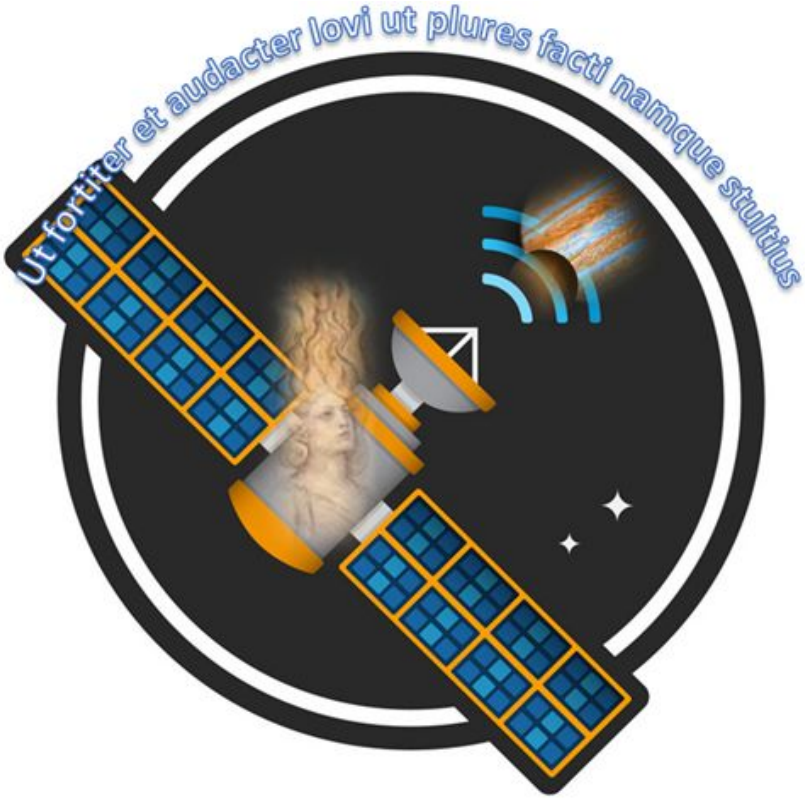

MANE 4850 Space Vehicle Design Capstone

Final Design Report

Professor Kurt Anderson

12/09/2019

Team Members:

Shruti Arumbakkam, Liam Fahey, David Hoddinott, Nathan Karwic,
Nidhi Perianayagam, Joe Pirro, and Clare Reilly

*Please See Section 4.3 for Authority and Responsibility

Table of Contents

List of Figures

List of Tables

List of Equations

List of Terms and Abbreviations

DSN - Deep Space Network
FEA - Finite Element Analysis
HGA - High Gain Antenna
Hz - Hertz, a measure of frequency
Kg - Kilograms
Km - Kilometers
KPa - Kilopascals
LGA - Low Gain Antenna
MLI- Multilayer Insulation
M-P - Minos Probe

N - Newtons
NASA - National Aeronautics and Space Administration
Kbps - kilobits per second, a measure of data transmission rate
R-O - Rhadamanthus Orbiter
RHU- Radioisotope Heating Unit
SAD - Solar Array Drive
UHF - Ultra High Frequency
W - Watts

1.0 Executive Summary

The Semele mission consists of the Minos Probe (M-P), which is to be placed on the surface of Jupiter's moon Europa, and the Rhadamanthus Orbiter (R-O) which is responsible for carrying the probe to its destination. The Semele mission is led by Rensselaer's Aerospace Systems Solutions, Inc. with additional funding from NASA and ESA. This report focuses on the R-O design.

Based on the decisions made in the Preliminary Design Report (PDR), this Final Design Report (FDR) provides an in-depth analysis and calculations regarding each subsystem. The report begins with a discussion of the mission objectives, including an examination of the scientific data gathered during the mission both by the M-P and the R-O. Additionally, the report discusses the constraints on the mission which are based on engineering factors such as mass, as well as the mission's larger political and environmental effect. Next, risks are considered; these include risks to the success of the mission as well as broader implications of specific systems used during the mission. The report then goes into a more specific description of the design of each individual subsystem. The selection of a design for each subsystem and the reasoning behind each selection is included in the PDR, included in Appendix 10.4.

A series of budgets is used to determine some of the overall metrics of the mission. This includes budgets pertaining to mass, power, volume, and cost. The section shows why specific values are set for each budget and how much each subsystem contributes to each budget. The report then gives a brief overview of the mission timeline in the form of a Gantt chart. The chart summarizes milestones for both the design process and the actual mission itself. The conclusion then summarizes the selected design and its benefits, as well as the predicted results of the mission.

Based on the analysis performed for the FDR, the Semele mission will take 3 years. During the bulk of this time the spacecraft is in transit from the Earth to Jupiter. It uses a monopropellant hydrazine engine along with 12 ADCS thrusters, a reaction wheel, and magnetic torque tubes to maintain the correct trajectory. The R-O then deposits the M-P on the surface of Europa and maneuvers itself into a Jovian orbit. In this orbit, the spacecraft generates energy

using gallium arsenide solar panels and stores excess energy in batteries for use while in eclipse. Multilayer insulation is used to keep all systems within operating temperature ranges. The R-O is capable of sensing characteristics of Europa's orbit as well as seismic activity during flyby. This information along with data transferred to the orbiter from the M-P is then transferred to Earth using a high gain antenna operating in the X band.

2.0 Acknowledgments

Dr. Anderson is a professor and associate dean of engineering at Rensselaer Polytechnic Institute with years of experience building spacecraft in industry. Dr. Anderson's advice has been instrumental for each part of the design of the R-O.

Sarah Cavanaugh is a graduate student at Rensselaer Polytechnic Institute, who has both reduced the load on Dr. Anderson and enabled quick design decisions which could otherwise be arduously impossible to accomplish.

3.0 Introduction

Jupiter's moon Europa has garnered a lot of scientific interest over the years, from the very first images of its frozen, cracked, icy surface sent from the Voyager missions in 1979 [1] to today. From here, the question as to whether there could still be a liquid ocean beneath what we could see, surfaced, as well as the notion that this moon could still harbour some form of life. While the ice shell is estimated to be between 15 and 25 km thick, the ocean below it is estimated to be 60 to 150 km deep, containing twice as much water as is held in all of Earth's oceans. [2]. Little is known about this vast body of water under the surface of Europa, and while there have been previous missions to Jupiter that included Europa flybys such as the Pioneer 10 and 11, Voyager, Galileo, and New Horizons, no mission including thorough exploration of Europa's surface and what is has to offer has been completed yet. Launching in the next decade, NASA's proposed Europa Clipper mission aims to image Europa's surface, as well as gather evidence as to the liquid ocean under its surface and characterize it through gravity, magnetic field, and thermal measurements across Europa's surface through a series of 45 flybys of Europa [3]. Before this point in time, no probe has ever landed on Europa's surface to sample its surface composition and relay the data back to Earth. This proposed mission, however, aims to change that by sending the R-O in orbit around Jupiter, which will then release the M-P onto Europa's surface. The M-P will detect the composition of ice on Europa's surface, and search for any potential organic precursor carbon-containing molecules with physical measurements made on the surface that could hint at the potential for extraterrestrial life. Meanwhile, the R-O will aim to detect the water under Europa's surface, radiation levels, seismic activity, and Europa's atmospheric composition through numerous flybys. The M-P will be in communication with the R-O, which

will relay the data it receives, as well as the data transmitted to it from the probe, back to the Earth.

Presented below is the final design of the R-O that will be used for this mission, complete with descriptions and classifications of the major risks of each subsystem, as well as potential future work that could be undertaken in order to improve the designs that are already in place here, as a stepping stone towards a robust orbiter that can play a part in probing into the mysteries that this moon holds.

4.0 Project Scope

4.1 Objectives

The Semele mission is made up of several phases. The first phase was to complete the PDR, where options for each of the eight subsystems were evaluated, and chosen. This document pertains to the second phase of the mission, which is to analyze the decisions made, give detailed descriptions, and perform calculations in each subsystem. A third phase will be to model and test each individual component to ensure their reliability. The final phase will be to fund and manufacture the Rhadamanthus-Orbiter according to the designs chosen.

Based on the decisions made in the PDR, this document, the FDR, contains in-depth analysis regarding those decisions, as well as detailing how the subsystems are integrated. The eight subsystems evaluated are structures, thermal systems, power management, telecommunications and data, mechanisms and deployables, propulsion systems, attitude dynamics and control, and orbital mechanics. For the month following the PDR, the team completed this more detailed analysis. The final design is presented in two ways: a detailed written report, and a presentation.

The mission itself also has several objectives. The two primary objectives are to reach the desired Jupiter orbit and release the probe to the moon Europa. These objectives are completed primarily by the orbital mechanics, propulsion, and mechanisms subsystems. The orbiter must also adequately protect its on-board sensors including the probe. This is accomplished by the thermal control and structures systems. Since the orbiter also has on-board sensors, part of the mission objectives is to collect atmospheric data of Europa, and relay this information back to Earth. This is the primary focus of attitude dynamics and control, communications, and mechanisms subsystems.

4.2 Constraints

The Semele mission is subject to political, environmental, and economic constraints, which are listed in Table 4.2.1 below. Additionally, a range of technical constraints will impact the mission design. These technical constraints are discussed in depth in each subsystem.

Table 4.2.1: Mission Constraints

Mission Constraints	
Type	**Constraints**
Economic Constraints	● Budget Constraints
Environmental Constraints	● Plutonium as a heat source ● Avoiding Europa contamination ● Hydrazine propellant is a health hazard
Political Constraints	● Use of a private launch vehicle ● Inclusion of Plutonium

4.3 Authority and Responsibility

Table 4.3.1 outlines which individual is responsible for each section of the FDR.

Table 4.3.1: FDR Responsibilities

Final Design Report Responsibilities	
Name	**Responsibilities**
Arumbakkam, Shruti	Introduction Propulsion Subsystem Mass Budget
Fahey, Liam	Executive Summary Orbital Mechanics Subsystem Timeline
Hoddinott, David	Constraints ADCS Subsystem Conclusion
Karwic, Nathan	Acknowledgements Power Subsystem Power Budget
Perianayagam, Nidhi	Objectives Mechanisms and Deployables Subsystem Telecommunications and Data Subsystem
Pirro, Joseph	Authority and Responsibility Structures Subsystem Volume Budget
Reilly, Clare (Team Leader)	Risk (Appendix 10.1) Thermal Controls Subsystem Monetary Budget

5.0 Design Approach

5.1 Structures

The following section consists of the final structural design for the Rhadamanthus Orbiter. This section contains a summary of the overall design, an in-depth finite element analysis of the main structure housing, a detailed model of the entire orbiter layout, and a risk assessment.

The structural design of the Rhadamanthus Orbiter does not follow traditional spacecraft designs because of the emphasis that has been placed on low cost for this mission. Hence, the exterior structure of the R-O consists of a cube-shaped design that is made out of aluminum. A cube shape was chosen because of its simplistic nature in terms of ADCS control, and aluminum was chosen as the main material of the spacecraft because of its low cost and low density, which is beneficial to both the cost and mass budgets. Unlike the exterior of the spacecraft, the interior of the R-O follows a more traditional 2-Deck layout. The 2-Deck interior structure consists of two cross beams that are made out of titanium, which will increase the structural integrity of the spacecraft. This layout was selected because it increases the structural supports on the interior of the spacecraft and provides organization amongst the interior components. For a detailed view of the overall design, refer to Figure 5.1.3.1.

5.1.2 Body Finite Element Analysis

Based on the preliminary research done in the PDR and further analysis after that report, it was determined that the Falcon Heavy was the most optimal launch vehicle choice for this mission because of the extra mass that it can lift into LEO. Table 5.1.2.1 displays the maximum payload specifications that the Falcon Heavy launch vehicle can support when delivering the R-O to the desired trajectory.

Table 5.1.2.1: Falcon Heavy Maximum Payload Specifications [4]

Space-X Falcon Heavy Maximum Payload Specifications	
Specification	**Value**
Mass (kg)	5400
Size (m)	4.8(Diameter) x 11(Height)
Volume (m^3)	796

One of the most critical parts of any space mission is the time between lift-off reaching orbit. This interval of time is the most dangerous for any spacecraft because of the high force exerted on the spacecraft by the launch vehicle. These forces are mainly in the form of acoustics and vibrations due to the natural frequencies of both the launch vehicle and the spacecraft. Because of this phenomenon, the natural frequencies of both the launch vehicle and the spacecraft need to be taken into account to ensure that neither of the bodies are vibrating at the same frequency along the same axis. If the two bodies are vibrating at the same frequency along the same axis, resonance occurs and the spacecraft will most likely be torn apart due to the extreme forces that it experiences.

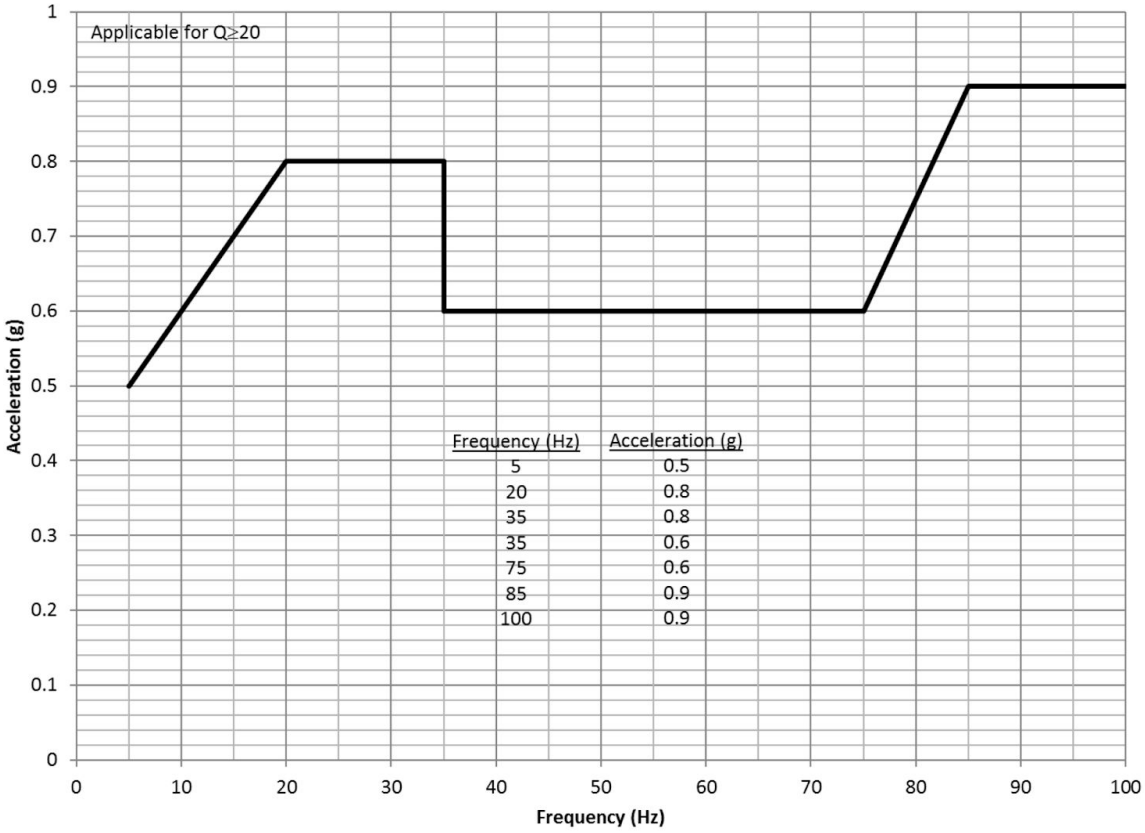

Figure 5.1.2.1: Falcon Heavy Axial Frequency Environment [4]

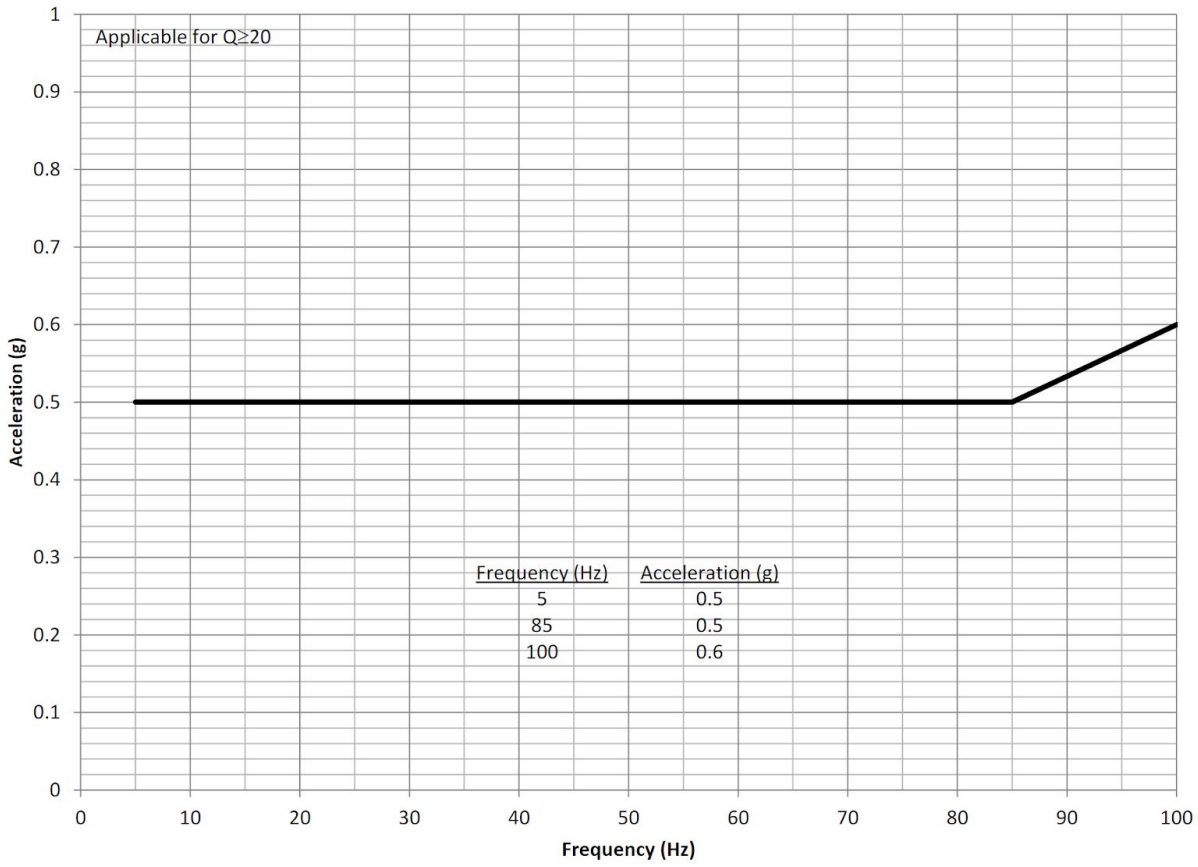

Figure 4-4: Maximum lateral equivalent sine environment for Falcon 9 and Falcon Heavy

Figure 5.1.2.2: Falcon Heavy Lateral Frequency Environment [4]

Figures 5.1.2.1 and 5.1.2.2 display the vibration frequency environment of the Falcon Heavy launch vehicle. As shown in the figures, the natural frequency range of the launch vehicle is between 5-100 Hz. Due to this, the vibration analysis that is performed on the R-O will only consider the natural frequencies between 5-100 Hz. Table 5.1.2.2 displays the list of natural frequencies that were calculated for the R-O by using Nastran Nx finite element analysis (FEA) software, as well as the overall structural design and tetrahedral meshgrid.

Table 5.1.2.2: Natural Frequencies of the R-O calculated by FEA software

Structural
Mode 1, 17.0231 Hz
Mode 2, 17.4634 Hz
Mode 3, 23.5797 Hz
Mode 4, 23.7299 Hz
Mode 5, 23.9101 Hz
Mode 6, 23.9536 Hz
Mode 7, 24.1573 Hz
Mode 8, 24.3791 Hz
Mode 9, 24.712 Hz
Mode 10, 24.8087 Hz
Mode 11, 28.3599 Hz
Mode 12, 28.4513 Hz
Mode 13, 28.6276 Hz
Mode 14, 29.7239 Hz
Mode 15, 29.9252 Hz
Mode 16, 31.3321 Hz
Mode 17, 31.4336 Hz
Mode 18, 31.8669 Hz
Mode 19, 34.0335 Hz
Mode 20, 34.4631 Hz
Mode 21, 36.7381 Hz
Mode 22, 36.8 Hz
Mode 23, 38.2248 Hz
Mode 24, 40.9936 Hz
Mode 25, 41.0649 Hz
Mode 26, 42.7385 Hz
Mode 27, 42.8358 Hz
Mode 28, 44.3699 Hz
Mode 29, 51.3014 Hz
Mode 30, 52.5643 Hz

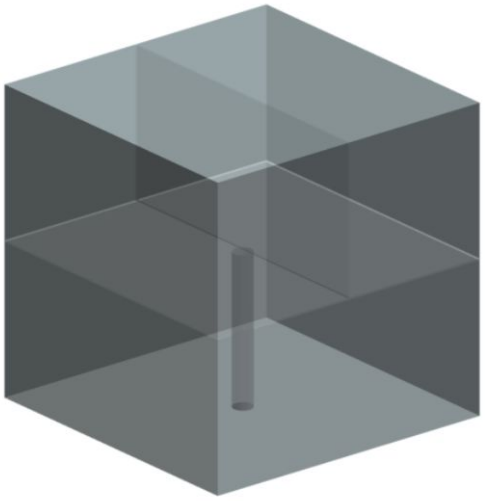

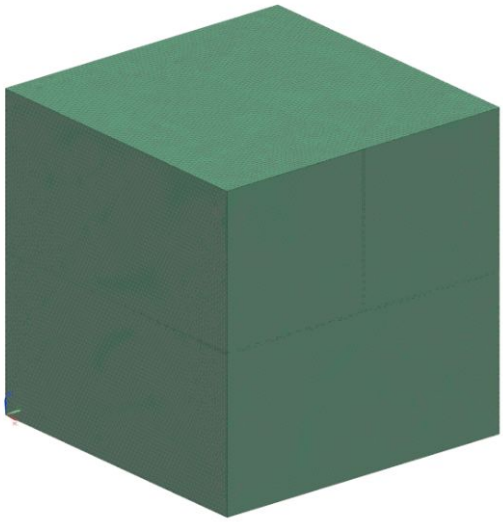

The vibration analysis calculated the first 30 modes, along with the natural frequencies associated with those modes for the structural design of the R-O. The Falcon Heavy launch vehicle has natural frequencies at 5, 20, 35, 75, 85 and 100 Hz, while the spacecraft has natural frequencies of 17, 23, 31, 34, 36, and 42. From the first 30 modes, it is clear that the natural frequencies of the spacecraft are not the same as the Falcon Heavy launch vehicle. Given this

analysis, it can be concluded that the R-O will survive the vibration stresses that are felt during launch.

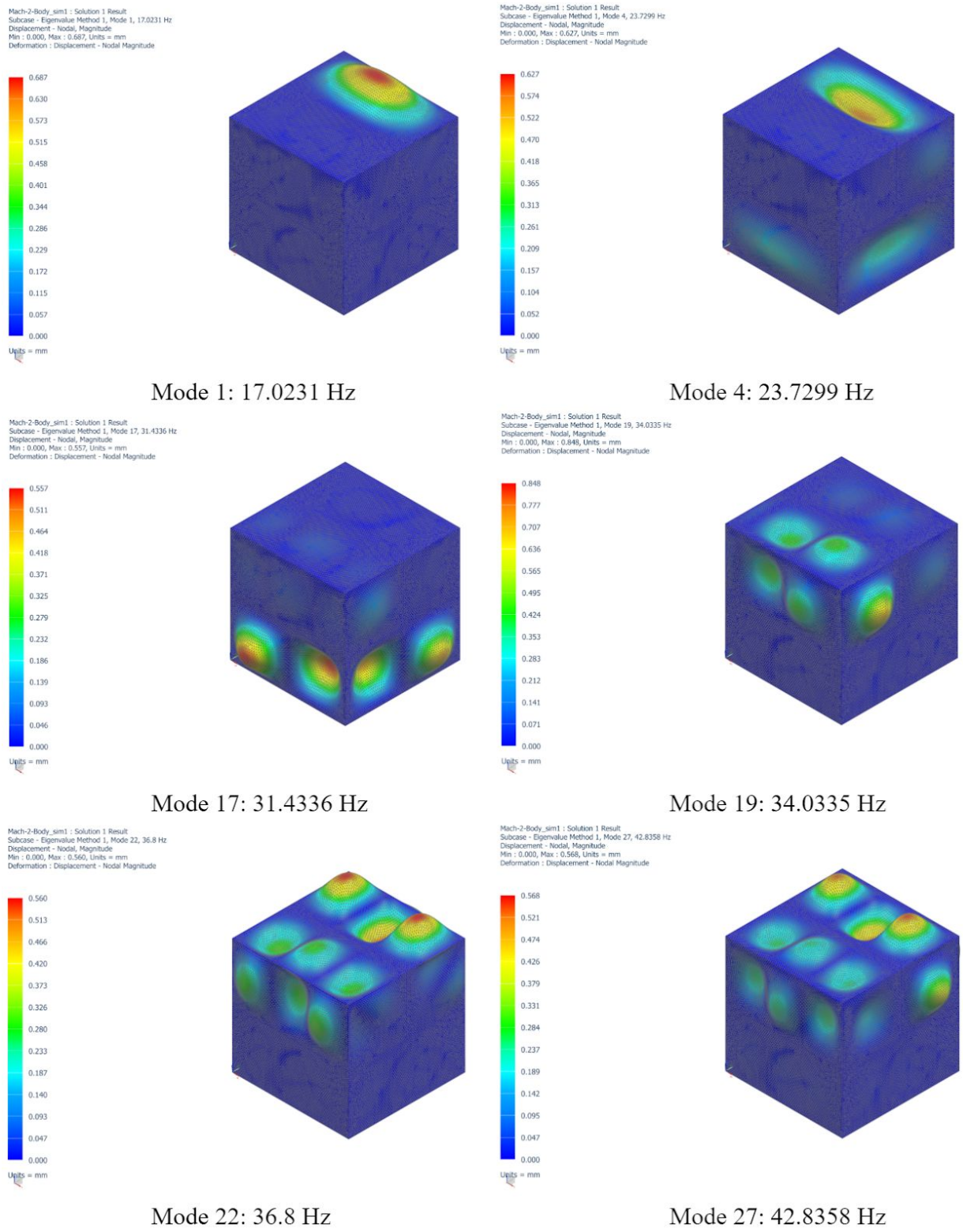

Figure 5.1.2.3: Simulated FEA Structural Deformations due to Natural Frequencies

The largest deformation due to vibration frequency occurred during mode 19, which experienced a deformation of .848 millimeters. This deformation is very miniscule when comparing the 5 millimeter thickness of the aluminum housing. However, this deformation can be further decreased through one of three ways, increasing the thickness of the aluminum housing, adding another cross member support, or adding a tie down point to the area to secure it in place. After analyzing each natural frequency and the deformation of the spacecraft structure due to vibrations, it can be concluded that this structural housing design of the R-O will accomplish the task of surviving launch.

5.1.3 Overall Structural Model

The overall structural model of the R-O consists of all the components required both on the exterior and interior of the spacecraft.

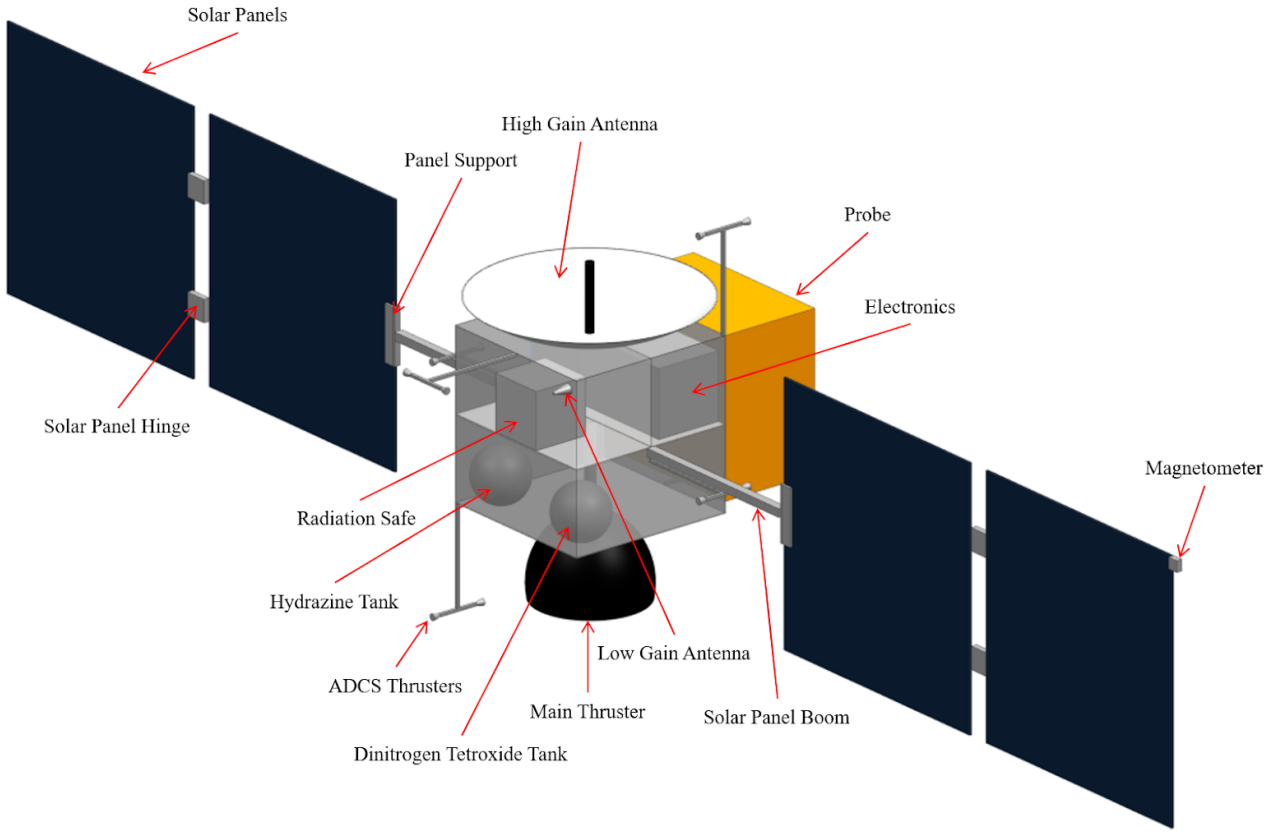

Figure 5.1.3.1: Overall Spacecraft Structure (Deployed Configuration)

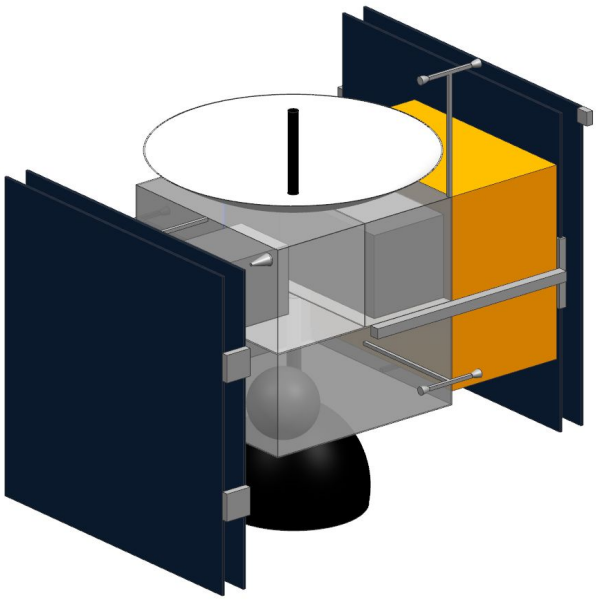

Figure 5.1.3.2: Overall Spacecraft Structure (Stowed Configuration)

The overall structure of the R-O has a total wet mass of 3525 kg and a volume of 2.47 m^3, for more information on the mass and volume budgets, refer to Sections 6.1 and 6.3 respectively. The dimensions of the Rhadamanthus Orbiter in the stowed configuration are 3.786 meters by 3.325 meters by 3.327 meters (LxWxH). From Table 5.1.2.1, the fairing size of the Falcon Heavy is 4.8 meters in diameter by 11 meters in height, therefore the R-O will easily fit inside the fairing. Overall, this structural design of the R-O will work extremely well with the chosen Falcon Heavy launch vehicle.

5.1.4 Risk and Risk Mitigation

There are two major risks when considering the structures subsystem. One as discussed previously is the risk of failure do to the acoustic and vibration forces inflicted by the launch vehicle. The second major risk is the impact of a micrometeorite on the spacecraft during flight. Both of these risks have been taken into consideration in this design of the R-O. The acoustic and vibration risk can be further mitigated through communication with SpaceX on the exact axial and lateral natural frequencies of the Falcon Heavy that may line up with the R-O; refer to Section 5.1.2 for ways to reduce the risk of acoustics and vibration. In addition, the risk of a micrometeorite impact can be further decreased by increasing the wall thickness of the aluminum housing or by adding another layer behind the aluminum to absorb the impact in addition to

aluminum. From Appendix Figure 10.1.1, in terms of overall risk to the R-O, the structures subsystem falls in the category of 2D or 3D, thus requiring that either a management team or supervisor to evaluate the analysis done on the natural frequencies of the spacecraft to ensure that failure does not occur.

5.1.5 Conclusions

The main body structure of the R-O consists of a combination of exterior aluminium and interior titanium. This configuration allows for the most structural integrity and achieves the goal of reducing weight and cost. The natural frequencies of the R-O as determined by FEA, do not overlap with the natural frequencies of the Falcon Heavy launch vehicle. However, a more in depth analysis needs to be performed to ensure that the natural frequencies that are close do not occur along the same axis, whether it be axial or lateral. The overall structural design of the R-O is compact and organized, thus allowing for easy storage inside the Falcon Heavy fairing and easy access to any subsystem. In general, the risk to the overall mission as a result of the structures subsystem is very small, hence this structural design of the R-O is the best choice because of its low risk and cost.

5.1.6 Future Work

The future work of the structures subsystem will consist of three major operations, evaluating building time, reevaluating the material selection for certain components, and increased FEA. Evaluating the building time of the R-O will allow for both a more accurate estimate of the launch date and the cost to build. Material selection of certain components will also be reevaluated since other materials may be cheaper or lighter which could further decrease the cost of the mission. The FEA performed in this report is very preliminary and a very in depth analysis needs to be performed to assess every natural frequency of the R-O to ensure that none of them align with the Falcon Heavy launch vehicle. In addition, the increased FEA will also have to take into account the entirety of the spacecraft, and not just the main body structure as was evaluated in this report.

5.2 Thermal Systems

The thermal subsystem ensures that all equipment requiring particular temperature conditions both inside and outside of the spacecraft operate efficiently for the entirety of the mission. This is done both with strategic placement of elements that aid in thermoregulation and choosing appropriate protection. Without ensuring all elements will survive the harsh conditions of space, multiple components could fail and cause mission issues. The options for thermal control were examined, and those best suited to the mission were selected and will be discussed.

Due to the limited time for the completion of this document and only one team member associated primarily with each section, analysis was not conducted with the aid of any programs and this design represents an overview of main components utilized in the thermals subsystem. A preliminary examination of mission requirements produced the results reported in this section, so this is not the final design decision. Although testing and analysis will need to be performed at a later time, the research conducted for this section is sound and should produce favorable results in the future.

5.2.1 External Environment

To begin the analysis for the thermal subsystem, environmental conditions were accounted for. The spacecraft will need to survive the launch, Earth's orbit, transit to Jupiter, and Jupiter's orbit. The transport of the spacecraft to the launch site will not be discussed. Although the spacecraft will not spend much time in the launch phase, it was considered in the analysis to ensure temperature limits for exposed equipment were not exceeded. Aerodynamic heating will cause external temperatures of 363 to 473 degrees Kelvin [5].

Once the spacecraft reaches its parking orbit of about 300 kilometers, new heating considerations including direct solar, albedo, and Earth IR heating will be considered. For direct solar radiation, the amount received by the spacecraft will differ based on whether the Earth is at perihelion or aphelion. The analysis performed by the orbital mechanics team used a circular orbit, but the values for the two elliptic cases are noted. The relationship between solar flux and distance is represented as $\frac{1367.5}{AU^2}\frac{W}{m^2}$, so with Earth in a circular orbit 1 AU from the sun, 1367.5 W/m^2 is considered the average flux. Another assumption made by the design team was that the spacecraft will be at zero degrees inclination facing the sun when determining maximum solar flux. This assumption was made knowing that although the inclination of the orbit around Earth will be 25 degrees, it will be such that the slant occurs facing the sun. Table 5.2.1.1 below provides values obtained by NASA of the conditions of Earth for a 24 hour observation period and a 2σ condition [5]. Using these values accounts for the higher risk nature of the mission. There is only a five percent chance that 2σ conditions will be exceeded, excluding any potential component failures.

Table 5.2.1.1: Earth Orbital Environments [5]

Earth Orbital Environments		
Characteristic	**Aphelion**	**Perihelion**
Solar Flux (W/m^2)	1322	1414
Albedo	0.17	0.19
IR (W/m^2)	236	257

As the spacecraft begins its transit from Earth, the direct solar, albedo, and IR drops were considered. These conditions typically apply whenever a spacecraft makes a close enough encounter with a planet, but will not be considered for the flyby of Mars at this time for simplicity. The Mars flyby will not consist of any of the extreme conditions for this mission. Empty space is estimated to be about 3 degrees Kelvin, and this will be the minimum temperature to prepare the spacecraft for. Approaching Jupiter and early into its orbit, the average solar flux of Jupiter, in a 5.2 AU circular orbit, will be about 50.57 W/m^2 . It is assumed there will be almost no inclination when in Jupiter's orbit, so any solar flux experienced will also be direct as it was in the Earth case. Table 5.2.1.2 below shows the values for aphelion and perihelion of Jupiter conditions.

Table 5.2.1.2: Jupiter Orbital Environments [5]

Jupiter Orbital Environments		
Characteristic	**Aphelion**	**Perihelion**
Solar Flux(W/m^2)	46	56
Albedo	0.343	0.343
IR(W/m^2)	13.4	13.7

5.2.2 External Protection

The mission will be focused on keeping the spacecraft warm, since the transit to Jupiter will be what takes a majority of the time. Additionally, the period of time the spacecraft will spend in Jupiter's radiation belt is significant enough that the protection of equipment susceptible to damage from this area will need to be a priority. The spacecraft is oriented in such a way that for the situation where it is in the direct line of the sun, the probe will face Earth as seen in Figure 5.1.3.1. This means that the probe will be receiving the IR and albedo thermal load, which is significantly less than if it were facing the sun. Most of the solar flux will be taken by the body of the spacecraft at the wall closest to the hydrazine tanks, which may keep them slightly warmer than if they had been placed elsewhere. This also means that for the case where the spacecraft is on the other side of Earth they will be facing the 3 Kelvin of space. How to maintain the appropriate operating temperature of the tanks will need to be a balance of the heater placements and heat removal to keep it around its ideal 291.7 kelvin, which will be explored at a later time.

The interior will be coated in black paint (Chemglaze Z306) to increase emittance, and the flat plate radiator will be coated in white paint (Z93) to minimize absorption [5]. Table 5.2.2.1 below highlights some of the values for the materials selected. Propellant lines and tanks will need to be aluminum coated to decrease emittance. It should be noted that the white and aluminum coatings will degrade more quickly in the space environment than the black coating, and so will need to be applied more heavily. The assumption is made that all antennas, panels, and relevant outside equipment that cannot be covered with the multilayer insulation used by the majority of the spacecraft will be more capable of handling harsh space conditions and covered more appropriately. For the antennas, this means using MLI with non-aluminized Kapton so as not to disrupt radio frequencies.

The MLI covering the body will consist of several layers, beginning with an outer layer then adding several interior layers. All layers will be separated by Dacron. Kapton will be used for the outer layer rather than Teflon because although it may not be as strong, it is more balanced in its absorptance and emittance, and is not as heavy. Kapton is also compatible with long term UV exposure which will be useful when encountering Jupiter. Aluminized Mylar will be used for the interior layers, because it is reliable but not as heavy as other options per layer while still operating within necessary parameters. The thickness for the Mylar will not be determined at this point for lack of time.

Table 5.2.2.1: External Protection Emittance and Absorption [5]

External Protection Emittance and Absorption		
Material	**Emittance**	**Absorption**
Chemglaze Z306	0.89	0.92-0.98
Z93	0.92	0.17-0.20
Aluminum	0.03-0.10	0.09-0.17
Kapton	0.62	0.44
Mylar	0.05	0.14

5.2.3 Internal Environment

The internal environment for the spacecraft has to be suitable for the removal of unnecessary heat produced by components while also making sure all parts are still warm enough to be within their operating temperatures. This will involve a combination of strategic placement of components, the addition of a heat source to the system, and transfer of excess heat to a radiator. The table below states many of the requirements for the operating temperatures for components both inside and outside the spacecraft, as well as considering the heat output for those inside. Since antennas and solar panels are external components, their heat output are not considered for simplicity. The mission is such that the environment will be colder for longer than hotter, so radiators will be smaller than they would for warmer missions. This means batteries may have to exceed their operating temperature for a short time, but with the assumption that nothing will be caused extreme damage. Table 5.2.3.1 are the operating temperature values that the team produced for their subsystems. However, when considering the formation of the actual orbiter, components that the design team did not consider in this document for simplicity will need to be considered more carefully at a later time. This means that the exact number of RHUs required for this mission may not be known, but it may be assumed that the number will be close to what Cassini had, which was 82 not including those on the probe [6].

Table 5.2.3.1: Component Thermal Attributes

Component Thermal Attributes		
Component	**Hot Operating**	**Cold Operating**
Low-Gain Antenna	358	253
High-Gain Antenna	408	98
Reaction Wheels	358	238
Star Tracker	360	240
Solar Panels	450	200
Li-Ion Batteries	330	270
Fuel Tanks	291.7	---

5.2.4 Internal Protection

Since one of the most difficult portions of the mission will be keeping all components within operating temperature while the environment is at 3 degrees Kelvin, Radioisotope Heating Units (RHUs) will be placed near operating components. One RHU outputs about 1 Watt [6]. Since certain components will need to be warmer than others, there will be an amount of excess heat in the interior that must be removed. The weight distribution of the RHUs was not considered because their individual mass is nearly negligible compared to the entirety of the orbiter.

Referring to Figure 5.1.3.1, the radiator will be placed in the lower right hand corner of the spacecraft, below the electronics and facing the solar panel. This is beneficial because it is assumed that the electronics will have a larger heat output than other components, and so if heat pipes are needed there will be less distance to travel. The heat rejection of the radiator and estimation of how large it should be is determined with

$$\frac{Q}{A} = \varepsilon\sigma T^4 \quad \ldots(5.2.4.1)$$

Where Q is the heat output, A is the area of the radiator, σ is the Boltzmann constant, ε is emissivity, and T is temperature in Kelvin [5]. Since this equation is heavily dependant on temperature, the lower the temperature of the internal environment is, the less heat that will be rejected by the system. To increase efficiency, heat pipes can be placed along the inside of the radiator. The overall efficiency of the radiators will degrade over time, making it harder to keep the interior cool, but it will be more important that only the necessary heat is ejected since the mission will be cold most of the time.

5.2.5 Risk and Risk Mitigation

The first large risk concerned with this mission is radiation. Jupiter's radiation belts could cause significant damage to functioning components if not properly protected. Therefore, having confidence that all surfaces are shielded with MLI appropriately or covered with paint is a priority. Additionally, there is risk associated with using RHUs because once they are placed on the spacecraft they cannot be turned off. Any leakage of the radiation on the interior of the spacecraft could be detrimental to the mission. The assumption is that this is an extreme case and will be unlikely so long as they are placed and secured properly. Should the MLI fail or be damaged, the exposure to the extreme temperatures could be damaging to equipment. Therefore, MLI must be selected thick enough to withstand mission requirements but not significantly affect cost. There is risk associated with using mostly passive thermal systems, since if any significant malfunction occurs they cannot be shut off. This will need to be mitigated by sufficient system testing and determination if an active system must be added, which will need to be done at a later time. The thermal system has an overall risk of 2C, as was determined from the Appendix Figure 10.1.1. There will need to be committee management and review before the system can be approved.

5.2.6 Future Work

There is still much to accomplish for the thermal system of this mission because much of it will rely on component testing as a unit. To provide a more detailed analysis of the conditions that the spacecraft will face, especially externally, analysis would be performed using finite element analysis or other programming that can accurately account for temperature distribution. The number of layers of MLI and thickness of each layer to provide the best conditions for equipment would be found. Furthermore, less assumptions would be made about the orientation of the spacecraft in its transit. An examination on the placement of the internal components and the overall space temperature will determine how many RHUs are required and if heat removal is sufficient.

5.3 Power Management

5.3.1 Power Needs

The nominal maximum concurrent power draw is expected to be 175W, so the power system will be able to supply this constantly at EOL. (see Power Budget in Section 6.2)

5.3.2 Solar Panels

Based on the new power requirements and an EOL power density of 11.09 W/m^2 [7, 8], the design solar panel area is 15.8m^2. There will be 4 solar panels, each 2.3m x 1.72m such that the total length of each 2-panel array is 4.6m. Orienting the panels so that they are thinner when stowed allows for more space for the probe attachment along the sides of the vehicle, while only slightly increasing the weight of the panel structure.

The structure of the panels will be a carbon fiber sandwich structure with aluminum honeycomb in order to keep the mass low while keeping most of the strength of the carbon fiber. In order to determine the thickness of the components, one needs to consider the maximum bending moment induced by the weight of the panels under the maximum acceleration by modifying the following equations:

$$M = \frac{w \times L \times a}{2} \quad ...(5.3.2.1)$$

$$S_{CF} > \frac{M \times (T_t/2)}{I} \quad ...(5.3.2.2)$$

$$S_{HC} > \frac{M \times (T_h/2)}{I} \quad ...(5.3.2.3)$$

Where w is the mass of the array, a is the maximum acceleration, L is the length of the array, T_t is the total thickness, T_h is the thickness of the honeycomb, S_{HC} is the shear strength of the honeycomb, and S_{CF} is the normal strength of the carbon fiber.

From the above equations, one can iterate using Matlab to find the minimum carbon fiber thickness for a given honeycomb thickness. By iterating through different thicknesses using the Matlab code in Appendix 10.2.11, and the material properties in Appendix 10.3, the code finds the minimum acceptable panel mass is 14.44kg with a honeycomb thickness of 8.3mm and a carbon fiber thickness of 0.288mm. Note that the maximum acceleration of up to 70 m/s^2 [4] is not from the motor on the R-O, but actually occurs during the burn to escape from Earth's influence.

5.3.3 Power Storage

5.3.3.1 Eclipse Time

In order to determine the eclipse time, one can determine the orbital angles between which the spacecraft will be in shadow, and determine the transit time based on the orbital model. Because Jupiter is far from the sun, solar rays can be assumed to be parallel. This means that the spacecraft will be in shadow when the height "y" of the ellipse is less than the radius of Jupiter:

$$R_J > y \quad ...(5.3.3.1.1)$$

Taking the generic relation for an ellipse and inserting the characteristics of the Jovian orbit, the spacecraft is in eclipse when:

$$R_J > \left| 763000 \times \sqrt{1 - \frac{(x+1963000)^2}{2037000^2}} \right| \quad ...(5.3.3.1.2)$$

This relation is satisfied when the spacecraft is within 47°, yielding a total eclipse time of 30 minutes.

5.3.3.2 Battery

The battery is designed to fulfill all the power requirements for twice the expected eclipse duration, or 1 hour. Due to its exceptional thermal tolerances and energy density, the battery will be a Li-ion cell. Based on the batteries on Juno, approximate energy density for a space-tolerant Li-ion battery is 110 Wh/kg. In order to provide 175W of power for a full hour, a similar battery will mass 1.6 kg.

5.3.4 Risk and Risk Mitigation

The largest risk is that all power to the vehicle is lost, which would result in a catastrophic failure and potential loss of the mission. The considered methods of catastrophic failure are impact on the solar panels and thermal damage to the batteries. Without mitigation, a rigid array would have a 2D (See Figure 10.1.1) risk due to impact. However, by slightly modifying the orbit to reduce time spent near areas of high object density, this risk can be dropped to a 2E classification. The battery not only pose a threat to themselves when experiencing a power draw, but the heat it gives off can also overheat other components if throwing off a lot of heat. As the R-O is designed for operation near Jupiter, the design environment has less solar radiation than is present near Earth. These effects mean that near Earth, the risk of component failure due to overheating is a 2C during battery use. In order to mitigate this risk, the batteries will be limited to a 100W output while within the orbit of Mars,

decreasing both the likelihood and severity of damage. The risk can be reclassified as a 3D after mitigation.

5.3.5 Future Work

In the future, the team will find a supplier for the battery and solar panel structure. Additionally, the team will find costs for all components in order to develop a full cost budget.

For a manufacturable design wiring must also be produced. This will occur while plans for component mounting are also being created.

5.4 Telecommunications and Data

The primary function of the communications system is to transmit and receive data from Earth, as well as relay information to and from the probe. Radio waves, which travel at the speed of light in a vacuum, can take anywhere from 35 to 52 minutes to reach Jupiter depending on their relative positions around the Sun. During the trajectory of the R-O and its orbit around Jupiter, the spacecraft is not able to have constant communication with Earth. The communication of the R-O with the probe relies heavily on where the probe is located on Europa. The trajectory is further detailed in Section 5.7.

5.4.1 Earth Communication

The High Gain Antenna (HGA) chosen was a dual reflector HGA, similar to that used on Juno. The HGA will have the ability to communicate on the X and S bands. The X band will be the primary method of communication with Earth, as it has little interference from other radio frequencies and is extremely powerful at long distances. There will also be a conical Low Gain Antenna (LGA) located on the body of the R-O. The LGA will only operate on the S band, which is weaker over very long distances, and remains stable against Earth's weather patterns [9].

The HGA is meant to transmit the high amounts of data received from the probe back to Earth. An important aspect of the HGA is to consider is uplink versus downlink. Uplink frequency is the transmission from Earth to the R-O, and downlink frequency is from the R-O back to Earth. An S/X band connection was chosen because there is significantly more data that needs to be transmitted to Earth compared to the data that is transmitted to the probe. The S/X band connection offers a turnaround ratio of 880/221 [10]. The distance between Earth and Jupiter varies from 600 million to 900 million km [11]. Using Equation 5.4.1.1 below, the maximum gain at a maximum distance could be calculated. The dual reflector shape of the HGA enables a higher bit rate for only a small amount of added mass.

$$G_t = 17.8 + 20log(f) + 20log(D) \quad ...(5.4.1.1)$$

Table 5.4.1.1 Downlink High Gain Antenna Summary [10]

Downlink High Gain Antenna Summary	
Parameter	**Value**
Frequency (*f*)	X Band (8420.432097 MHz)
Data Rate	580 kbps
Max Range	9.6e8 km
Dish Diameter (*D*)	2 m
Max Gain	102.33 dBi

Communication to Earth will primarily be done using the Deep Space Network (DSN). The DSN is a series of United States satellites on Earth in 3 locations: California, Madrid (Spain), and Canberra (Australia). The location of these satellite groups allows for nearly all of Earth's surface area to be communicable. The channel chosen for the DSN connection was Channel 18 due to its downlink frequency for the X band. At this frequency, there will be little interference from other spacecrafts, which is the main concern at such a distance from Earth. Channel 7 (2110.58 MHz) was chosen for the S band uplink frequency.

Another important factor to consider when designing a HGA is the physical structure. With the Falcon Heavy as the launch vehicle, SpaceX recommends limiting the minimum resonant frequencies of secondary structures to 35 Hz [4]. A CAD model of the HGA was produced in order to find the resonant frequencies. This is shown below in Figure 5.4.1.1 with the resonant frequencies listed in Table 5.4.1.2.

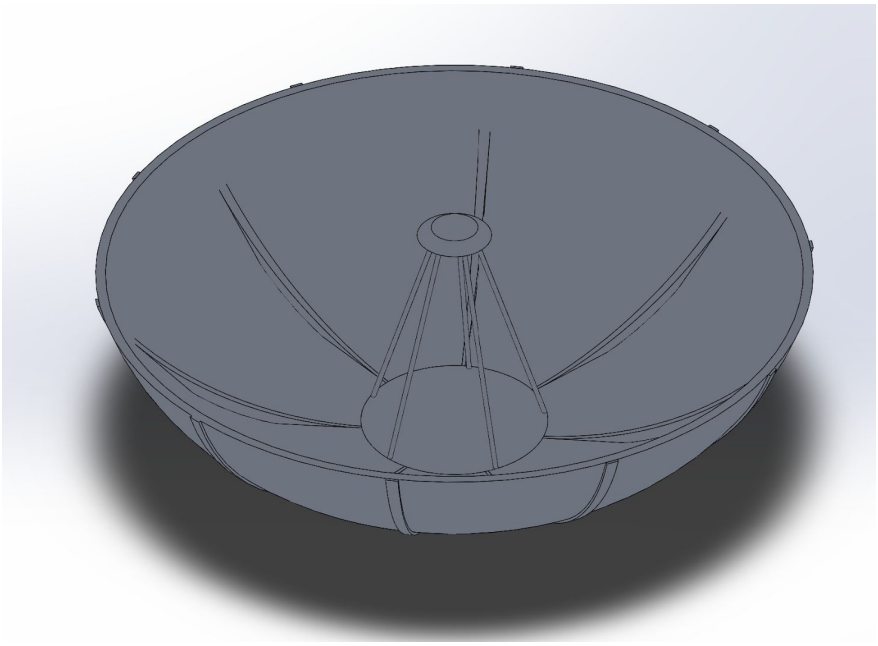

Figure 5.4.1.1. HGA CAD model from Solidworks

Table 5.4.1.2. Resonant Frequencies of the HGA

Resonant Frequencies of the HGA	
Mode	**Frequency (Hz)**
1	29.6572
2	39.5125
3	53.4233
4	79.3740
5	102.3937

The first natural frequency mode is 29.6572 Hz, according to the Solidworks Analysis performed. Although this is below the recommended natural frequency from SpaceX, the risk of the HGA failing is very low due to its deployment and gimbal mechanism, which is further discussed in Section 5.5.

The LGA has minimal structural impact, since it has a total volume of 0.3 m^2 and a minimal density because it is mostly hollow. The LGA operates only on the S band, which gives the S/S connection a turnaround ratio of 240/221 [10]. The LGA is meant to act as a backup to the HGA in case of emergencies or issues with the HGA. The maximum gain of the LGA can be calculated using Equation 5.4.1.2 below. Channel 14 was used for the LGA downlink frequency.

$$G_t = 5log(\frac{D}{\lambda}) + 3.5 \text{ ...(5.4.1.2)}$$

Table 5.4.1.3 Downlink Low Gain Antenna Summary

Downlink Low Gain Antenna Summary	
Parameter	**Value**
Frequency (λ)	S Band (2295.000 MHz)
Data Rate	23 kbps
Max Range	7e8 km
Cone Diameter (D)	.14 m
Max Gain	17.57 dBi

The range that the LGA was designed for is much lower than that of the HGA. This also results in a significantly lower maximum gain and data rate. The LGA is only intended to be used in case of emergency, or if the HGA is not able to see the Earth due to the orientation of the craft. It will be used minimally throughout the flight. There was no medium gain antenna considered to reduce the mass and power as much as possible. A CAD model of the LGA is shown below in Figure 5.4.1.2.

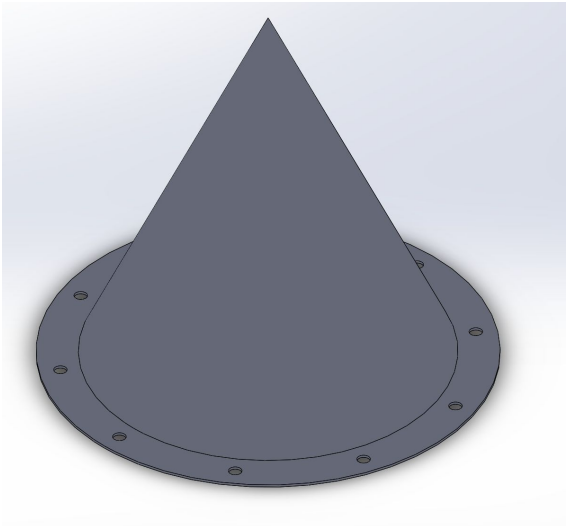

Figure 5.4.1.2. Low Gain Antenna model from Solidworks

5.4.2 Probe Communication

After reviewing the choices of the M-P communications team, it was decided that an Ultra-High Frequency (UHF) antenna would be used for the back and forth data transmissions between the R-O and the M-P. This UHF antenna would be omni-directional, so there would be no need for a gimbal. It will also be designed to fit the range of the R-O orbit around Jupiter relative to Europa. Unfortunately due to lack of time and available probe teams, the exact choices for this antenna could not be determined.

5.4.3 Sensor Suite

The main roles of the onboard sensors are to learn about Europa's atmosphere and surface. This includes the detection of water and ice, seismic activity, detection of radiation, and atmospheric composition. Sensors are also needed for attitude dynamics and controls systems.

The sensors onboard the orbiter will include a plasma spectrometer, a gravity gradiometer, composite infrared spectrometer, and a cosmic dust analyzer. These sensors satisfy the conditions listed above in that order. For attitude dynamics and control, the sensors will be gyros, celestial trackers, and a magnetometer. In order to reduce the weight of the sensor suite, sensors with little overlap in function were chosen.

The sizes and weights of many of the sensors could not be adequately determined due to lack of available resources and manufacturer specifications. The information used in other sections of this report are approximated from the sensor specifications from the Cassini and Juno orbiters.

5.4.4 Risk and Risk Mitigation

The primary risk surrounding the communication system involves the failure of the system. Without communication, there would be no way to send commands to or retrieve data from the orbiter. In order to reduce risk while still maintaining a low mass, there will be one LGA to supplement the HGA with Earth communication, and one UHF antenna to communicate with the probe. The chosen LGA and UHF antennas have been used before, and pose little to no risk of failure individually.

A second risk to consider with the communication system is blackout. This occurs when there is a celestial body blocking the path of radio frequencies between the R-O and Earth, or the R-O and the probe. Blackout will occur during certain orbital maneuvers, such as the gravity assist around Mars. Blackout between the R-O and the M-P will occur when they are opposite sides of Europa. With the chosen maneuvers, blackout will always be a problem with the communication system. In order to ensure communication has been re-established, the R-O will send short signals as soon as Earth is in its line of sight.

Political, environmental risk to the Earth, and economic risks were considered in regards to the communication system, but these were deemed not applicable in this case. Using Appendix Figure 10.1.1, the communications system poses an overall risk of 2D to the R-O. An overall risk of 2D means that the failure would severely affect the mission, but it is not very probable. This requires that a management team or supervisor must evaluate the analysis before manufacturing and testing can be completed.

5.4.5 Future Work

Before the antenna can be fully designed and manufactured, proper decisions must be made specifically about the UHF antenna to communicate with the M-P. In addition, further calculations must be done to determine the amount of time the orbiter will be able to communicate with Earth and the probe. This relies heavily on the Orbital Mechanics and Attitude Dynamics and Control Systems. Additionally, calculations must be completed for the antenna in worst case scenarios, which would take interference and antenna pointing into account. The calculations shown in the above analysis are preliminary, and should not be taken as the final decisions. Lastly, diagrams must be completed to show the connections between the antennas, data storage, and power systems.

5.5 Mechanisms and Deployables

Deployables are used in order to move appendages from launch configuration to orbit configuration. The main components that get deployed are the solar arrays, as well as the high gain antenna. Due to the high risk of breakage for the HGA during deployment and available space during launch, there is no deployment mechanism to open the HGA. Another component that must be deployed are the sensors for detecting conditions of Europa's atmosphere and the attitude dynamics control system. The main non-deployment mechanisms used are for pointing the solar arrays and HGA towards the Sun and Earth respectively in order to optimize their usage. Lastly, a mechanism for the probe release is decided.

5.5.1 Solar Array Mechanisms

Solar arrays are deployed far from the body of the R-O in order to minimize the shadow experienced from the spacecraft as well as to maximize the total surface area. The power system chose to use rigid solar panels with a necessary area of 50 m^2. A preliminary CAD model of the solar arrays is shown in Figure 5.5.1.1. Unfortunately, due to time constraints the natural frequencies of the solar arrays could not be calculated.

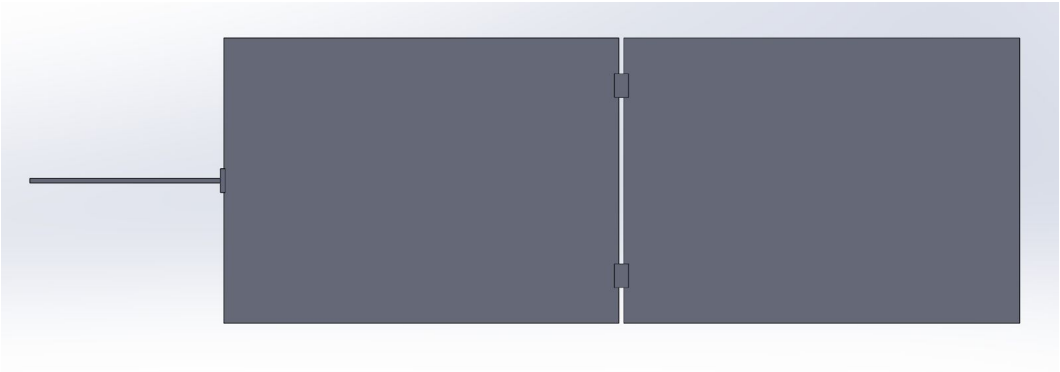

Figure 5.5.1.1. Solar Array Model from Solidworks

Once the solar arrays are deployed, they will not need to fold up again. In order to prevent the solar arrays from 'refolding' themselves, the hinges will have positive latching mechanisms. This also helps to prevent flapping of solar arrays during times of acceleration [12]. Since the solar panels are crucial for powering the R-O, there are two positive latching hinges between each panel. This gives some redundancy, but with little more mass. Again, because the solar arrays will remain deployed, it was decided that kickoff springs would be used to release them from the stowed position. A use of a motor would use more power and mass than necessary for the orbiter. Kickoff springs work to overcome the restrainment device, without causing severe damage or vibrations [12].

The solar arrays must be able to rotate in order to face the Sun. A typical method for the bidirectional rotation is a Solar Array Drive (SAD). The SAD device consists of a motor, gear train, clutch, slip ring and potentiometer [12]. Due to the relatively low overall mass of the solar arrays compared to other spacecrafts, a brushless direct-current motor was chosen to reduce power consumption. This type of motor provides a finite number of steps to reach the desired orientation without compensating for the moment of inertia.

5.5.2 High Gain Antenna Mechanisms

In order to reduce the risk of deployment failure as well as overall mass the HGA will stay fully opened from launch. There is adequate space for the 2 m diameter in the launch vehicle fairing.. For this reason, only pointing mechanisms were researched for the HGA.

A classical gimbal method will be used to point the HGA. A Cardan gimbal suspension consists of a pair of pivot bearings and a gimbal plane. See Figure 5.5.2.1 for a full diagram. The approximate error for a Cardan gimbal mechanism is 0.0014° is common, as this gimbal is widely used and tested [12]. Each axis is independently controlled, allowing for maximum precision. The center of gravity of the pivot points reduces the vibrations that could potentially affect the HGA. This will help stabilize the HGA during launch at a frequency of less than 35 Hz.

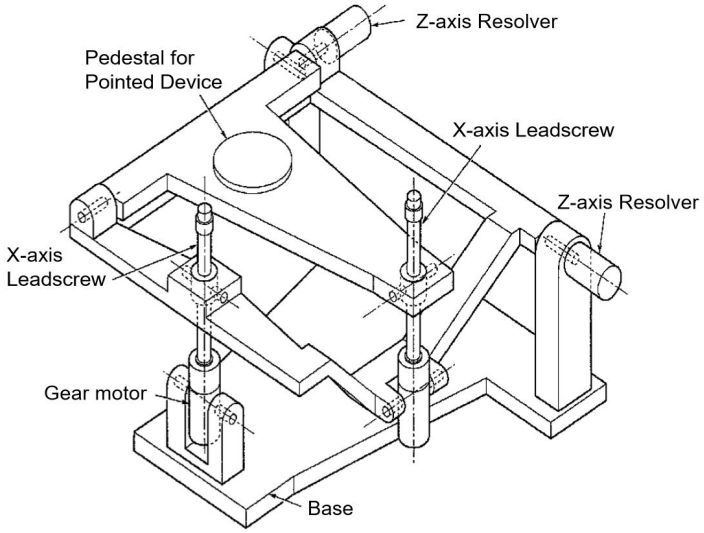

Figure 5.5.2.1. Cardan Gimbal Suspension [12]

5.5.3 Probe Release Mechanism

From analysis in the PDR, the chosen probe launch release mechanism is ball-lock separation. The ball-lock mechanism will be triggered by separation bolts. Unfortunately, due to delayed communication with the probe development team, further analysis and decision could not be made regarding the release of the probe.

5.5.4 Sensor Deployment

In order to accurately the atmospheric conditions on Europa, the sensors must be deployed away from the body of the orbiter. See Section 5.4.3 for the full sensor suite. Due to the lack of publicly available resources, the necessary distances the sensors must be from the body could not be determined. Accurate masses and sizes could also not be determined for the sensors, and so they were left out of the inertia calculations. There are a total of 7 sensors, 4 of which need to be deployed. The magnetometer will be located on the outermost edge of the solar arrays, to provide the least electrical interference from the spacecraft body. Data and diagrams from Cassini and Juno were used to estimate the relative sizes of the sensors to the orbiter.

The sensors will be deployed away from the spacecraft using telescoping booms, which will not be restowable. Keeping the sensors in the deployed positioning allows for kickoff springs to be used for each section, instead of using motors. This reduces the overall weight and power consumption. An example of a spring-loaded telescoping boom is shown below in Figure 5.5.4.1.

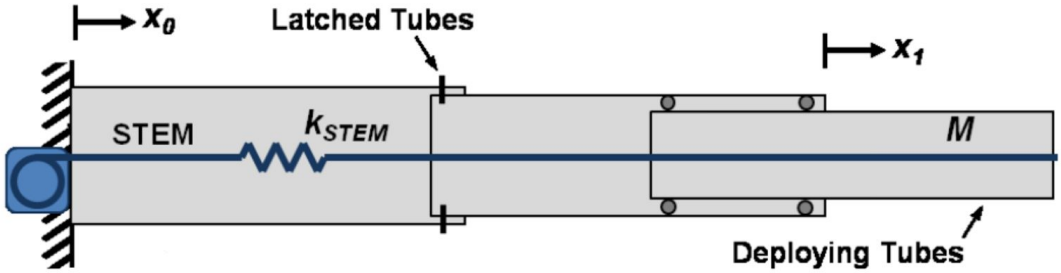

Figure 5.4.1.1. Telescoping Boom for Sensor Deployment [13]

5.5.5 Risk and Risk Mitigation

The main risk considered is the failure of any of these deployables. All of the mechanisms have been used in a wide variety of sizes and conditions, ensuring that they will work when necessary. The biggest concern regarding the HGA was eliminated by altering the original design from an opening deployment of the HGA to a fixed open HGA.The primary environmental risk to the deployables and mechanisms is the extremely cold temperatures experienced in space. These materials become less mobile in extreme conditions. The joints and moving parts should be properly lubricated and insulted to ensure they work in any conditions they will experience. According to Figure 10.1.1, the overall risk for the mechanisms and deployment subsystem is 2D which means an overseer or manager must oversee and approve of calculations and analysis before manufacturing can begin.

5.5.6 Future Work

The solar array natural frequencies could not be calculated due to the lack of information regarding the specifics of the solar array mass, materials, and arrangement. This will be done in the future before manufacturing and testing. The gimbal mechanism for the HGA must also be tested to verify the weight of the antenna does not overload it. The final decision regarding the release of the probe must also be decided before further analysis can be completed.

5.6 Attitude Dynamics and Control Systems

5.6.1 Summary

The Attitude Dynamics and Control system (ADCS) is responsible for the measurement and control of spacecraft orientation. The orbiter is required to change orientation multiple times during the duration of its mission. Since the mission trajectory includes a gravity assist maneuver, a very high degree of pointing accuracy is required during burns to ensure that the gravity assists are successful. Additionally, the ADCS must counteract disturbances such as solar pressure or gravity-gradients, and must be capable of de-tumbling the spacecraft.

The ADCS will include two subsystems; control and measurement. The components of each of these can be seen in Table 5.6.1.1.

Table 5.6.1.1: Subsystem Parts [14][15][19][20]

Subsystem Parts	
Control	**Measurement**
Honeywell 4820 reaction wheel	Honeywell HG5700 RLG IMU
MOOG Monarc 22-6 Hydrazine	Honeywell HG1930 MEMS IMU
128- gram magnetorquers	Ball Aerospace CT-2020 Star Tracker

The control system will include a Honeywell 4820 reaction wheel, sixteen MOOG Monarc 22-6 Hydrazine thrusters, and three custom 128-gram magnetorquers. The Honeywell 4820 has three primary reaction wheels, and a fourth which allows the system to maintain control authority in the event of flywheel failure. It is capable of producing 65 N-m-s of angular momentum. The Monarc thrusters are 22 Newton thrusters with an I_{sp} of 230 seconds. The thrusters are mounted on 1.55 m booms to increase the maximum moment they can impart on the spacecraft. Sixteen thrusters are included on this mission as twelve are required to control the spacecraft exclusively with couple moments, and four additional thrusters add redundancy. The magnetorquers are 7.5 cm in radius, have 1000 turns, and use a 0.1 mm wire gauge. With a 1-A nominal current, they require 7.25 W to operate. By including 6 magnetorquers, each with a different orientation, the local magnetic field will never completely align with the axis of the tube, thus ensuring that at least 1 magnetorquers has control authority at any time.

The Honeywell HG5700 RLG inertial measurement unit (IMU) is the primary inertial sensor, which uses a combination of laser ring gyros and vibrating beam accelerometers to

measure angular position and rate, with an accuracy of 0.01 deg/hr [19]. Additionally, a Honeywell HG1930 will serve as a backup IMU, which will be used in the event that the main IMU fails. The HG1930 uses micro-electromechanical systems, and has an accuracy of 1 deg/hr. Three Ball Aerospace CT-2020 Star trackers will allow for precise measurement of angular position of the spacecraft. The CT-2020 have an accuracy of 0.000278 degrees. Including three Star trackers will allow the system to take an accurate measurement from any orientation. The CT-2020 has a field of view that is large enough (8 degrees, [20]) to negate the need to include a sun-tracker.

5.6.2 Disturbances

The primary function of the ADCS is to maintain the spacecraft's orientation. There are several space phenomena that are capable of imparting a moment on the spacecraft. The two most prominent ones are solar pressure and gravity gradient. Calculations were completed to determine the total angular momentum that these perturbations can impart on the R-O during both its Jupiter transfer and the Jovial orbiting period of the mission.

The magnitude of disturbance effects are highly dependent on the orientation of the spacecraft. Currently, a detailed plan does not exist for the orientation of the orbiter during its mission. There are some details available (for example, the solar panels must be facing the Sun), but these are not accurate enough for precise calculations. As a result, all calculations done for the disturbances are of a worst-case scenario. That is to say, for each calculation, whenever a variable is unknown due to lack of a detailed mission plan, that variable is set to the value that would maximize the external torque acting upon the R-O. This allows for an upper bound to be created for the sizing of the ADCS system.

5.6.2.1 Solar Pressure

The sun emits light in the form of photons, which transfer a very small amount of momentum onto any object that they strike. This force is characterized Equations 5.6.2.1.1 - 5.6.2.1.4.

$$F_{abs} = P_s * A * (1 - q) * cos(\alpha) \quad \text{...(5.6.2.1.1)}$$

$$F_{ref} = 2 * P_s * A * q * cos(\alpha) \quad \text{...(5.6.2.1.2)}$$

$$F_{total\ solar} = F_{ref} + F_{abs} \quad \text{...(5.6.2.1.3)}$$

$$T_{solar} = \sum F_{total\ solar} * D \quad \text{...(5.6.2.1.4)}$$

Where F_{abs} is the force of the absorbed sunlight, P_s is the local solar pressure, A is the cross sectional area exposed to the solar pressure, q is the reflectivity of the material (nominally

0.5, [14]), α is the angle the face is from the incoming sunlight, and F_{ref} is the force of the reflected solar pressure. T_{solar} is the total torque imparted on the system from solar pressure, and D is the distance each surface is from the spacecraft's center of mass. The local solar pressure, P_s, can be approximated using by r, the distance from the sun. This can be seen in equation 5.6.1.2.5 [17].

$$P_s = \frac{1.03^{11}}{r^2} \quad \ldots(5.6.1.2.5)$$

This results in solar pressure decreasing exponentially as a function of distance. Using Equations 5.6.2.1.1- 5.6.2.1.5, the torque from the solar pressure is calculated for the duration of the transfer orbit (Figure 5.6.2.1.1).

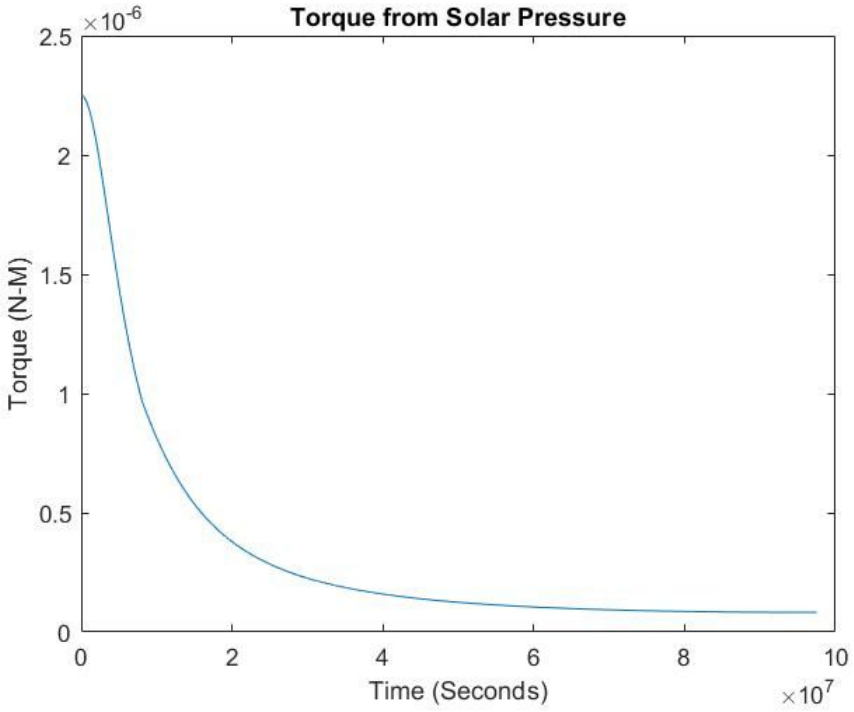

Figure 5.6.2.1.1: Torque from Solar Pressure

Figure 5.6.2.1.1 is numerically integrated to determine that the total angular momentum that will be imparted onto the R-O by solar pressure is 31.228 Newton meter seconds (N-m-s). This is also calculated for the Jupiter-orbiting phase of the mission, and it was found that approximately $5.34 * 10^{-4}$ N-m-s of angular momentum is exerted by solar pressure per orbit.

5.6.2.2 Gravity Gradient

The gravitational field around attracting bodies varies as a function of distance. This non-uniformity can create a torque on bodies in the field, which is characterized in Equation 5.6.2.2.1 [18].

$$T_{grav} = \frac{3*mu}{2*r^2} * I_3 - I_2 * sin(\theta) \quad \ldots(5.6.2.2.1)$$

Here, T_{grav} is the resultant torque, r is the distance from the attracting body, and mu standard gravitational parameter. I_3 and I_2 are the R-O's moments of inertia, and θ is the angle between the gravity vector and the alignments of the spacecraft if there is a zero gravity gradient. For these calculations, the moments of inertia and θ are chosen to maximize the gravity gradient. It is assumed that the gravity gradient of each planet would only be sufficiently large within its sphere of influence.

The torque on the spacecraft as a result from the gravity gradient of solar bodies is calculated for both the transfer orbit and the Jupiter-orbiting phase of the R-O's mission. During the transfer phase of the mission, the spacecraft experiences gravity from four sources; Earth as the R-O leaves low earth orbit, Mars as the R-O performs a gravity assist, Jupiter as the R-O approaches the planet before capture, and the Sun for the duration of the transfer. The effects of each of these planets are calculated using Equation 5.6.2.2.1. The resulting torques can be seen in Figure 5.6.2.1.1.

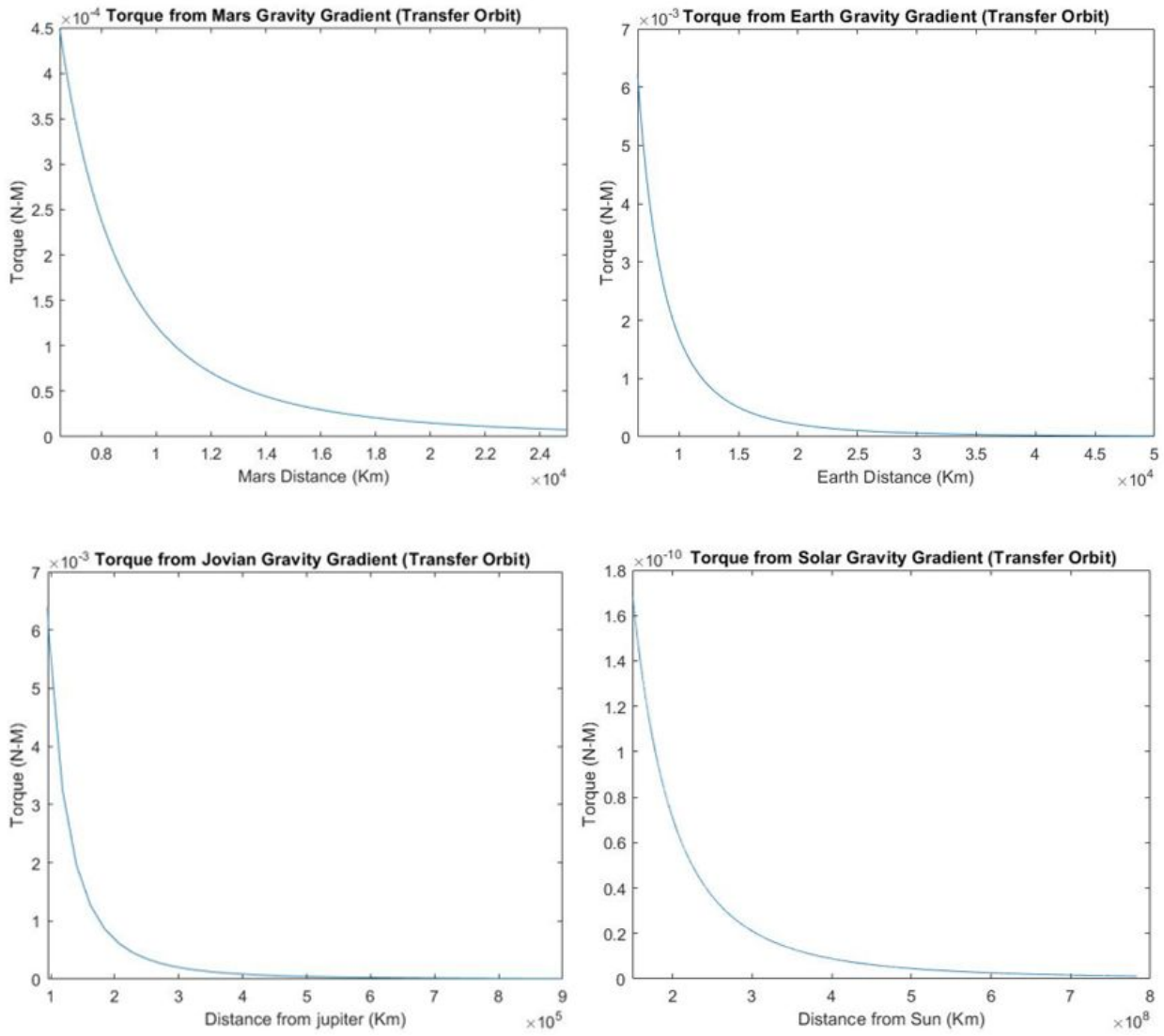

Figure 5.6.2.1.1: Torque from Gravity-Gradient

These torques are integrated with respect to time in order to determine that the total angular momentum imparted on the spacecraft from the gravity gradients of each body is 14.95 N-m-s. This is repeated for the Jupiter-orbiting phase of the mission (Figure 5.6.2.1.2), and it is determined that the gravity gradient of Jupiter will impart 1.0012 N-M-S of angular momentum on the R-O per orbit.

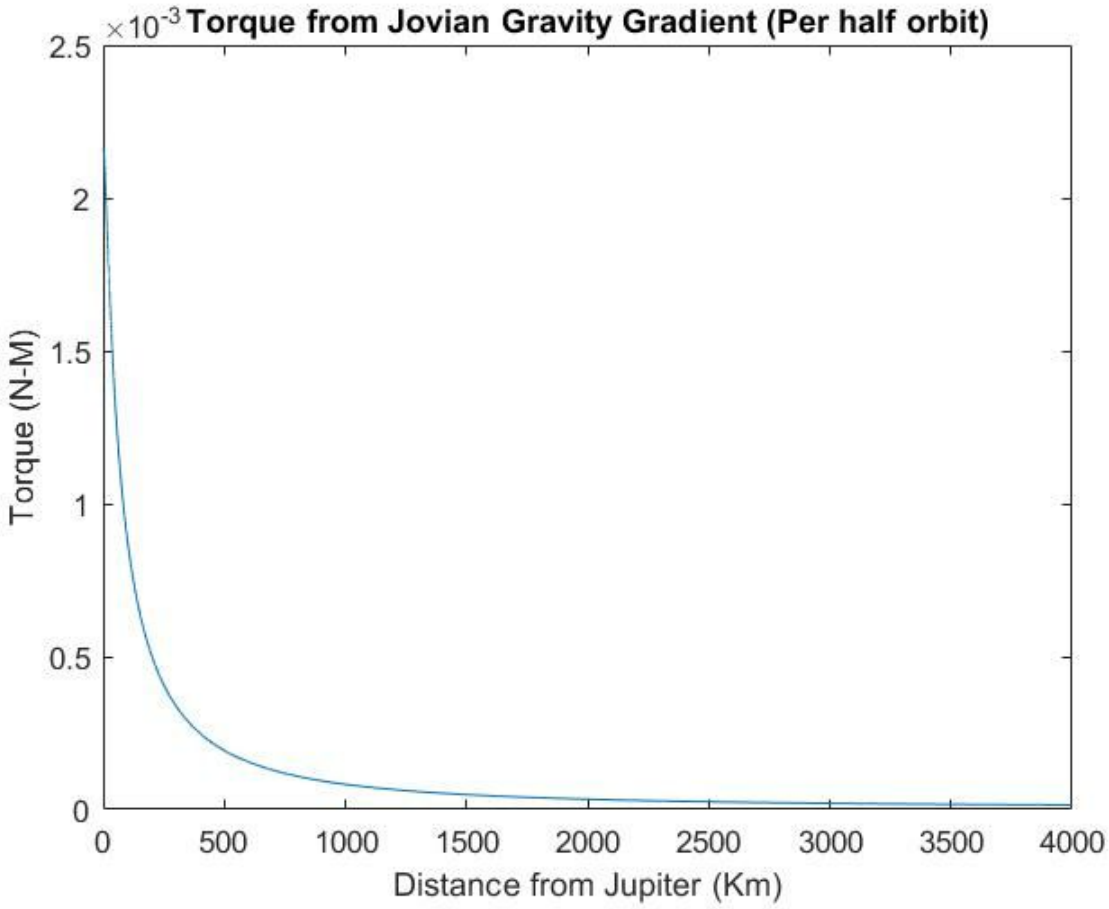

Figure 5.6.2.1.2: Torque from Jupiter Gravity-Gradient per Half Orbit

5.6.2.3 Total Disturbance Angular Momentum

The the total angular momentum during the transfer orbit is 46.172N-M-S. During the Jupiter-orbiting phase of the mission, 1.00173 N-m-s of angular momentum will be imparted on the R-O per orbit. A more detailed breakdown of these can be seen in table 5.6.2.3.1.

Table 5.6.2.3.1: Disturbance Effects

Disturbance Effects		
Parameter	**Transfer orbit magnitude (N-m-s)**	**Jupiter-Orbiting phase magnitude (N-m-s)**
Gravity-Gradient	14.95	1.0017
Solar Pressure	31.228	0.00053
Total	46.172	1.00173

5.6.3 De-saturation of Reaction Wheels

During both the transfer orbit and the Jupiter-orbiting phase of the mission, it is necessary to desaturase the reaction wheels. Deasturating the reaction wheels is necessary for two reasons: First, in order to regain control authority from the wheels if they have accelerated to their maximum speed. Secondly to keep the flywheel speed low to prevent bearing friction from imparting another torque that must be countered by further accelerating the wheels.

In order to counter the torque from a solar disturbance, the reaction wheels will spin up to impart an opposing torque, and thus maintain the spacecraft's desired orientation. The reaction wheels will continuously accelerate to combat the input torques. As the wheels' spin, the friction associated with their bearings creates a torque opposite to the wheel motion. Thus, the reaction wheels must accelerate further in order to maintain orientation. This continues, and eventually the reaction wheels reach their maximum speed without changing the orientation of the spacecraft. Eventually the reaction wheel speed cannot be increased further, and must be desaturated to reset the system [16].

5.6.3.1 Transfer Orbit Phase

During the Transfer orbit, desaturating the reaction wheels must be done with propellant, as during interplanetary transit there are no outside phenomena strong enough provide a control moment. The amount of propellant required for de-saturating the reaction wheels during the transfer phase can be found using Equations 5.6.3.1 - 5.6.3.4 [18].

$$F_{thruster} = I_{sp} * m_{dot} * g_0 \quad ...(5.6.3.1)$$

$$T_{motor} = F_{thruster} * L_{boom} \quad ...(5.6.3.2)$$

$$Time_{burn} = \frac{L_{total}}{T_{motor}} \quad ...(5.6.3.3)$$

$$Mass_{propellant} = Time_{burn} * m_{dot} \quad ...(5.6.3.4)$$

Where $F_{thruster}$ is the force of single ADCS thruster, T_{sp} is 225 [15], g_o is 9.81, L_{arm} is 2.3 meters. These equations result in a total propellant mass to desaturate the reaction wheels during the transfer orbit of 8.707 Kg of fuel.

5.6.3.2 Jupiter-Orbiting Phase

During the Jupiter-orbiting phase of the mission, it will be possible to use Jupiter's magnetic field to desaturate the reaction wheels. This is advantageous, as reducing the propellant requirements of the system can extend mission life. This is done via the use of a magnetorquer, also known as a magnetic torque tube. A magnetorquer is a coil of wire wrapped around a tube. If the magnetorquer is in a magnetic field when a current is applied to the coil, it produces a torque as described in Equation 5.6.3.2.1 [18].

$$T_{mag} = (N * I * A)\,\hat{i} \times B_{local}\,\hat{n} \quad ...(5.6.3.2.1)$$

Where T_{mag} is the magnetorquer torque, N is the number of turns in the coil, A is the cross sectional area of the coil I is the current, and B_{local} is the local magnetic field.

The local magnetic field strength of Jupiter can be approximated using Equation 5.6.3.2.2.[17]

$$B_{local} = \frac{B_0 * {r_0}^3}{{r_{local}}^3} * \sqrt{3 * sin(lat) + 1} \quad ...(5.6.3.2.2)$$

Where B_0 is the magnetic field strength at the 'surface' of Jupiter ($4.3 * 10^{-4}$ Teslas), R_0 is the radius of Jupiter, and lat is the local latitude. The strength of Jupiter's magnetic field as a function of distance can be seen below in Figure 5.6.3.2.1.

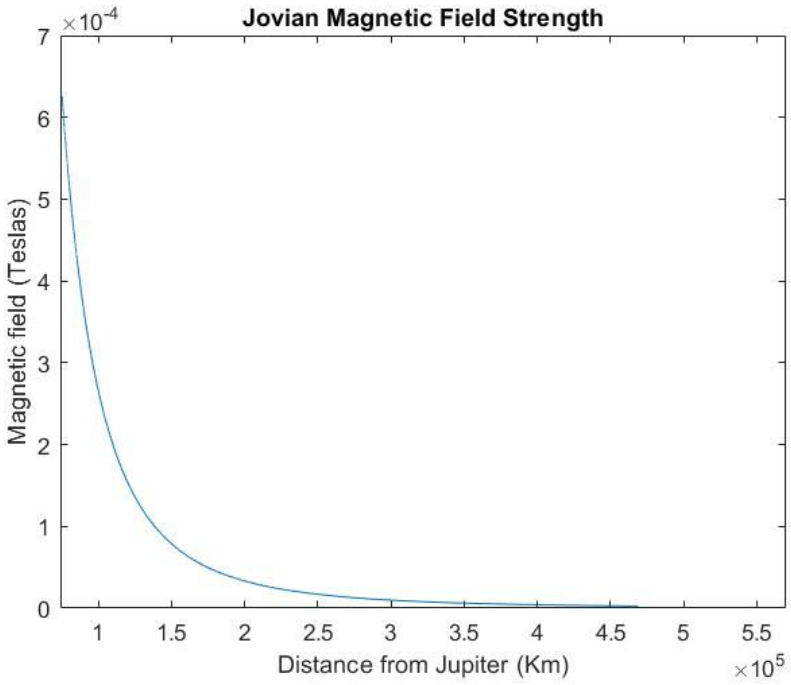

Figure 5.6.3.2.1: Jovian Magnetic Field Strength

Using this data, as well as the known total angular momentum imparted on the R-O per orbit, a magnetorquer was designed. The designed magnetorquer has radius of 7.25 cm, with 1000 turns, and is designed to use 1-A of current, built with a standard 0.1 mm copper wire. This coil weighs 128 g. Using this design, the torque available during each of the R-O's orbits is described in Figure 5.6.3.2.2.

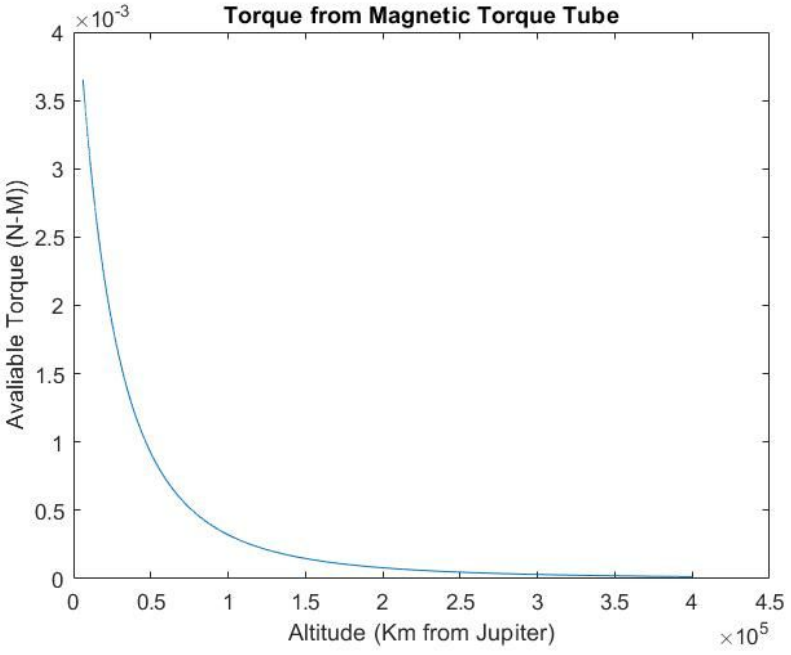

Figure 5.6.3.2.2: Magnetorquer Torque

By integrating the torque from the magnetic torque tube, it is found that the magnetorquer is able to impart 3.326 N-m-s of angular momentum per orbit. This is sufficient to completely negate the effects of Jupiter's gravity gradient, as well as the relatively minor solar pressure affects. The power required to do this is 36.37 Watt-Hours per orbit. By applying equations 5.6.3.1-5.6.3.4 to the Jupiter-orbit phase of the mission, it is found that these magnetorquers save 53.624 kilograms of propellant that would otherwise be used to desaturate the reaction wheels during the Jupiter orbits.

5.6.4 De-tumbling

If a sufficiently large disturbance is applied to a spacecraft, it can cause the craft to enter a 'tumble', where the spacecraft spins quickly and in multiple directions. A sample of the orientation of a spacecraft in an uncontrolled tumble can be seen in Figure 5.6.3.2.2.

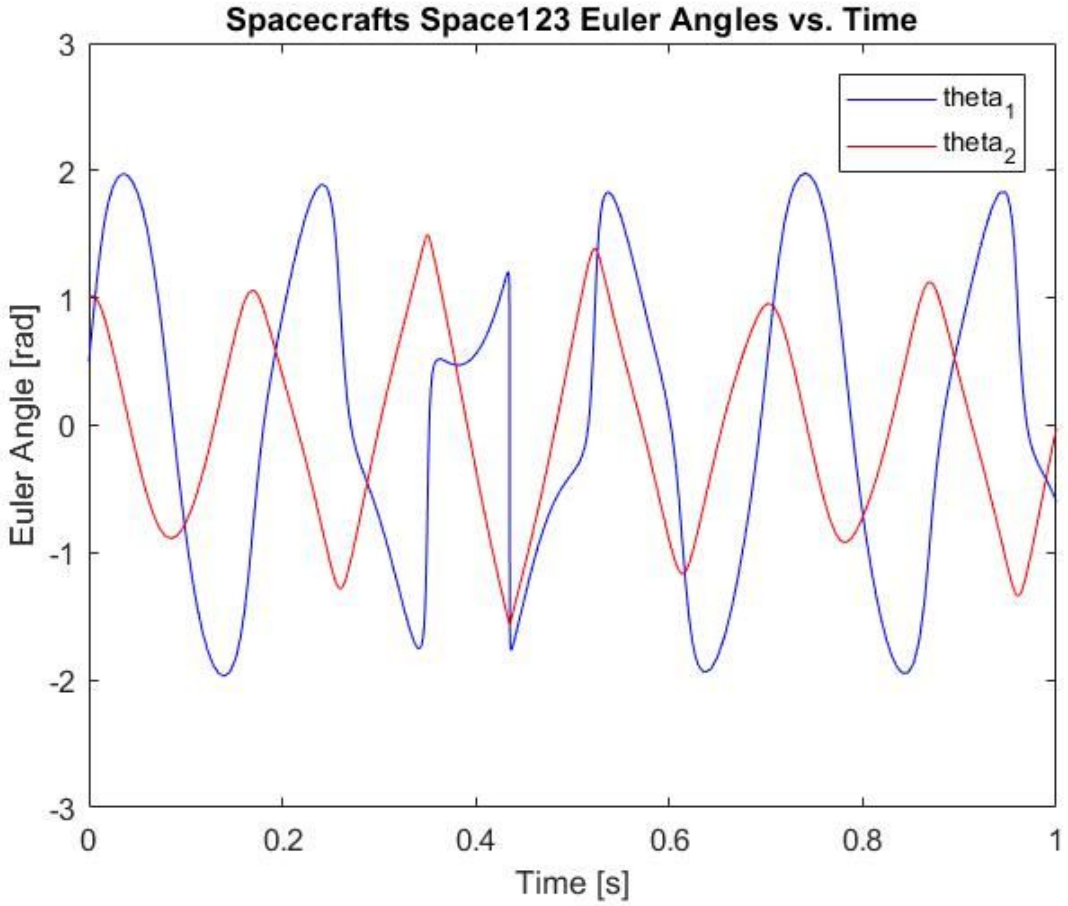

Figure 5.6.3.2.2: Tumble Angles

A tumble can be initiated by a collision, malfunction, or any other event capable of applying a large moment to the craft. When tumbling, a spacecraft likely will not be able to communicate with Earth, take scientific measurements, adjust course, or properly regulate temperature. If a tumble is severe enough, the rapid changes in angular momentum can cause damage to the spacecraft. As a result, if a tumble occurs, it is imperative that the ADCS detumbles the spacecraft quickly.

In order to control the spacecraft in the event of a tumble, a sliding linearization kalman filter (or Linear Quadratic Regulator) was developed. A nonlinear model of a tumbling spacecraft was developed, which is then linearized at each state. This nonlinear model uses Euler angles and direction cosine matrices. The Kalman filter then uses the linearized model to develop an optimal control gain for the current craft state. This control gain is then applied to the current states to create a control moment. This moment is then checked to ensure that it is within the capabilities of the control system, and is then applied to the model. The HG1936 IMU is capable of reading data at 600 Hz [19], thus the controller is subject to this delay. Then each state is updated, and the process repeated.The overall control system diagram can be seen in Figure 5.6.3.2.4. For a complete control system diagram (including each subsystems diagram), as well as control code, see Section 10.2.12 of the Appendix.

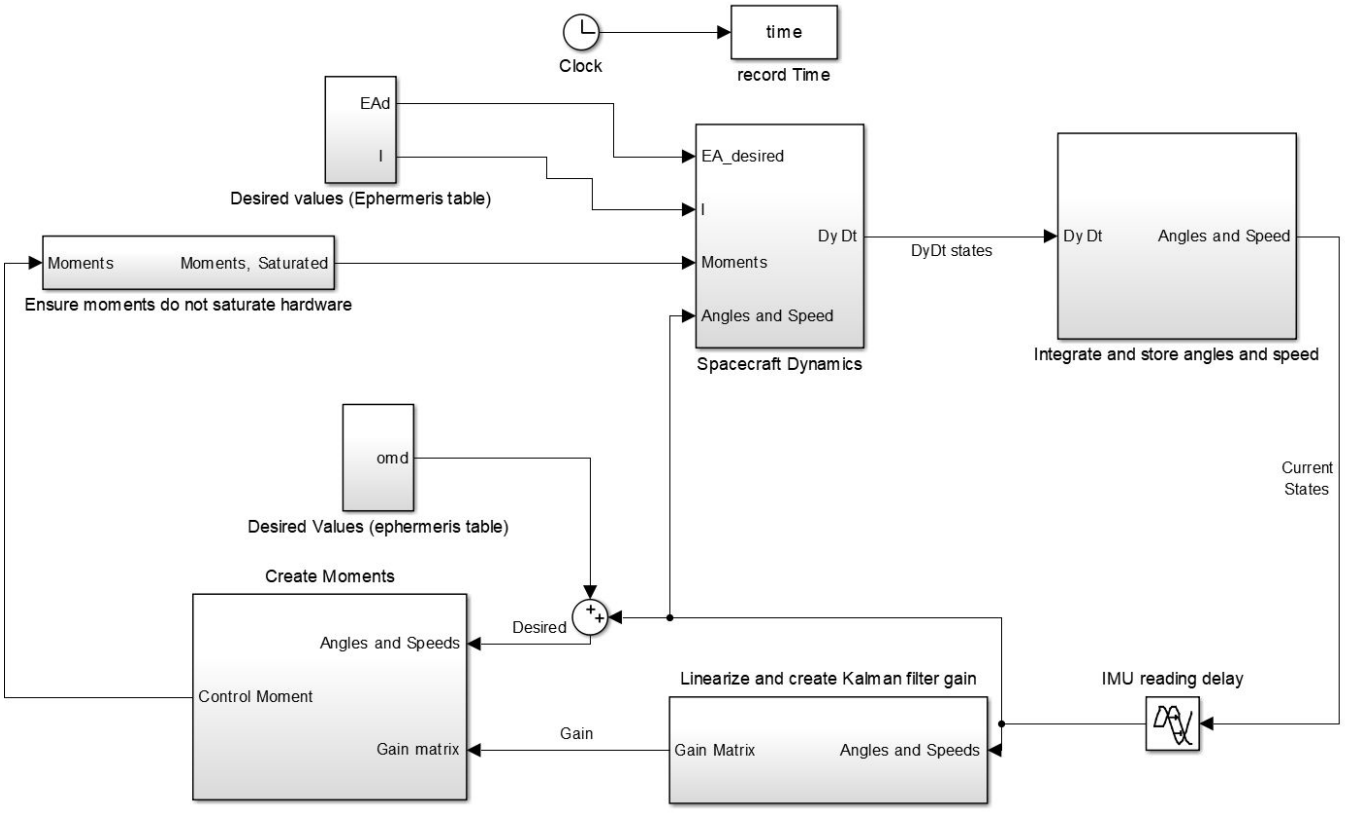

Figure 5.6.3.2.4: Control System Diagram

In order to verify that the control system works effectively, it was simulated with a range of initial conditions. An example of the response to these input conditions can be seen in Figure 5.6.3.2.4.

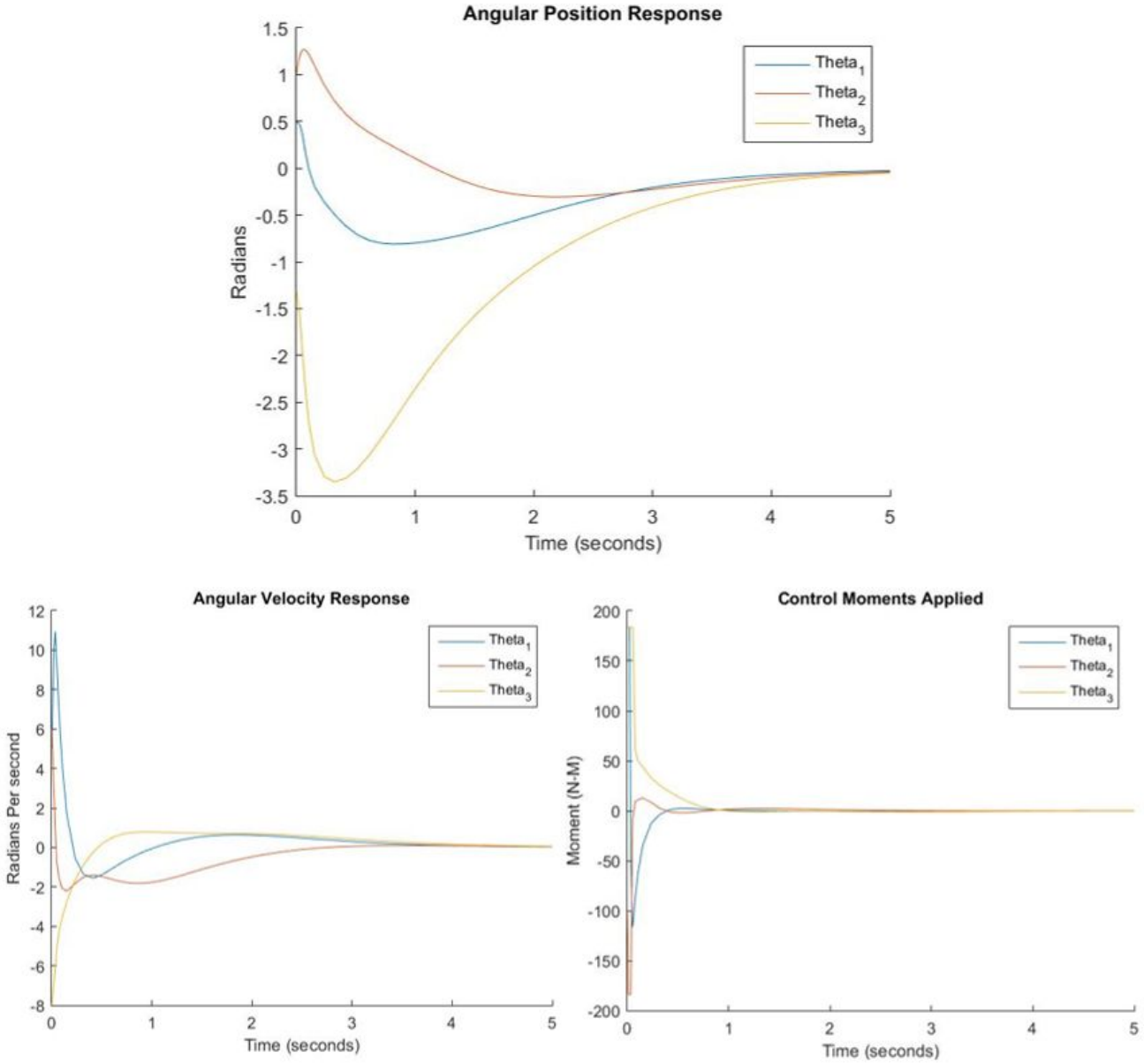

Initial angular velocity: $\omega_1 = 5\ \frac{Radians}{sec}$, $\omega_2 = 6\ \frac{Radians}{sec}$, $\omega = -6\ \frac{radians}{sec}$

Initial angular position: $\theta_1 = 0.5\ Radian$, $\theta_2 = 1\ Radian$, $\theta_3 = -1.33\ Radian$

Figure 5.6.3.2.4: Control Algorithm Response to a Tumble

This control system is capable of correcting a tumbling R-O with angular velocities of up to 45 radians per second, and can stabilize (reduce angular velocity to less than 0.1 radians per second) any tumble less than 15 radians per second in under 5 seconds.

5.6.5 Risk and Risk Mitigation

The ADCS is a critical system in any spacecraft. Any significant loss of attitude control could result in the loss of the mission or mission effectiveness. As a result, redundancies are included in each component. The Honeywell 4820 reaction wheels include a fourth wheel, so if any of the three main flywheels malfunctions, the system can maintain control authority in all three axis. Sixteen thrusters are included instead of the nominal twelve, so if any one thruster fails, there is still thruster control authority in any direction. The three star trackers provide both the ability to take accurate orientation measurements in any position, but also adds redundancy to the system, as if any one star tracker fails, either of the other two can still be used. An the HG1930 IMU is included, serves as a backup to the HG9900 IMU.

Although the ADCS system as a whole acts as a single point of failure to the mission, each subsystem includes redundancies to make the ADCS system more robust. The failure of the ADCS would result in the loss of the mission, however the multiple layers of redundant components make the probability of this low. This allows the ADCS system to be classified as a 1E risk (see Appendix 10.1).

5.6.6 Future Work

It is possible to counter the effects of solar pressure on the spacecraft orientation by flipping the spacecraft 180 degrees in order to invert the solar moment exerted on the craft. This has been performed successfully on past missions, such as on TDRSS [17]. Once a detailed mission profile has been developed for the Semele mission, future work can include exploring this possibility as a means to reduce the effect of solar pressure, or to desaturate the reaction wheels. Additionally, a detailed mission profile will enable future work to include more precise calculations of disturbance torques.

The current control algorithm assumes that the onboard computer can compute a control moment instantly. Additionally, it assumes that the reaction wheels and thrusters can apply control moments without delay. This is not representative of a realistic system. The delay associated with the calculation and application of the control moments causes a significant decrease in ADCS performance during a tumble. Modern systems combat this via the use of a model-based predictive control system. This system uses a multibody dynamic model of the spacecraft in order to predict the movement of the spacecraft, and apply the control moment at

the correct time. Future work for this mission will include the development of such a system for the R-O.

The nonlinear model of the R-O's angular movement currently uses Euler angles and direction cosine matrices. This is a suboptimal three-axis attitude representations, as Euler angles have the possibility of encountering singularities, as well as requiring trigonometric functions to be computed. Future work for this mission will switch this nonlinear model to quaternions, which do not use trigonometric functions, and will not encounter singularities.

5.7 Orbital Mechanics

The Orbital Mechanics subsystem is responsible for determining the path the spacecraft follows to Jupiter and its final orbit. As discussed in the preliminary design report, the selected trajectory involves a gravity assist off Mars along with a gravity braking maneuver off of Ganymede to slow down for capture. The R-O orbiter's final Jovian orbit is a highly eccentric orbit with minimal time in eclipse to facilitate maximum power generation and very large communication window with the minos probe on Europa. Optimization algorithms are used with the method of patched conics to produce an estimation of the transfer trajectory used for this mission. The results presented in this section are predicated on the assumption that all celestial bodies are in the equatorial plane and have perfectly circular orbits.

5.7.1 Transfer Trajectory

The transfer trajectory to Jupiter involves a single gravity assist off of Mars. By flying past Mars, the spacecraft receives a momentum boost which puts it into a higher energy orbit that is capable of reaching the mission target. For this analysis, the method of patched conics is used to simplify the dynamics of the system. This method assumes that the spacecraft only feels the effects of one body's gravity at any given time. In order to minimize the propellant requirements, the patched conics analysis is run through Matlab's optimization algorithm, fmincon.

The trajectory of the spacecraft to Jupiter has two parameters which can be selected by the design team; the initial heliocentric trajectory and how close the spacecraft gets to Mars during its flyby. These parameters are optimized such that the mission requires as little propellant as possible. The associated script is reproduced in Appendix 10.2.1.

Several constraints are placed on this optimization problem to ensure the success of the mission. These constraints are a combination of linear constraints and non-linear constraints, which need to be passed to fmincon differently. The linear constraints are given in the form of Equation 5.7.1.1. Fmincon is given the A matrix and b vector as two arguments for the function.

$$Ax \geq b \quad ...(5.7.1.1)$$

The linear constraints on the initial orbit require that the orbit must have an apoapsis equal to or greater than Mars's orbit radius to ensure that it meets with mars, and the apoapsis must be less than Jupiter's orbital radius, otherwise there would be no benefit to using a gravity assist[20]. Additionally the periapsis of the Martian flyby are subject to 2 constrains. The orbiter must pass within Mars's sphere of influence to ensure that Mars's gravity affects the trajectory, and the minimum distance from Mars be large enough to ensure that the spacecraft does not slow down due to atmospheric drag from Mars's atmosphere. For this analysis it is assumed that a 200 km altitude is high enough that the spacecraft would experience negligible air resistance. This altitude is selected because it is where the atmospheric density on Mars is equivalent to the atmospheric density on earth at 300km as shown in Figure 5.7.1.1. A 300km earth orbit is generally considered high enough to not experience any aerodynamic drag [22].

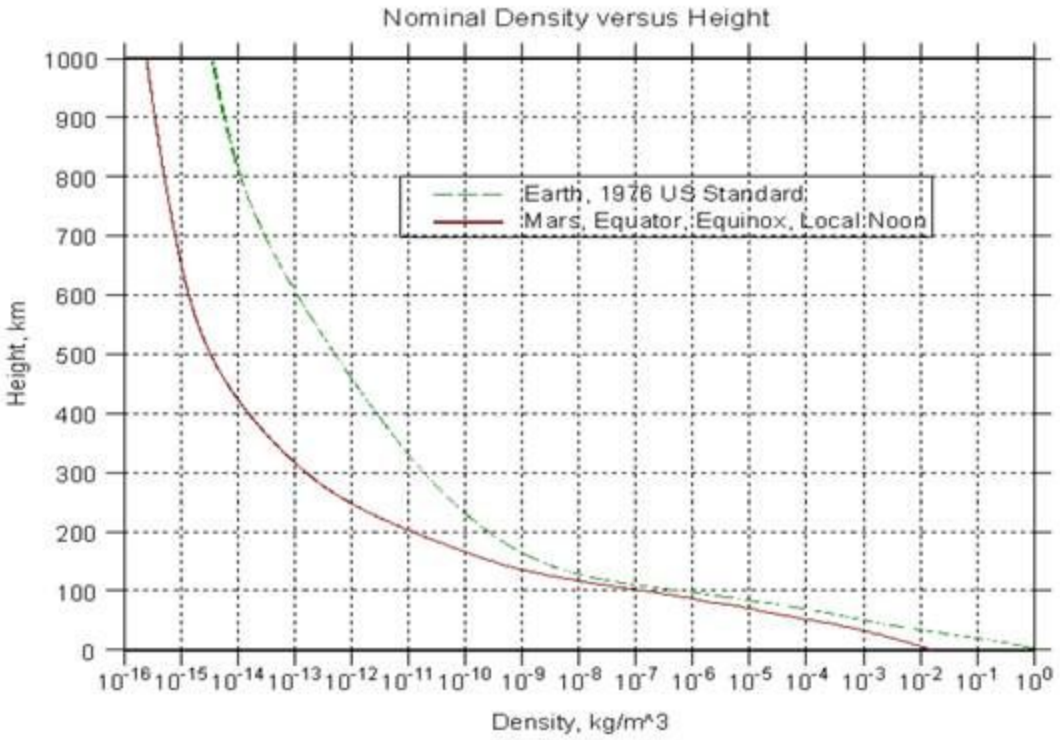

Figure 5.7.1.1: Comparison of the Atmospheric Density of Earth and Mars [22]

The only nonlinear constraint on the problem is that the spacecraft must reach Jupiter at its final apoapsis.This constraint is provided by a separate Matlab function which calculates the apoapsis of the final orbit and compares it to Jupiter's orbital radius. This function is provided in Appendix 10.2.2. In order to increase the accuracy of the calculations the final orbital distances are normalized by Jupiter's orbital radius as shown in Equation 5.7.1.2.

$$c = 1 - \frac{Rmax}{Rmin} \quad ...(5.7.1.2)$$

Fmincon ensures that for a trajectory to be considered as an optimal solution, the calculated c value must be less than or equal to zero, which implies the maximum distance the spacecraft reaches is equal to or greater than Jupiter's mean orbital radius. This optimization found the ideal trajectory has an initial apoapsis of 6.012 x 10^8 km and passes by mars with a minimum radius of 3783 km. The minimum delta-V required when escaping earth from a low earth orbit is 5.76 km/s. The transfer orbits and planet orbits are shown in Figure 5.7.1.2.

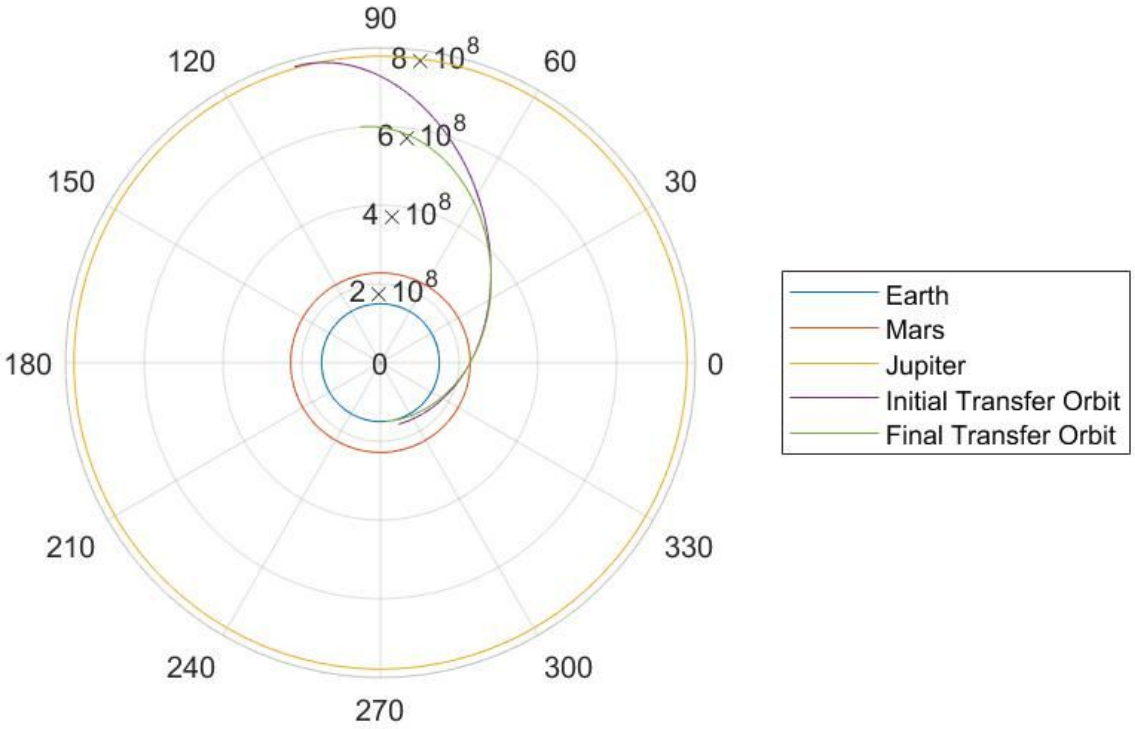

Figure 5.7.1.2: Semele Mission Transfer Trajectory

Upon reaching Mars, the spacecraft is deflected from the initial transfer orbit to the final orbit until it rendezvous with Jupiter. However this code assumes that the planets are all in the correct locations when the spacecraft leaves earth. In order to ensure the spacecraft reaches its destination, launch windows are calculated to determine when the spacecraft should leave earth to ensure it follows the correct trajectory and meets with Jupiter. Based on the initial heliocentric orbit the true anomaly of the spacecraft when meeting Mars is calculated using Equation 5.7.1.3.

$$\theta_m = acos\left(\frac{\frac{h^2}{\mu R_m}-1}{e}\right) ...(5.7.1.3)$$

Here θ_m is the spacecraft's true anomaly when its distance from the sun is equal to R_m, Mars's mean orbital radius. To ensure mars is in this location when the spacecraft reaches it, the angle Mars travels during the spacecraft's transit is calculated using Equation 5.7.1.4.

$$\Delta\theta = \omega t ...(5.7.1.4)$$

ω is Mars's angular velocity, which is assumed constant for a circular orbit. t is the amount of time the spacecraft takes to reach θ_m, which is calculated using Kepler's equations [23], given as Equations 5.7.1.5 - 5.7.1.7.

$$E = 2tan^{-1}(\sqrt{\frac{1-e}{1+e}}tan(\theta/2)) ...(5.7.1.5)$$

$$M = E - esin(E) ...(5.7.1.6)$$

$$t = \frac{MT}{2\pi} ...(5.7.1.7)$$

In these equations, E is the eccentric anomaly, e is the eccentricity of the orbit, and θ is the true anomaly. M is the mean anomaly and T is the period of the orbit. Travel time for a body between two specific angles is calculated several times throughout the astrodynamic analysis. To expedite these calculations, a Matlab function, 'TravelTime', is used for calculating times between specific locations in a given orbit. This function is included in Appendix 10.2.5. The resulting $\Delta\theta$ mandates that the spacecraft must leave earth at a time when Mars is 0.6325 radians ahead of earth. A similar analysis is performed to determine Jupiter's location. Here the entire travel time of the mission is considered, rather than just the time to reach Mars's orbit. Jupiter must lead Earth by 1.8399 radians when the mission begins.

5.7.2 Capture Orbit

After reaching Jupiter's orbit the spacecraft must be captured by Jupiter's gravity and enter a Jovian orbit. Based on the results from the transfer optimization the spacecraft has a hyperbolic excess velocity of 5.4838 Km/s upon meeting Jupiter. Two methods are used in conjunction to slow the spacecraft for capture. First a gravity brake is performed off ganymede to decrease the spacecraft's momentum without the use of fuel. Second, the propulsion system is

used to reduce the spacecraft's velocity relative to Jupiter enough for it to enter an elliptical Jovian orbit.

Similar to the gravity assist analysis for the transfer trajectory, an optimization is performed to determine the ideal conditions for the gravity brake. The design variables in this system are the minimum distance the spacecraft flies past Ganymede and the minimum distance the spacecraft flies past Jupiter. Unlike the transfer trajectory analysis, this optimization only contains linear constraints. The periapsis of the spacecraft's Jovian orbit must be greater than Jupiter's radius to prevent a collision with the planet and it must be less than Jupiter's sphere of influence to ensure the primary attractor for the problem is Jupiter, allowing the sun's gravity to be neglected. Similarly, the periapsis of the hyperbolic flyby trajectory must be greater than Ganymede's radius but within its sphere of influence [24].

The fitness function of the optimization is the eccentricity of the final Jovian orbit. The fitness function is the result of the analysis which fmincon tries to minimize. This analysis finds the minimum eccentricity rather than minimum delta V because the exact final orbit is not as important to the mission as becoming captured by jupiter. If the eccentricity after the brake could be less than 1 the spacecraft would be captured without any fuel burn, optimizing for a minimum delta V requires a fixed final orbit, which places an unnecessary constraint on the design space. The optimal eccentricity found was 1.0108. Therefore the spacecraft requires some delta V for capture. A delta V of 0.6604 Km/s places the spacecraft into an elliptical orbit. Figure 5.7.2.1 shows the pre and post ganymede flyby hyperbolic Jovian orbits as well as the final captured orbit and the orbits of moons considered during the mission.

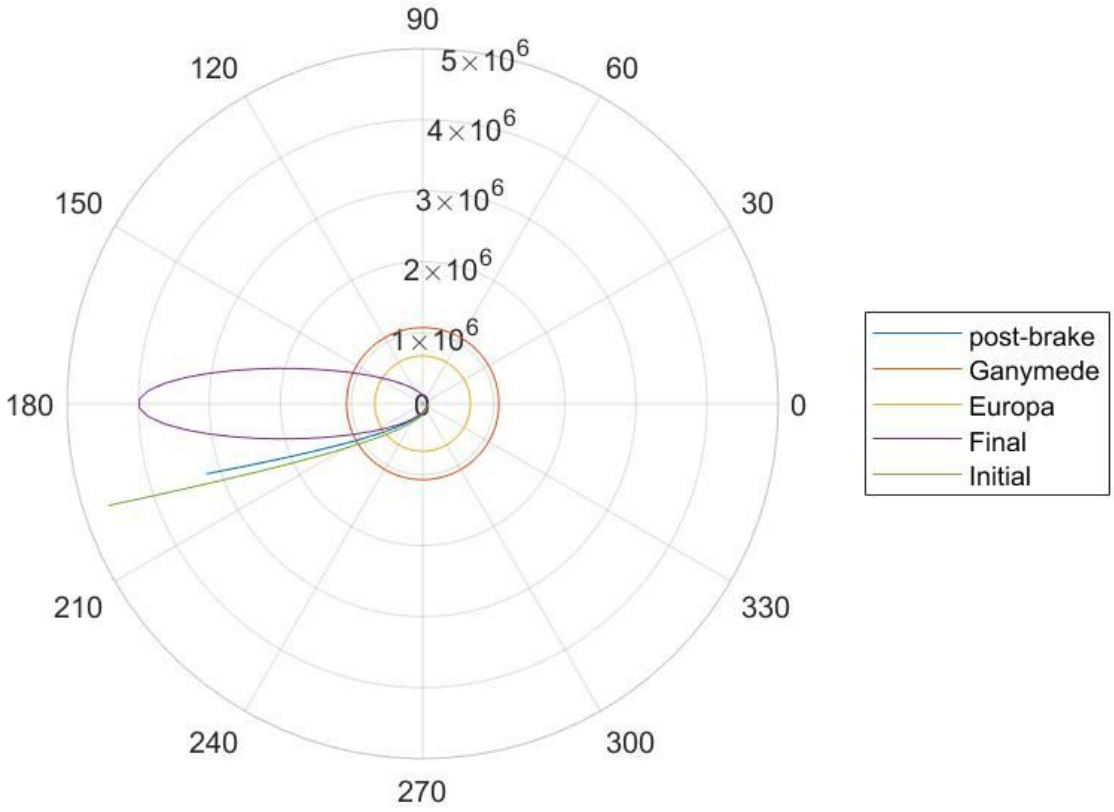

Figure 5.7.2.1: Spacecraft Capture Orbit and Incoming Trajectory

The final orbit of the spacecraft has an apoapsis of 4 x 10^6 Km and a periapsis of 6.1594 x 10^4 Km. The total orbital period is 18.6980 Earth days. The probe will be deposited on Europa upon the first pass of its orbit. The relatively long orbital period allows the orbiter to maintain communication with the probe as the moon passes beneath it. Based on Europa's orbital speed the M-P will be able to communicate with the R-O for 2 days followed by a black out of 1.5 days. The strength of the telecoms as discussed in Section 5.4 means that even at the maximum distance of 4 x 10^6 Km the two systems will be able to communicate.

An added benefit of the highly eccentric capture orbit is that the spacecraft spends very little time in eclipse. This reduces the size of batteries required to maintain power when the solar panels are in shade. For this analysis it is assumed that the spacecrafts apoapsis is aligned with the direction of the sun. The time spent in eclipse is determined using the TravelTime function based on the approximate time in the shade produced in Section 5.3. The analysis determined that the spacecraft is only in eclipse for 30 minutes.

5.7.3 3-Body Problem

After using the method of patched conics to find a relatively accurate trajectory for the mission, a three body analysis is performed. This analysis continues to assume the celestial bodies are in the equatorial plane and have perfectly circular orbits. However, it creates a significantly more accurate depiction of the forces on the spacecraft based on the gravity from both the sun and Mars.

The equation of motion for the spacecraft in this 3 body system is a second order time dependent ordinary differential equation shown in Equation 5.7.3.1. Additionally, the vector from Mars to the spacecraft, denoted as $\widehat{R}_{m\to s/c}$, must be expressed with another time dependant equation because mars is moving relative to the sun. This relation is given in Equation 5.7.3.2.

$$\widehat{a} = \frac{-\mu_{sun}\widehat{R}}{R^3} - \frac{\mu_{mars}\widehat{R}_{m\to s/c}}{R_{m\to s/c}^3} \quad ...(5.7.3.1)$$

$$\widehat{R}_{m\to s/c} = [R_m cos(\omega t),\ R_m sin(\omega t)] \quad ...(5.7.3.2)$$

These equations define the motion of the spacecraft through its transfer orbit to Jupiter, however unlike the method of patched conics there is no analytic solution to these equations. Therefore they are solved using Matlab's numerical integrator ODE 45. While this does allow the system to be solved numerically, it introduces new inaccuracies.

ODE 45 limits the minimum step size to 3.72529 x 10^{-9} [25]. Running the simulation for extended periods of time forces the step size of the solver to decrease below this value in order to meet integration tolerances. Because the gravity assist trajectory is so sensitive to slight changes in the location of the spacecraft, often a very small step size is required to accurately show the trajectory of the spacecraft. In this case running the simulation for a long enough time to reach Jupiter results in a minimum step size of several kilometers. As a result the spacecraft cannot be aimed at mars accurately enough to be placed in the correct final orbit.

One way to improve this loss of accuracy is to break the transfer trajectory up into multiple trajectories for much shorter time periods. Instead of using ODE 45 once to model the entire mission, the function is used multiple times to model shorter durations of time. The first run of ODE 45 starts with the spacecraft leaving Earth with the optimal velocity calculated using the method of patched conics. This is propagated for a period of time and then its final time step values for the spacecraft's position and velocity are set as the initial conditions for a subsequent run of ODE 45. This process is continued until the full duration of the mission is modeled.

While this does increase accuracy it also greatly increase the computational cost of the model and even with this accuracy increase the model will run into accuracy problems. The step size of the model cannot be made arbitrarily small for increased accuracy, as Matlab only stores numbers to double precision accuracy. While this is generally more than enough significant figures for most applications, the extremely precise requirements of a gravity assisted trajectory

often requires more accuracy. When the velocity of the spacecraft is rounded to double precision accuracy it has very little effect on its location within a short time. However because the system is being modeled for years. An alteration in velocity of a few meters per second can result in a change in final location of several kilometers. This perturbation is then magnified by the flyby of another planet.

Due to time limitations, a proper 3-Body flyby was not achieved. Figure 5.7.3.1 shows the spacecraft trajectory using the 3-Body analysis. The spacecraft does not intersect mars and as a result its trajectory is unaltered, resulting in the spacecraft reaching an apoapsis well below the mission requirements.

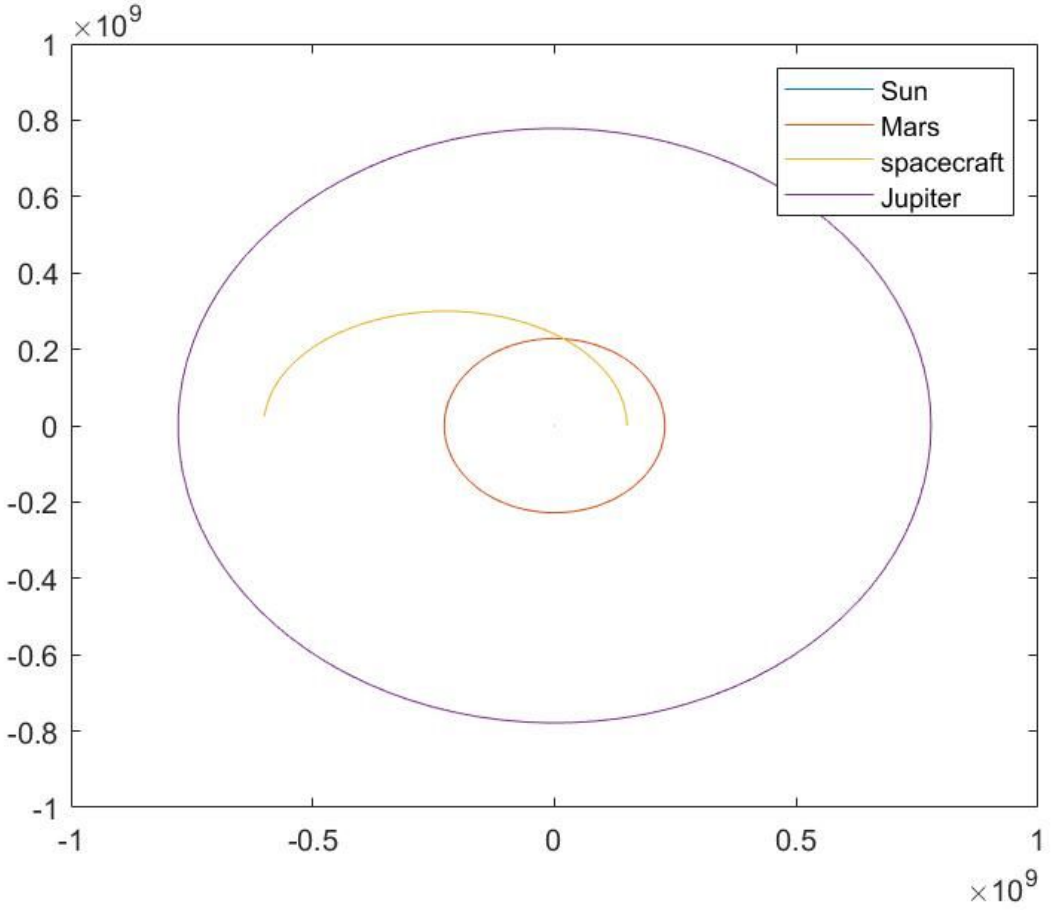

Figure 5.7.3.1: Initial Transfer Orbit Based on 3-Body Analysis

5.7.4 Risk and Risk Mitigation

The major risks associated with the orbital mechanics section include loss of mission, increased fuel costs, less power availability due to increased time shaded by Jupiter or other bodies blocking the sun, and extended mission time. Increased fuel costs are associated with a

mission trajectory which needs a large number of corrective burns, and errors entering the planned Jovian orbit will result in less time facing the sun and therefore less power available for all subsystems, these risks fall into the category 3B from Appendix Figure 10.1.1. More robust analysis as discussed in Section 5.7.5 will reduce the risks to category 3D.

The largest risk is loss of mission. If the trajectory analysis is not performed correctly, the spacecraft may not reach Jupiter and become lost in the solar system. Based on current models this risk falls into category 1B. However, this risk can be reduced to 1E through more robust modeling methods. This includes, the method of patched comics, 3-body analysis, and STK. As the design process progresses the model accuracy increases. Additionally, the propulsion system will be capable of restarting the engine to make small changes in velocity during the three year trajectory to Jupiter, as well as, while performing planetary and lunar flybys. This will ensure that small perturbations to the orbit can be correct before the spacecraft path diverges too heavily from the mission trajectory.

5.7.5 Future Work

Further analysis needs to be performed to complete the 3-body analysis. Due to the difficulties in precisely meeting Mars for a gravity assist future analysis will be performed using STK's astrogator software. This still produces challenges in accurately aiming the spacecrafts initial trajectory, however, STK's astrogator has a targeting sequence object which alters specific system inputs until a specified stopping condition is reached. This automates the need for different aiming conditions needed for the Matlab 3-body script. For this analysis, the target sequence alters the launch time until reaching the stopping condition of the spacecraft reaching Jupiter. Additionally astrogator has the benefit of not assuming the planets lie in the equatorial plane or that they have perfectly circular orbits [26].

Unfortunately, STK still has a minimum step size when determining the trajectory of the spacecraft and the initial launch conditions. Similar to the Matlab 3-body analysis this may result in the proper launch conditions lying between individual steps of the propagator and as a result the stopping condition may not be reached. Additional analysis for gravity assist trajectories must be performed with custom high fidelity integrators running on supercomputers to minimize the inaccuracies to a reliable level. Unfortunately, this is beyond the capabilities of the orbital mechanics team at this time.

As a proof of concept STK was used to determine the proper delta V required for a hohmann transfer to Jupiter. For this analysis the stopping condition is an apoapsis equal to Jupiter's orbital radius. The targeting sequence incrementally increases the delta V at Earth until this value is reached. The results are shown in Figure 5.7.5.1.

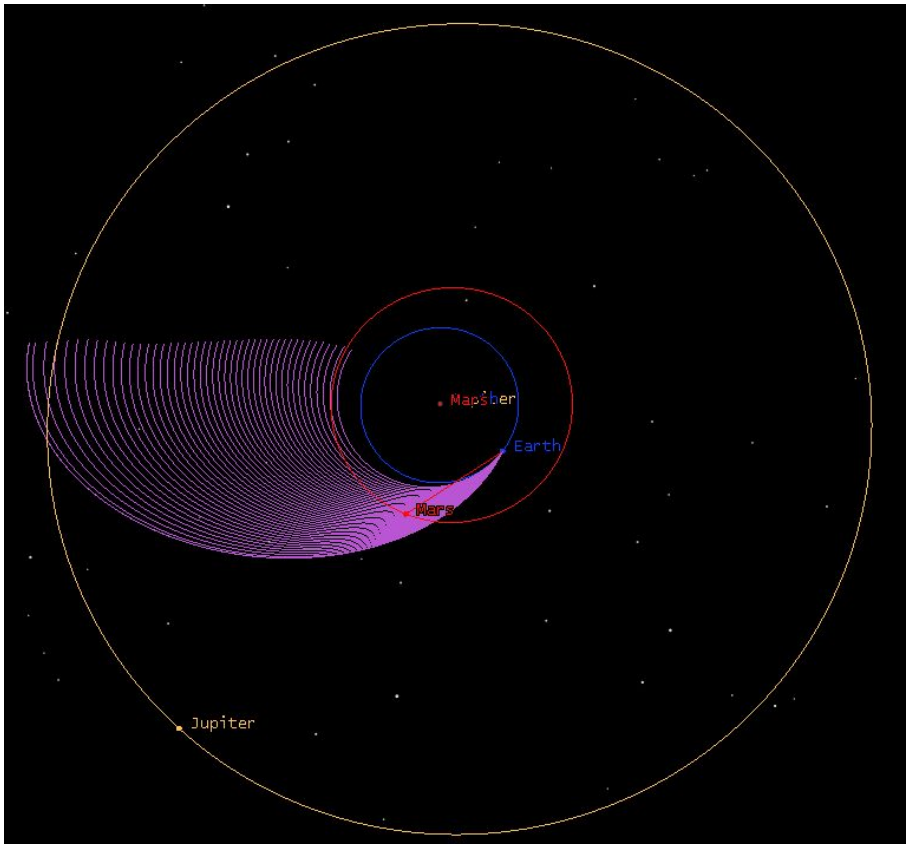

Figure 5.7.5.1: STK Targeting Sequence for Direct Flight to Jupiter

This image shows all trajectories astrogator checked when determining the delta V required to meet Jupiter. It shows that while a very large number of iterations are tested, the distances between trajectories is still several kilometers in size. Due to the highly sensitive nature of gravity assisted trajectories it is very likely that the ideal trajectory lies between 2 iterations, when the proper analysis is performed. Overall, while STK is far more accurate when working with the governing differential equations of orbital mechanics problems, it is still not a perfectly accurate method.

5.8 Propulsion Systems

Following the changes made to complete the final trajectory of the R-O, the delta-V requirements of this mission have increased to an impulsive burn of 0.6604 km/s, and no longer follow the original estimates of approximately 50 low magnitude longer burns of 0.02 km/s throughout the trajectory from Earth to Jupiter. For this reason, the original potential choice of pulsed plasma thruster was changed to a dual-mode propulsion system which is capable of performing the required delta-V maneuver in a reasonable time. The dual-mode propulsion system was chosen over a monopropellant system that acted as a second option in place of the pulsed plasma thruster in the PDR, due to its overall higher specific impulse for a smaller total system mass. A short analysis is provided below, highlighting these changes.

5.8.1 Monopropellant vs Dual-Mode System

The dual-mode system examined for this mission was the Aerojet R-4D-15 HiPAT Dual Mode High Performance Rocket Engine, accommodating a fuel of hydrazine and an oxidizer of dinitrogen tetroxide (MON-3). Six different monopropellant Aerojet Rocketdyne engines currently in production were compared to the Aerojet R-4D-15 HiPAT Dual Mode High Performance Rocket Engine, compared in terms of mass, and specific impulse. The masses of the monopropellant engines ranged from 1- 6.4 kgs with specific impulses that ranged from 223 - 237 s, the dual mode engine has a mass of just 5.44 kgs, with a specific impulse of 329. This much higher specific impulse greatly reduces the amount of propellant required onboard in order to complete the delta-V maneuver, without the main thruster itself adding a significant amount of extra mass, and so, was chosen as the propulsion system for this mission.

5.8.2 Dual-Mode System Specifications

The modified delta-V is a 0.6604 km/s burn for capture into Jupiter's orbit, which will be accomplished with the Aerojet R-4D-15 HiPAT Dual Mode High Performance Rocket Engine. The main technical specifications of this engine are outlined below in Table 5.8.2.1 For a more comprehensive list of technical specifications, see [27].

Table 5.8.2.1 Main Thruster Technical Specifications

Main Thruster Technical Specifications	
Specification	**Description**
Oxidizer	N_2O_4 (MON-3)
Fuel	N_2H_4
Nominal Thrust	445 N
Chamber Pressure	940 kPa
Inlet Pressure Range	1520 - 2140 kPa
Expansion Ratio	375:1
Mixture Ratio	1
Steady State Firing Duration	1800 s
Total Impulse	9.55 x 10^6 N-s

In order to meet the delta-V requirements, the Tsiolkovsky equation can be used to calculate the mass of fuel that would be required for this operation. This equation is given below as Equation 5.8.2.1 [28].

$$\Delta V = I_{sp} g_o ln \frac{m_o}{m_f} \quad \ldots (5.8.2.1)$$

Here, I_{sp} is the specific impulse of the engine used, g_o is the gravitational acceleration on the surface of the Earth, m_o is the total wet mass of the R-O, and m_f is the total dry mass of the R-O.

Given a total dry mass of 2814 kgs, the mass of propellant required is calculated to be 638.934 kgs. 25% more of this calculated mass to be held in reserves for any unforeseen emergency maneuvers, should the R-O be required to perform them. Taking into account the 69 kgs of hydrazine that are required for the sixteen MOOG Monarc thrusters, the total fuel system requirements are presented below in Table 5.8.2.2 [28] .

Table 5.8.2.2 Propellant Requirements

Propellant Requirements			
Propellant Use	**N_2H_4 (kg)**	**N_2O_4 (MON-3) kg**	**Total (kg)**
Usable propellant	468.33	399.33	867.66
Trapped propellant (~3%)	14.05	11.98	26.03
Outage (~1%)	4.68	3.99	8.67
Loading error (~0.5%)	2.34	1.10	4.33
Total loaded propellant	489.4	416.4	906.69

With the specific impulse and mass characteristics outlined in the section above, this engine is capable of completing the required delta-V maneuver with a total burn time of 4364.38 s. This value is calculated with Equation 5.8.2.2 below:

$$\Delta T = \frac{M_l I_{sp} g_o}{F}(1 - e^{\frac{-\Delta V}{Isp * g_o}}) \qquad \ldots(5.8.2.2)$$

Here, M_L is the total mass of the rocket at the time of the burn, F is the thrust provided by the main thruster, and ΔV is the total change in velocity required. Assuming an approximately full tank at the time of this maneuver, this total burn time requires 2.42 total steady state burns on this engine, or 3 initiations and 2 completions of a steady state burn.

Next, the weight of the helium required for the pressure regulation system was calculated. A pressure regulated system is required in this case to order to allow for easier control of inlet pressure to the engine, as well as in keeping the pressure constant in both tanks. For this, the volume of helium is initially estimated using Equation 5.8.2.3 below [28].

$$V = \frac{P_r V_u}{P_1 - P_2} \qquad \ldots (5.8.2.3)$$

Here, P_r is the regulated propellant tank pressure, V_u is the volume of usable propellant, P_1 is the initial pressurant sphere pressure, and P_2 is the final pressurant sphere pressure. Next, the initial mass of helium required is calculated from the Equation 5.8.2.4 of state given below:

$$w_s = \frac{P_1(V)}{2078.6(294.3)} \qquad \ldots(5.8.2.4)$$

Here, V is the volume of helium calculated using Equation 5.8.2.4. Finally, the total mass of helium is calculated through taking into account the amount of helium that is already loaded into the propellant tanks; this is given by the ullage volume of each propellant tank.

$$w_u = \frac{P_r(V_{ullage})}{2078.6(294.3)} \qquad \ldots (5.8.2.5)$$

The pressure of the propellant tank was taken to be the maximum expected operating pressure of the ArianeGroup Surface Tension Propellant Tank OST 25/0 [29] which is 1860 kPa. The initial pressurant sphere pressure is taken to be 27579.03 kPa [30] modelled after a comparable F_2/N_2H_4 bipropellant, pressure regulated system. The final helium sphere pressure is taken to be 7.5 times lower than it's initial pressure [28]. From here, the volume of helium pressurant required is calculated to be 0.0596 m^3. This yields the final mass of helium to be 2.758 kgs. The tank mass required to hold this amount of helium would then be 19.44 kgs, as a tank of 3.2 kgs contains 0.454 kgs of Helium [28].

The propellant tank used here is capable of holding the oxidizer, but is too small to accomodate the hydrazine. Because the next sized tank available for reference accommodates 700 litres of volume with a maximum operating pressure increase of only 1 bar (or 100 kPa), the mass of helium calculated here was approximated using the maximum expected operating pressure of the OST 25/0 tank. The main technical specifications for this tank are given below in Table 5.8.2.3 below. For a more comprehensive list of technical specifications, see [29].

Table 5.8.2.3: Propellant Tank Technical Specifications

Propellant Tank Technical Specifications	
Specifications	**Description**
Maximum Expected Operating Pressure (MEOP)	18.6 bar
Mass	21.0 kg
Diameter	0.753 m
Length	0.652 m
Pressure Vessel Material	Ti6414V STA(3.7164.7)

A conventional solenoid three-way isolation valve can separate the pressurization lines between the fuel and the oxidizer, with a two-way solenoid valve allowing in place for helium to flow into the oxidizer tank. The inlet of each propellant tank is equipped with a burst disc and a relief valve in line with each other, to ensure that no leakages occur in the system. Finally, an isolation valve, filter, return relief valve, and a return check valve are kept in place at the outlet of both propellant tanks, with a manual fill valve going into the propellant tanks so that the fuel and oxidizer can be pumped into their respective tanks. While the isolation valve serves to prohibit any fuel or oxidizer from flowing for all stages except the pre-firing and firing stages, the return relief valve and check valve allow fuel/oxidizer to flow one way back into their respective tanks should any be trapped between the isolation valve and engine propellant valve after firing. This will ensure that no heat is absorbed by this residual propellant that could cause a pressure rise in the feedlines [30]. The masses of these valves are given in Table 5.8.2.4 below:

Table 5.8.2.4: Valve Masses

Valve Type	Mass (kg)
Fill valve	0.454
Regulator	0.907
Check valve	0.227
Burst disc + relief valve	0.454
Solenoid valve	0.907
Filter	0.454

The mass flow rates of the oxidiser and fuel are estimated to be 0.6762 kg/s, from the relation given below in Equation (5.8.2.6)

$$M_P = \frac{T}{I_{sp}} \qquad \ldots(5.8.2.6)$$

Here, M_p is the propellant mass flow rate, T is the thrust provided, and I_{sp} is the specific impulse of the engine used.

For this system, a conventional unlike-doublet injector is chosen to be employed, as pictured below in Figure (5.8.2.1) [31]. This type of injector mixes the two separate fuel streams at an angle theta relative to each other, with all of the oxidizer passing through a single opening and all of the fuel passing through a separate, single opening.

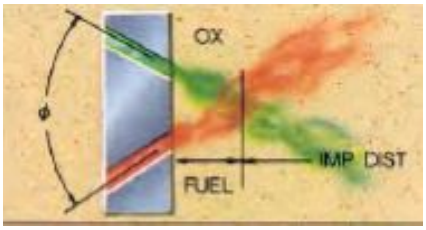

Figure 5.8.2.1: Unlike-Doublet Injector

While these valves are commonly used, to allow for optimal mixing of the two propellants and inhibit any oxidizer-rich, or fuel-rich zones within the combustion chamber resulting from liquid-phase interactions that could cause the streams of oxidizer and fuel to separate, an impinging sheet formation is used instead of an impinging jet, with an injector orifice diameter of 0.08 in, or 0.00203 m [32].

5.8.3 Risk and Risk Mitigation

One risk that could occur in this system is vapour mixing in the check valves caused by a leakage in a regulator valve, which could cause result in a single point failure for this system, which could ultimately result in the loss of the mission [33]. This would be classified as a 2D risk under the guidelines presented in Appendix Figure 10.1.1. The best way to mitigate this risk would be to check all systems beforehand, and thoroughly test the valves to ensure that this event will not occur during the mission. This requires that a management team or supervisor must evaluate the analysis before manufacturing and testing can be completed.

The flow of both oxidizer and fuel would need to stay regulated in order to ensure that the inlet conditions at the thruster were appropriate at all times; any severe pressure changes in the system would result in wrong mixing ratios of the fuel, or the non-functioning of the pressure regulator valve delivering the oxidizer and fuel into the main thruster. This would be classified as a 2D risk under Appendix Figure 10.1.1. One way to mitigate this would be to ensure as best as possible that no leaks would occur during the mission through robust testing of the regulator valve. This requires that a management team or supervisor must evaluate the analysis before manufacturing and testing can be completed.

Finally, should the R-O encounter the need to start a maneuver to course correct in the event of an emergency, a sufficient amount of propellant might not be available, even while accommodating for an additional 25%, which could also result in the loss of the mission. Depending on the situation, this would be classified as a 1D risk level according to the guidelines presented in Appendix Figure 10.1.1.

5.8.4 Future Work

Some future work for this section would include a complete static and dynamic analysis on the stresses experienced by the tanks and supporting structure during the mission, as well as a more in-depth look into the heating loop that would be required to keep the fuel and oxidizers at the right temperatures. A full analysis could be performed in order to pinpoint any combustion instabilities within the system, from interactions between the chamber and the feed system [31], the chamber and its structure (to prevent resonance), or even interactions between the combustion process and internal chamber acoustics. A final estimate of all the masses of the pressure lines, valves, and other elements could also be collected and presented in a final system design.

6.0 Budgets

6.1 Mass Budget

Based on further orbital analysis, it has been determined that the burn to escape from Mars needs to be larger than originally estimated. Due to this increase, the launch vehicle is changed to a Falcon Heavy. Given the launch vehicles capabilities the mass budget is 5400kg. Figure 6.1.1 assumes the Falcon Heavy is in a maximum-reusability configuration in order to minimise cost. Any mass not used by the R-O and M-P will be used to send smaller missions to Mars or Jupiter.

Table 6.1.1: Mass Budget

Mass Budget Breakdown	
Subsystem	**Percentage of Total Mass**
Structures	5%
Thermals	5%
Power	20%
Telecommunications & Data	4%
Mechanisms & Deployables	3%
ADCS	4%
Propulsion	19%
Probe	40%
Total Mass: 3525 kg	

6.2 Power Budget

To properly size power systems and schedule commands, it is necessary to know the power requirements of each subsystem. These requirements are listed in Table 6.2.1.

Table 6.2.1: Power Requirements of Systems

Power Requirements of Systems	
System	**Power (W)**
Computer	50
Reaction Wheels	50(max)
HGA	75
LGA	10-15
Instruments	75(total)
RCS Thrusters	120(emergency)

To maintain control of the spacecraft, the main computer and reaction wheels always have power. In an emergency scenario such as an uncontrolled tumble or unexpected reaction wheel saturation, all operations are suspended while the computer and all ADCS systems work to regain control of the spacecraft. During normal operation, the power draw is low enough that the batteries are being charged while in sunlight, for depletion when in the shade. The power requirements of different systems throughout the mission life are shown in Table 6.2.2.

Table 6.2.2: Power Distribution to Systems

Power Requirements of Systems						
Component	**Data Collection**	**Probe Comm.**	**Earth Comm.**	**Desaturation**	**Hold**	**Emergency**
Computer						
ADCS Wheels						
ADCS Thrusters						
Instruments						
LGA						
HGA						

This table shows systems in green when they will be operating at the same time. An emergency (shown in red) will override any other mission phase and activate the ADCS thrusters.

6.3 Volume Budget

The volume budget is a breakdown of how much space each subsystem uses in the current design of the R-O. These values are subject to change based on future analysis and needs.

Table 6.3.1: Volume Budget

Volume Budget Breakdown	
Subsystem	**Percent of Total Volume**
Structures	4%
Thermals	1%
Power	16%
Telecommunications & Data	2%
Mechanisms & Deployables	1%
ADCS	3%
Propulsion	7%
Probe	66%
Total Volume: 2.47 m^3	

6.4 Monetary Budget

Due to difficulty finding individual component costs and an unclear idea of how many hours and resources are budgeted for such a mission, the design team could only base the cost of the mission on the costs of previous missions. The Europa Clipper was selected as the mission to base the budet from due to its similar nature. This mission will cost just under 4 billion dollars, and so as of this document the Semele Mission is expected to as well [34].

7.0 Timeline

A Gantt chart and mission timeline is included in Figure 7.0.1. This chart outlines the major milestones of the design process including the PDR and FDR. Additionally, the mission timeline shows the major events of the spacecraft's trajectory. For the timeline, Phase 1 begins at Earth and encompasses the transfer to Mars, Phase 2 is the bulk of transfer time and includes the orbit from Mars to Jupiter and rendezvous, and Phase 3 contains all the events occuring in Jovicentric orbit, including gravity braking with Ganymede, capture, and Europa flyby.

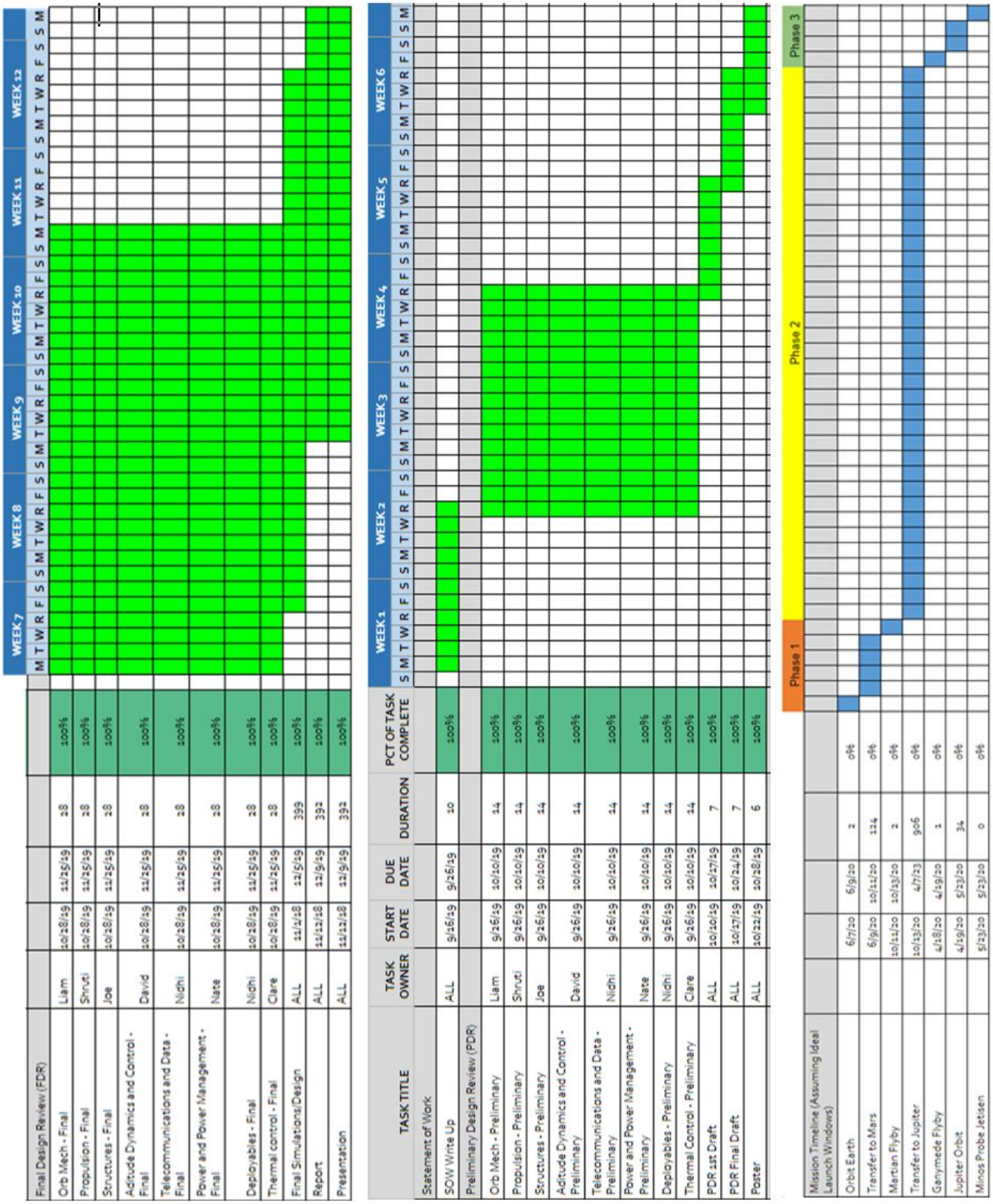

Figure 7.0.1: Gantt Chart

8.0 Conclusion

To successfully complete the mission as described by the customers, the Radamanthus - Orbiter will be built on an aluminum bus with titanium reinforcements. The orbiter's attitude will be controlled via reaction wheels, thrusters, and magnetorquers, and measured via a suite of IMU's and star trackers. The R-O will be placed on a trajectory that includes a gravity assist from Mars, and gravity braking from Ganymede, and will be placed in a highly elliptical orbit around Jupiter. The orbiter's temperature will be regulated with RHUs, insulation, and radiators. Power will be provided via solar panels, and stored in lithium-ion batteries, deployed via a rigid arm. A dual mode propulsion system will provide propulsion for the mission. Communication with Earth and the Minos-probe will be accomplished via an X-band high gain antenna, and 2 low gain antennas. The Minos-probe will be deployed via the use of a ball and lock mechanism. This system will be able to successfully deposit the M-P on the surface of Europa, and deliver the R-O into an elliptical Jovian orbit, where it will be capable of taking a myriad of scientific measurements.

9.0 References

[1] Clark, Stuart. (2015). *Why NASA's Europa mission has people excited.* Retrieved from https://www.theguardian.com/science/across-the-universe/2015/feb/04/nasa-europa-mission-has-people-excited

[2] *Europa.* Retrieved from https://solarsystem.nasa.gov/moons/jupiter-moons/europa/in-depth/

[3] Jet Propulsion Laboratory. *Mission to Europa Europa Clipper.* Retrieved from https://www.jpl.nasa.gov/missions/europa-clipper/

Structures

[4] SpaceX. (2019). *Falcon User's Guide*. Retrieved from https://www.spacex.com/sites/spacex/files/falcon_users_guide_10_2019.pdf

Thermal Systems

[5] Gilmore, David G. (2002). *Spacecraft Thermal Control Handbook.* Vol 1, The Aerospace Press.

[6] Light-Weight Radioisotope Heater Unit. (2017, November 2). Retrieved from https://rps.nasa.gov/power-and-thermal-systems/thermal-systems/light-weight-radioisotope-heater-unit/.

Power Management

[7] SolAero Technologies. (2018). *Space Solar Cells / Coverglass Interconnected Cells*. Retrieved 20 Oct. 2019. Web.

[8] Oberhaus, Daniel. (Jan 2, 2012). *Scientists Are Automating Plutonium Production So NASA Can Explore Deep Space*. Motherboard. Retrieved 20 Oct, 2019. Web.

Telecommunications and Data

[9] *Radio Frequencies for Space Communication*, https://www.spaceacademy.net.au/spacelink/radiospace.htm.

[10] D.K.Shin. (2014). *201 Frequency and Channel Assignments.* Deep Space Network. JPL. Retrieved from https://deepspace.jpl.nasa.gov/dsndocs/810-005/201/201C.pdf

[11] Coffey, J. (2015, December 25). How Far is Jupiter from Earth. Retrieved from https://www.universetoday.com/14514/how-far-is-jupiter-from-earth/.

Deployables and Mechanisms

[12] Fusaro, R. L. (1999). *NASA Space Mechanisms Handbook.* Glenn Research Center, NASA.

[13] Mobrem, M., Spier, C., (2012). *Design and Performance of the Telescopic Tubular Mast.* Aerospace Mechanisms Symposium, JPL. Retrieved from https://pdfs.semanticscholar.org/2a31/f767de09f0ace84aebc1a4f6ebac9eadd746.pdf

Attitude Dynamics and Control Systems

[14] Honeywell Inc. (2018) *Inertial Measurements units*., Honeywell. Retrieved from https://aerospace.honeywell.com/en/learn/products/sensors/inertial-measurement-units][https://www.ball.com/aerospace/Aerospace/media/Aerospace/Downloads/D3408_CT2020_0118.pdf?ext=.pdf

[15] Moog Inc. (2017) *Monopropellant Thrusters Datasheet*, Moog. Retrieved from https://www.moog.com/content/dam/moog/literature/Space_Defense/spaceliterature/propulsion/Moog-MonopropellantThrusters-Datasheet.pdf

[16] Yang, Yaguang. (2016). *Spacecraft Attitude and Reaction Wheel Desaturation Combined Control Method.* Retrieved from:https://arxiv.org/abs/1603.09629

[17] Anderson, Kurt, 2019. Lecture for Space Vehicle Design

[18] Brown, Charles D. *Elements of Spacecraft Design*. American Institute of Aeronautics and Astronautics, Inc., 2002.

[19] Honeywell. (2018). *HG1936 Rate Sensor*. Phoenix, AZ.

[20] Ball Aerospace. (2019). *CT-2020*.

Orbital Mechanics

[21] Williams, David. "Jupiter Fact Sheet." *NASA*, NASA, 18 July 2018, nssdc.gsfc.nasa.gov/planetary/factsheet/jupiterfact.html.

[22] jlowe. (n.d.). A better Mars atmosphere model. Retrieved from http://www.agi.com/news/blog/november-2010/a-better-mars-atmosphere-model?feed=AGIBlogsFeed.

[23] Curtis, Howard D. (2005). *Orbital Mechanics for Engineering Students*. Oxford: Elsevier Butterworth-Heinemann. Print.

[24] *Natural Satellites Ephemeris Service*. IAU: Minor Planet Center. Retrieved 8 January 2011. Note: some semi-major axis were computed using the μ value, while the eccentricities were taken using the inclination to the local Laplace plane"

[25] Shampine, L. F. and M. W. Reichelt, "The MATLAB ODE Suite," *SIAM Journal on Scientific Computing*, Vol. 18, 1997, pp. 1–22.

[26] Sellers, J. J., Larson, W. J., (1996). *Satellite Tool Kit Astronautics Primer.* McGraw-Hill Inc.

Propulsion Systems

[27] Aerojet Rocketdyne. (2019, September 13). *In-Space Propulsion Data Sheets.* Retrieved from https://www.rocket.com/sites/default/files/documents/In-Space Data Sheets 9.13.19.pdf

[28] DEleuterio, G. M. T., & Baines, P. J. (1987). *Elements of spacecraft design*. Toronto: University of Toronto, Faculty of Applied Science and Engineering.

[29] Surface Tension Propellant Tank OST 25/0. (n.d.). *Surface Tension Propellant Tank OST 25/0*. Taufkirchen, Germany.

[30] NASA. (1971). Space Storable Propellant Nodule Thermal Control Technology. *NASA Cr 117959*, *N71*(25578). Retrieved from https://ntrs.nasa.gov/archive/nasa/casi.ntrs.nasa.gov/19710016102.pdf

[31] Purdue Propulsion. (n.d.). *Liquid Rocket Propulsion (LRP) Systems.* AAE 439

[32] Evans, D. D., Stanford, H. B., Reibling, R. W.. (1967). *The Effect of Injector-Element Scale on the Mixing and Combustion of Nitrogen Tetroxide-Hydrazine Propellants.* NASA. Retrieved from https://ntrs.nasa.gov/archive/nasa/casi.ntrs.nasa.gov/19680002968.pdf

[33] Brown, C. D. (1996). *Spacecraft propulsion*. Washington, DC: American Institute of Aeronautics and Astronautics.

Non Subsystem References

[34] Foust, J., & Foust, J. (2019, August 22). Europa Clipper passes key review. Retrieved from https://spacenews.com/europa-clipper-passes-key-review/.

[35] Hurst, Joshua, 2019.State Space Linearization for Mechatronics 4520

[36] Toray Composites. (2019, Aug. 6). *Aluminum Honeycomb, Aerospace Grade Product Data Sheet.* Retrieved Nov. 14, 2019. Web.

10.0 Appendix

10.1 Risk

Risk Assessment Matrix

(excerpt from NASA MPR 8715.15)

Probability (P)	Severity			
	1 Catastrophic	2 Critical	3 Marginal	4 Negligible
A - Frequent	1A*	2A	3A	4A
B - Probable	1B	2B	3B	4B
C - Occasional	1C	2C	3C	4C
D - Remote	1D	2D	3D	4D
E - Improbable	1E	2E	3E	4E

* 1A, 2A, 3C, 4E, etc. are examples of Risk Assessment Codes (RAC) which roughly catagorized the severity/probability of the risk

Risk Acceptance and Management Approval Level	
Severity - Probability	Acceptance Level/Approving Authority
High Risk	Unacceptable: Documented approval from the MSFC EMC or an equivalent level independent management committee.
Medium Risk	Undesirable: Documented approval from the facility/operation owner's Department/Laboratory/office Manager or designee(s) or equivalent level management committee.
Low Risk	Acceptable: Documented approval from the supervisor directly responsible for operating the facility or performing the operation.
Minimal Risk	Acceptable: Documented approval not required, but an informal review by the supervisor directly responsible for the operation of the facility or performing the operation is highly recommended. The use of generic JHA (Job Hazard Analysis) posted on the Safety, Health, Environment (SHE) webpage is recommended, if a generic JHA has been developed.

Figure 10.1.1: Risk Assessment Matrix

10.2 Matlab Scripts

10.2.1 Transfer Optimization

```
%optimizing orbit
clc; clear all;
global muSun muMars Re Vp Rj Rm Ve Vm
%% notes

%% set up
muSun = 1.32712e11;
muEarth = 398600;
muJupiter = 1.2669e8;
muMars = 42828;

Re = 149.6e6; %orbital radius of earth
Rj = 778.57e6; %orbital radius of jupiter
Rm = 227.92e6; %orbital radius of mars

Ve = sqrt(muSun/Re);
Vm = sqrt(muSun/Rm);
Vj = sqrt(muSun/Rj);

%parking orbit around earth
rp = 6678;
Vp = 7.7258;

%design  initial guesses
ropt = 4000e5; %how close we get to mars multiply by e5 to keep things same order of
magnitude
Rx = 530e6; %some place in space past mars that are first yeet is aimed at

%% optimization
r0 = [ropt, Rx]; %initial guess
LB =[3589.5e5,Rm]; %first entrys are mars radius plus 200km to get out of atmosphere(times
e5) and sphere of influence
UB =[.576e11,Rj];
```

```
options = optimoptions('fmincon', 'Display','iter','Algorithm', 'active-set'); %display each iteration and use the sqp algorithm for fmincon, include constraint gradient

tic
%function minimization finding the optimal r values
[R, dv] = fmincon(@deltaV, r0, [], [], [], [], LB, UB, @orbit, options);%minimize volume is the same as minimizing weight
toc %end timer for computational cost

%% Final orbit calculation
[hf, ef, hsc, esc] = orbitTest(R);

%% Velocity relative to jupiter
thetaJ = acosd((hf^2/(muSun*Rj) - 1)/ef); %true anomoly at Jupiter (big accuracy loss here)
VJ(1) = muSun*ef*sind(thetaJ)/hf; %radial velocity at jupiter of space craft
VJ(2) = muSun*(1 + ef*cosd(thetaJ))/hf; %tangential velocity at jupiter

VJ(2) = VJ(2) - Vj; %velocity relative to jupiter at the end
format long
VJmag = norm(VJ);

%% orbits and intersects
n = 100;

%earth, mars,jupiter
re = Re*ones(1,n);
rm = Rm*ones(1,n);
rj = Rj*ones(1,n);
theta1 = linspace(0,2*pi,n);

%first send
theta2 = linspace(0,pi,n);
rt = hsc^2/muSun *1./(1 + esc*cos(theta2));
theta_intersect1 = acos(((hsc^2/(muSun*Rm))-1)/esc);
theta2 = theta2 - theta_intersect1; %offset for change inperi due to grav assist

%final orbit
theta3 = linspace(0, pi,n);
```

```
rf = hf^2/muSun *1./(1 + ef*cos(theta3));
theta_intersect2 = acos(((hf^2/(muSun*Rm))-1)/ef);
theta3 = theta3 - theta_intersect2;


%% plotting stuff
%plots
polarplot(theta1,re,theta1,rm,theta1,rj); %planets
hold on
polarplot(theta3,rf)
polarplot(theta2,rt);
legend('Earth','Mars','Jupiter','Initial Transfer Orbit', 'Final Transfer Orbit')

%% Travel time
t1 = TravelTime(hsc,esc,0,theta_intersect1,muSun); % time from earth to mars
t2 = TravelTime(hf,ef,theta_intersect2,pi,muSun); % time from mars to jupiter
tTots = t1 + t2; %transfer time in sec
tTot = tTots/(3600*24*365.25) %time in years

%% launch windows
wm = Vm/Rm; %angular velocity of mars [rad/sec]
travel_angle1 = wm*t1; %angle mars travles after we leave earth in radians
M_Eangle = theta_intersect1 - travel_angle1; %start yeet when mars is this far infront of earth

%theta_intersect2 is angle from peri to mars crossing
wj = Vj/Rj; %angular velocity of jupiter [rad/sec]
travel_angle2 = wj*tTots; %angle jupiter travles after we leave earth in radians

J_Eangle = (theta_intersect1 + (pi - theta_intersect2)) - travel_angle2; %start yeet when jupiter is
this far in front of earth

%% David's Data
N = 50;
Theta1 = linspace(0,theta_intersect1,N);
Theta2 = linspace(theta_intersect2,pi,N);
Rt = hsc^2/muSun *1./(1 + esc*cos(Theta1));
Rf = hf^2/muSun *1./(1 + ef*cos(Theta2));

for i = 1:N
```

```
    T1(i) = TravelTime(hsc,esc,0,Theta1(i),muSun);
    T2(i) = TravelTime(hf,ef,theta_intersect2,Theta2(i),muSun);
end

plot(T1,Rt)

figure(2)
plot(T2,Rf)
```

10.2.2 Orbit Function

```
function [c, ceq] = orbit(ri)
global muSun muMars Re Rj Ve Rm Vm
%flyby parameters
approach = 1; %darkside
x = 1; %mars is "above" earth
r = ri(1)/10^5; %how close we get to earth
flybyParameter = [approach,r,x];

Rx = ri(2); %initial orbit apoapsis
VinfEx = sqrt(muSun/Re)*(sqrt(2*Rx/(Re + Rx))-1); %hyperbolic access velocity

%% relative to the sun
Vsc = [ 0, VinfEx + Ve]; %velocity relative to the sun
esc =(Rx - Re)/(Rx + Re); %eccentricity
hsc = sqrt(muSun*Re*(1 + esc)); %angular momentum of orbit
orbit = [hsc, esc]; %initial orbit

%planet for flyby is mars
planet = [Rm, muMars];

%% calculating new orbit
NewOrbit = flyby(planet,orbit,flybyParameter);
hf = NewOrbit(1);
ef = NewOrbit(2);
Rmax = hf^2/(muSun*(1 - ef));

c = 1 - Rmax/Rj; %make sure c is less than 0, normalized values
```

```
ceq = []; %no equality constraint
end
```

10.2.3 Flyby Function

```
%planetary flyby
%everything in SI except km not m
%flybyParameters are for if its a sunside approach(-1) or
%darkside approach (1) and r is periapsis of planetary hyperbolic flyby,
%determined by mission or optimized
%x determines if planet is above (1) or below (-1) starting location
%example: x = 1 when going from earth to fly by mars x = -1 when going from earth to flyby
venus
%%
function [NewOrbit] = flyby(planet,orbit,flybyParameter)
muSun = 1.32712e11;

R = planet(1); %planets mean orbital radius assuming circular orbit
muPlanet = planet(2); %planets gravitational constant
Vplanet = sqrt(muSun/R); %planets velocity

h = orbit(1); %initial orbit angular momentum
e = orbit(2); %initial orbit eccentricity
%defines argument of periapsis as 0 cuz planet orbit is circular so dont matter

sunapproach = flybyParameter(1); %sunside approach or darkside approach
r = flybyParameter(2); %how close we get to the planet
x = flybyParameter(3); % is this planet above or below the starting location

%% relative to sun
theta = acosd((h^2/(muSun*R) - 1)/e); %true anomoly at planet (big accuracy loss here)
theta = x*theta; %changes sign depending on if the planet is above or below original orbit
V(1) = muSun*e*sind(theta)/h; %radial velocity at planet of space craft
V(2) = h/R; %tangential velocity at planet
gamma = atan2d(V(1), V(2)); %flight path angle
V(1) = -V(1); %text beq 8.89

%% relative to planet
```

```
Vrel = V;
Vrel(2) = Vrel(2) - Vplanet; %velocity relative to planet
Vrelmag = norm(Vrel); %velocity magnitude
hm = r*sqrt(Vrelmag^2 + (2*muPlanet/r)); %angular momentum of planet orbit
e = 1 + r*Vrelmag^2/muPlanet; %eccentricity of planet orbit

%% angle change
delta = 2*asind(1/e); %turn angle
phi1 = atan2d(Vrel(1), Vrel(2)); %angle between mars velocity and VM_m

%sunside approach or dark side approach
delta = sunapproach*delta;
phi2 = phi1 + delta;

Vrel2 = Vrelmag*[sind(phi2), cosd(phi2)];

%% leaving planet relative to sun
Vf = Vrel2;
Vf(2) = Vf(2) + Vplanet; %velocity relative to the sun
Vf(1) = -Vf(1); %text eq 8.89
Vfmag = norm(Vf); %spacecraft speed
hf = R*Vf(2); %angular momentum

%intermediate cals for finding theta
ecos = hf^2/(muSun*R) - 1;
esin = Vf(1)*hf/muSun;

thetaf = atan2d(esin, ecos); %true anomoly of sun orbit when meeting mars
ef = (Vf(1)*hf)/(muSun*sind(thetaf)); %eccentricity

NewOrbit(1) = hf;
NewOrbit(2) = ef;

end
```

10.2.4 DeltaV Function

```
function dv = deltaV(ri);
```

```
r = ri(1)/10^5;
Rx = ri(2);
global muSun Re Vp
   VinfEx = sqrt(muSun/Re)*(sqrt(2*Rx/(Re + Rx))-1); %delta V relative to earth purely theta
direction cuz this is a hohmann eq
   dv = Vp*(sqrt(2 + (VinfEx/Vp)^2) - 1); %the send to get us there
end
```

10.2.5 Travel Time Function

```
function t = TravelTime(h,e,theta1,theta2,mu)
%time it took to get here NOTE: E is in radians
T = 2*pi*(h/sqrt(1 - e^2))^3/mu^2; %period of orbit in seconds
x = sqrt((1 - e)/(1 + e))*tan(theta1/2); %intermediate calculation
E = 2*atan(x); %the big E in kepler's equation
Me = E - e*sin(E); %mean anomaly
t1 = Me*T/(2*pi); %travel time in seconds to theta1 in sec

x = sqrt((1 - e)/(1 + e))*tan(theta2/2); %intermediate calculation
E = 2*atan(x); %the big E in kepler's equation
Me = E - e*sin(E); %mean anomaly
t2 = Me*T/(2*pi); %travel time in seconds to second location

t = t2 - t1; %time between 2 locations
End
```

10.2.6 Capture Optimization

```
%gravity breaking
clc; clear all;
%% notes
%{
juno went into an orbit of 74111 km
closest spacecrat to jupiter
didnot aero brake
%}
%% Set up
global vinf muJupiter muGanymede Rg
```

```
G = 6.67408e-11; % THE gravitational constant
Mg = 1.48e23; %Mass of ganymede
Rg = 1070412; %ganymede's mean radius orbit
Re = 671.1e3; %europa
muJupiter = 1.2669e8;
muGanymede = G*Mg/1e9; %converting to km instead of meters
%% constants for constraints
rj =69911; %jupiter radius
rg =2634.1; %ganymede radius
SOIj =48.2e6; %jupiter sphere of influence
SOIg = 24340; %ganymede shpere of influnce

%% design Variables
r1 = 74111; %how close we get to jupiter %THIS IS WHERE WE GOTTA THINK
r2 = rg + 200; %how close we get to ganymede

%good values [Re,rg]
%reducing r1 makes it better Why is fmincon not picking up on this

%% relative to jupiter
MarsAssist = 5.483784230999427; %km/s relative to jupiter based on big yeet optimization
vinf = MarsAssist;

%% optimization
r0 = [r1, r2]; %initial guess
LB =[rj,rg]; %bodies radius
UB =[SOIj,SOIg]; %bodies sphere of influence

options = optimoptions('fmincon', 'Display','iter','Algorithm', 'sqp'); %display each iteration and
use the sqp algorithm for fmincon, include constraint gradient

tic
%function minimization finding the optimal r values
[R, e] = fmincon(@gravBrake, r0, [], [], [], [], LB, UB, [], options)%minimize eccentricity
toc %end timer for computational cost

%% final orbit
[e2, h2] = gravBrake(R);
rperi = h2^2/muJupiter * 1./(1 + e2);
```

```
%% post brake deltaV for capture
Vph = h2/rperi; %post brake periapsis velocity
ra = 4e6; %WE CAN CHANGE THIS ask nate and nidhi what they need
efinal = (ra - rperi)/(ra + rperi); % where we wanna be
hfinal = sqrt(rperi*(1 + efinal)*muJupiter);
Vpc = sqrt(muJupiter*(1+efinal)/rperi); %capture orbit perigee velocity
deltaV = Vph - Vpc; %better with smaller R

%% original orbit
n = 200;
Vperi = sqrt(vinf^2 + (2*muJupiter/R(1)));
hi = Vperi*R(1);
ei = hi^2/(muJupiter*R(1))-1;
theta3 = linspace(-9*pi/10, 0,n);
ri = hi^2/muJupiter *1./(1 + ei*cos(theta3));
theta_intersect = acos(((hi^2/(muJupiter*Rg))-1)/ei);
%theta3 = theta3 + theta_intersect; %offset for change inperi due to grav assist

%% post flyby and final orbit
theta1 = linspace(-9*pi/10, 0,n);
rt = h2^2/muJupiter *1./(1 + e2*cos(theta1));
theta_intersect = acos(((h2^2/(muJupiter*Rg))-1)/e2);
%theta1 = theta1 + theta_intersect; %offset for change inperi due to grav assist

theta2 = linspace(0,2*pi,n);
rc = hfinal^2/muJupiter *1./(1 + efinal*cos(theta2));

T = 2*pi*(hfinal/sqrt(1 - efinal^2))^3/muJupiter^2; %period of orbit in seconds
T = T/(3600*24) %time in days

%% Time in shade
a = (ra + rperi)/2;
enew = (ra - rperi)/(ra+rperi);
phi = 47; %use angle of eclipse
T = 2*pi*sqrt(a^3/muJupiter);
x = sqrt((1 - enew)/(1 + enew))*tand(phi/2); %intermediate calculation
E = 2*atan(x); %the big E in kepler's equation
Me = E - enew*sin(E); %mean anomaly
```

```
t = Me*T/(pi); %travel time in seconds time in eclipse is symmetric about peri thats why its not 2*pi


%% plots
polarplot(theta1,rt) %post braking
hold on
polarplot(theta2,Rg*ones(n,1)) %gany
polarplot(theta2,Re*ones(n,1)) %Europa
polarplot(theta2, rc) %capture orbit
polarplot(theta3, ri) % initial
legend('post-brake','Ganymede','Europa','Final','Initial')

%% David's Data
N = 100;
Theta1 = linspace(0,pi,N);
Rt = hfinal^2/muJupiter *1./(1 + efinal*cos(Theta1));


for i = 1:N
   T1(i) = TravelTime(hfinal,efinal,0,Theta1(i),muJupiter);
end

plot(T1,Rt)
```

10.2.7 Gravity Braking Function

```
%gravity breaking
function [ef,hf] = gravBrake(r)
%% Set up
global vinf muJupiter muGanymede Rg
r1 = r(1);
r2 = r(2);
Vg = sqrt(muJupiter/Rg);

%% relative to jupiter
Vph = sqrt(vinf.^2 + (2*muJupiter/r1)); %velocity at periapsis
esc = 1 + r1*vinf^2/muJupiter; %eccentricity of hyperbolic orbit
hsc = r1*Vph; %angular momentum of orbit
```

```
orbit = [hsc, esc]; %starting orbit

%% stuff for flyby
moon = [Rg, muGanymede];
approach = -1; %darkside
x = -1; %sc is "above" gany when coming in
r = r2; %how close we get to gany
flybyParameter = [approach,r,x];

%% calculating new orbit
NewOrbit = flybyjup(moon,orbit,flybyParameter);
hf = NewOrbit(1);
ef = NewOrbit(2);

end
```

10.2.8 Jupiter Fly-By Function

```
%planetary flyby
%everything in SI except km not m
%flybyParameters are for if its a sunside approach(-1) or
%darkside approach (1) and r is periapsis of planetary hyperbolic flyby,
%determined by mission or optimized
%x determines if planet is above (1) or below (-1) starting location
%example: x = 1 when going from earth to fly by mars x = -1 when going from earth to flyby
venus

%%
function [NewOrbit] = flybyjup(planet,orbit,flybyParameter)
muJupiter = 1.2669e8;;

R = planet(1); %planets mean orbital radius assuming circular orbit
muPlanet = planet(2); %planets gravitational constant
Vplanet = sqrt(muJupiter/R); %planets velocity

h = orbit(1); %initial orbit angular momentum
e = orbit(2); %initial orbit eccentricity
%defines argument of periapsis as 0 cuz planet orbit is circular so dont matter
```

```
sunapproach = flybyParameter(1); %sunside approach or darkside approach
r = flybyParameter(2); %how close we get to the planet
x = flybyParameter(3); % is this planet above or below the starting location

%% relative to Jupiter
theta = acosd((h^2/(muJupiter*R) - 1)/e); %true anomoly at planet (big accuracy loss here)
theta = x*theta; %changes sign depending on if the planet is above or below original orbit
V(1) = muJupiter*e*sind(theta)/h; %radial velocity at planet of space craft
V(2) = h/R; %tangential velocity at planet

%% relative to moon
Vrel = V;
Vrel(2) = Vrel(2) - Vplanet; %velocity relative to planet
Vrelmag = norm(Vrel); %velocity magnitude
hh = r*sqrt(Vrelmag^2 + (2*muPlanet/r)); %angular momentum of planet orbit
eh = 1 + r*Vrelmag^2/muPlanet; %eccentricity of planet orbit

%% angle change
phi1 = atan2d(Vrel(1), Vrel(2)); %angle of sc velocity above theta direction in jup coordinate
system
delta = 2*asind(1/eh); %turn angle
%sunside approach or dark side approach
delta = sunapproach*delta;
phi2 = phi1 + delta;

Vrel2 = Vrelmag*[sind(phi2), cosd(phi2)]; %velocity leaving moon in sun coordinate system rel
to moon

%% leaving planet relative to sun
Vf = Vrel2;
Vf(2) = Vf(2) + Vplanet; %velocity relative to the sun
Vfmag = norm(Vf); %spacecraft speed
hf = R*Vf(2); %angular momentum

%intermediate cals for finding theta
ecos = hf^2/(muJupiter*R) - 1;
esin = Vf(1)*hf/muJupiter;

thetaf = atan2d(esin, ecos); %true anomoly of sun orbit when meeting mars
```

```
ef = (Vf(1)*hf)/(muJupiter*sind(thetaf)); %eccentricity

NewOrbit(1) = hf;
NewOrbit(2) = ef;

end
```

10.2.9 3-Body Analysis

```
%3-body problem gravity braking
clc; clear all; clear plot;
clear global variable;
%% Notes
%keeps drawing on figure 1 not figure 2
%ode45 fucks up if you run the simulation too long because the time step
%cannot be reduced, looks like you can used patched conics pretty ok though
%trying to time meet up with hyperbolic trajectory
%% set up
% making global variable
global   muSun muMars Rm Mangle

muSun = 1.32712e11;
muMars = 42828;

Rm = 2.28e8; %orbital radius of ganymede in m
Re = 149.6e6; %orbital radius of earth
Ve = sqrt(muSun/Re); %earths velocity
Rj = 778.57e6; %orbital radius of jupiter


%% velocity and location when leaving earth
%based on mars optimization
peri = Re; %periapsis at earth
apo = 6.011601174529805e8;
e = (apo - peri)/(apo + peri);
h = sqrt(muSun*Re*(1 + e)); %angular momentum of orbit
vel = sqrt(muSun/Re)*(sqrt(2*apo/(Re + apo))-1); %hyperbolic access velocity rel earth
vel = vel + Ve; %vel rel sun
```

```
%% Mars starting location
Mangle = .5; %keep trying currently between .677 and .679
%0.632488933603221; %true anomaly of mars when mission begins assuming earth is at zero in
radians
%this value is from optoimization
%theta_intersect =  1.485638086206234; %angle in radians when s/c should
%reach mars based on optimization

%% ODE 45
%initial location
%this occurs after 6e6 sec after entering the sphere of influence of jupiter
x0 =  Re;
y0 = 0; %in m
% inital velocity
Vx0 = 0;
Vy0 = vel;

%ran initial location and selected new initial location at later time to
%improve accuracy

intervals = 1; %how many intervals the simulation is broken into
%at ten thousand intervals it takes 34 sec. max radius stabalizes much
%before that

tf = 30000000/intervals; %run time for each interval
X0 = [x0; y0; Vx0; Vy0];
tspan = [0 tf];
odeoptions = ['RelTol', 1e-15, 'AbsTol', 1e-15]; %reducing stepsize
[t,x] = ode45(@Body3transfer, tspan, X0, odeoptions);
xsc = [x(:,1),x(:,2)]; %storing location after each run
Mangle = Mangle + tf*sqrt(muSun/Rm)/Rm; %update mars location
tic
for run = 1:intervals %runs ODE 45 5 times
X0 = x(end,:);
[t,x] = ode45(@Body3transfer, tspan, X0, odeoptions);
xsc = [xsc;[x(:,1),x(:,2)]];
Mangle = Mangle + tf*sqrt(muSun/Rm)/Rm; %update mars location
end
Runtime = toc;
```

```
%% timing mars flyby
for i = 1:length(x)
   rs(i) = sqrt(xsc(i,1)^2 + xsc(i,2)^2); %distance from space craft to sun
   if (rs(i) - Rm) <= 0 %when we pass mars
      tclose = t(i); %what time is it
      xp = xsc(i,1); %where are we
      yp = xsc(i,2);
   end
end
theta_intersect = atan2(yp,xp); %true anomaly of spacecraft when meeting martian orbit
location = tclose*sqrt(muSun/Rm)/Rm + Mangle; %true anomaly of mars when s/c meets orbit
Test = location - theta_intersect; %change Mangle until this is zero


%% plotting shit
%used to plot jupiter and ganymede
rsun = 695510; %radius of sun [m]
rm = 3389.5;% radius of mars in m
theta = linspace(0,2*pi);
%the sun
xs = rsun*cos(theta);
ys = rsun*sin(theta);

%mars
xm = Rm*cos(theta);
ym = Rm*sin(theta);
%jupiter
xj = Rj*cos(theta);
yj = Rj*sin(theta);

%big picture
figure (1)
plot(xs,ys) %sun
hold on
plot(xm,ym) %mars
plot(xsc(:,1),xsc(:,2))
plot(xj,yj)
legend('Sun','Mars','spacecraft','Jupiter')
```

```
axis([-1e9,1e9,-1e9,1e9]); %square axis

MAX = sqrt(max(x(:,1))^2 + max(x(:,2))^2) %distance from space craft to sun
%% mars location
t1 = linspace(0,tf,length(x));
Theta_m = t1*sqrt(muSun/Rm)/Rm; %true anomaly of mars
offset = Mangle; %starting location for mars
Theta_m = Theta_m - offset;
RM = [Rm*cos(Theta_m); Rm*sin(Theta_m)]; %mars orbit
RM = RM';




%% animate shit
%animated orbit
h1 = animatedline('color','r'); %need 1 animated line object for each moving thing
h2 = animatedline('color','k');

figure(2)
plot(xj,yj) %jupiter
hold on
axis([-1e9,1e9,-1e9,1e9]); %stabalize axis

for k = 1:length(x)
   addpoints(h1,x(k,1),x(k,2));
   addpoints(h2,RM(k,1),RM(k,2));
   drawnow
end
```

10.2.10 3-Body Transfer Function

```
%%notes
function [dydt] = Body3transfer(t,X)
global   muSun muMars Rm Mangle %bringing in global variables
%split X into understood variable names
x = X(1);
y = X(2);
```

```
x_dot = X(3);
y_dot = X(4);

R = [X(1), X(2)];

%% individual force over mass approach
fs = -muSun*R/(norm(R)^3); %acceleration due to gravity of sun

theta_m = t*sqrt(muSun/Rm)/Rm; %true anomaly of mars
offset =  Mangle; %starting location for mars
theta_m = theta_m + offset;

rm = [Rm*cos(theta_m), Rm*sin(theta_m)]; %moving mars
rnew = R - rm; %vector from mars to s/c
fm = -muMars*rnew/(norm(rnew)^3); % acceleration from mars


a = fs + fm; %total acceleration

%% final vector of velocity and acceleration
dydt(1)= x_dot;
dydt(2)= y_dot;
dydt(3)= a(1);
dydt(4)= a(2);
dydt = dydt';
end
```

10.2.11 Solar Panel Optimization

For each type of honeycomb, there exists a configuration of carbon fiber and honeycomb that minimise the mass required to carry a certain acceleration. To find this point, the code iterates through potential honeycomb thicknesses and finds the minimum carbon fiber thickness such that neither the carbon fiber nor the honeycomb will under the given loads at the root of the array. For each honeycomb type, the code produces a plot similar to the one below which shows the total mass and mass of each part of the panel:

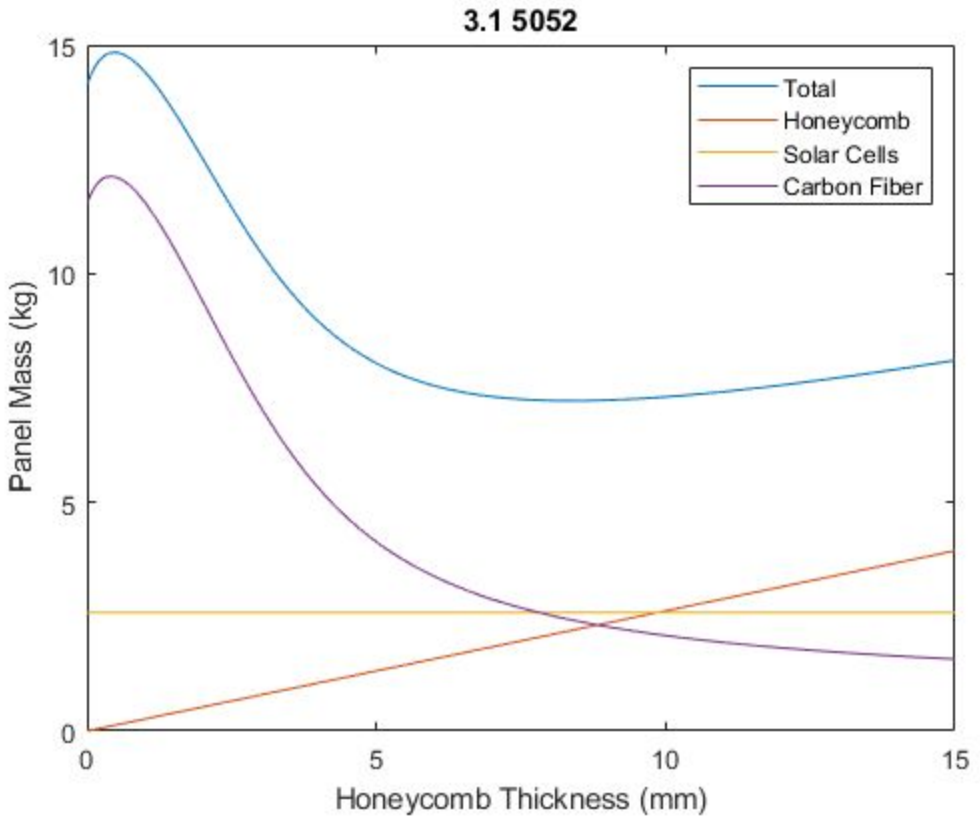

Figure 10.2.11.1: Solar Panel Mass

In the above figure, the optimal characteristics occur at the minimum of the total mass.

The code to produce optimal results based on acceleration and material properties is shown below:

```
aMax=70;
p=[3.1;4.5;5.2;8.1;4.5;6.1;8.1]*16.0185;
sStr=[155;255;307;543;350;525;740]*6894.76;
names={'3.1 5052','4.5 5052','5.2 5052','8.1 5052','4.5 5056','6.1 5056','8.1 5056'};
carStr=800e6; % 800 MPa
area=2.3*4.6;
th=(0.01:0.01:15)'/1000; %Thickness in mm converted to m
mmass=[0;0;0;0;0;0;0];
mth=mmass;
mtc=mmass;
for i=1:7
  massmf=zeros(length(th),1);
  tcmf=zeros(length(th),1);
```

```
  masshmf=zeros(length(th),1);
  masscmf=zeros(length(th),1);
  masssmf=zeros(length(th),1);
  for j=1:length(th)
    tc=0;
    force=inf;
    shear=inf;
    while and(force>carStr,shear>sStr(i))
      tc=tc+(10^(-7));
      massh=(th(j)*p(i)*area);
      massc=(tc*area*1600);
      masss=(area*.49);
      mass=massh+massc+masss;
      I=2.3*tc*(tc^2/6+2*(th(j)/2+tc/2)^2);
      force=(mass*aMax)*2.3*(tc/2+th(j))/I;
      shear=(mass*aMax)*2.3*(th(j)/2)/I;
    end
    massmf(j)=mass;
    masshmf(j)=massh;
    masscmf(j)=massc;
    masssmf(j)=masss;
    tcmf(j)=tc;
  end
  [mmass(i),pt]=min(massmf);
  mth(i)=th(pt);
  mtc(i)=tcmf(pt);
  figure(i)
  hold off
  plot(th*1000,massmf/2)
  hold on
  plot(th*1000,masshmf/2)
  plot(th*1000,masssmf/2)
  plot(th*1000,masscmf/2)
  xlabel('Honeycomb Thickness (mm)')
  ylabel('Panel Mass (kg)')
  title(names(i))
  legend({'Total','Honeycomb','Solar Cells','Carbon Fiber'})
end
```

10.2.3 ADCS

10.2.3.1 Control system Simulink diagram

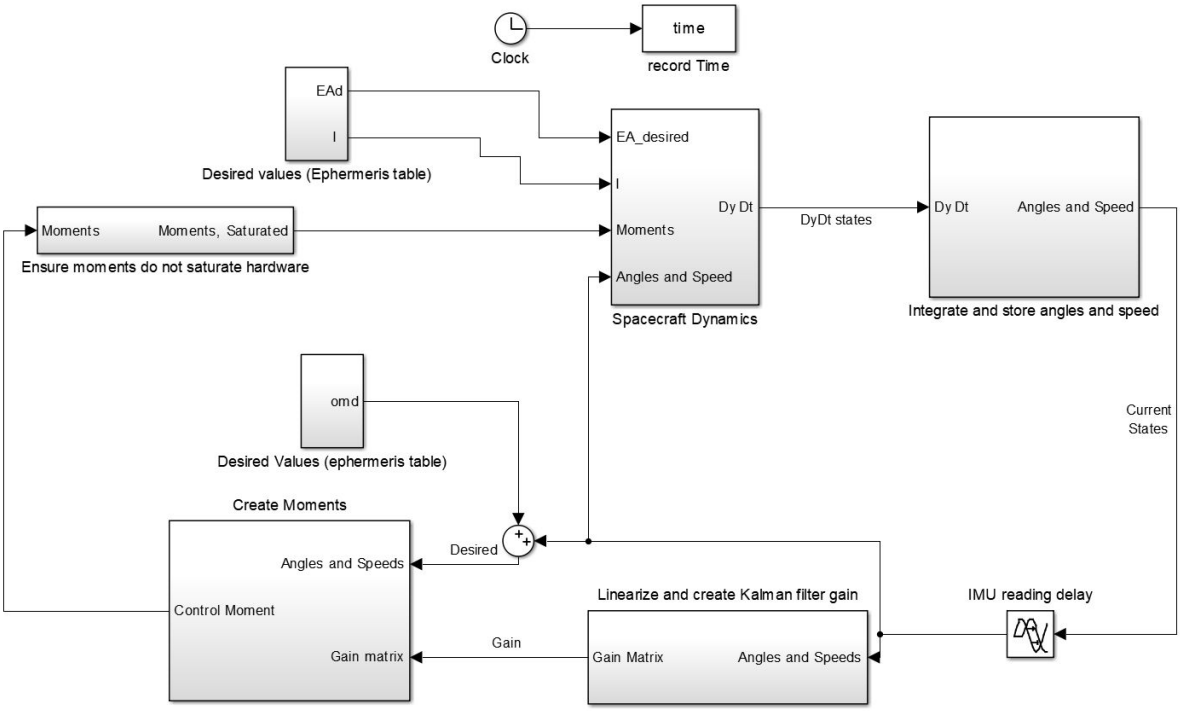

Figure 10.2.3.1.1: Overall Control System

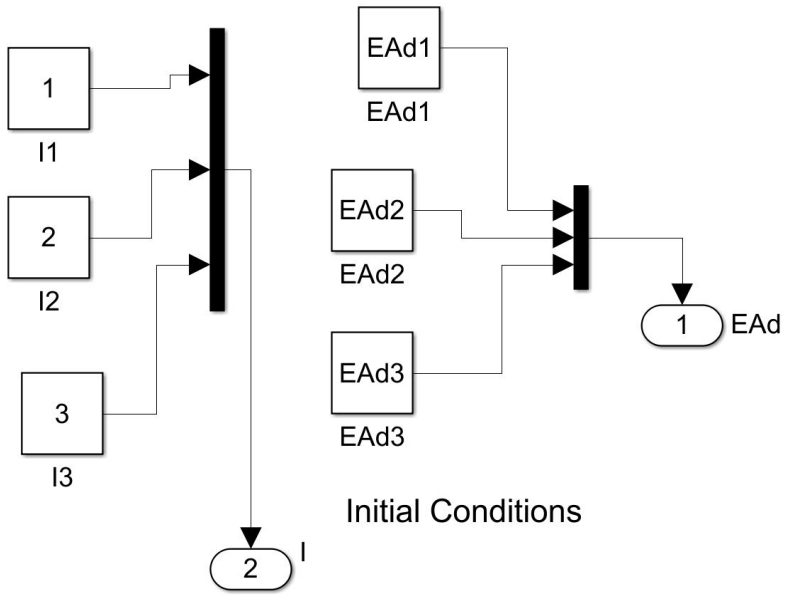

Figure 10.2.3.1.2: Initial Conditions

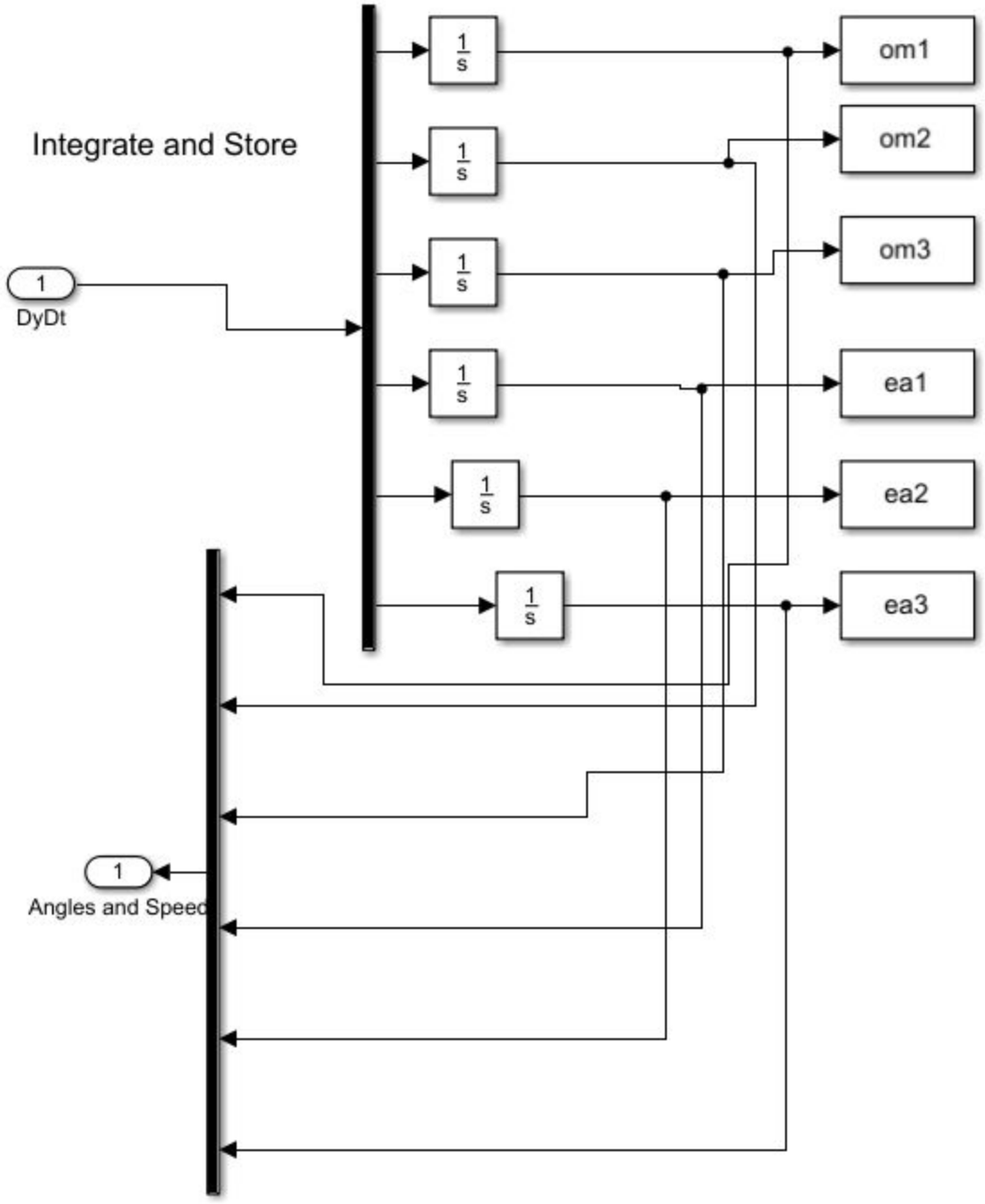

Figure 10.2.3.1.3: Integrate and Store Data

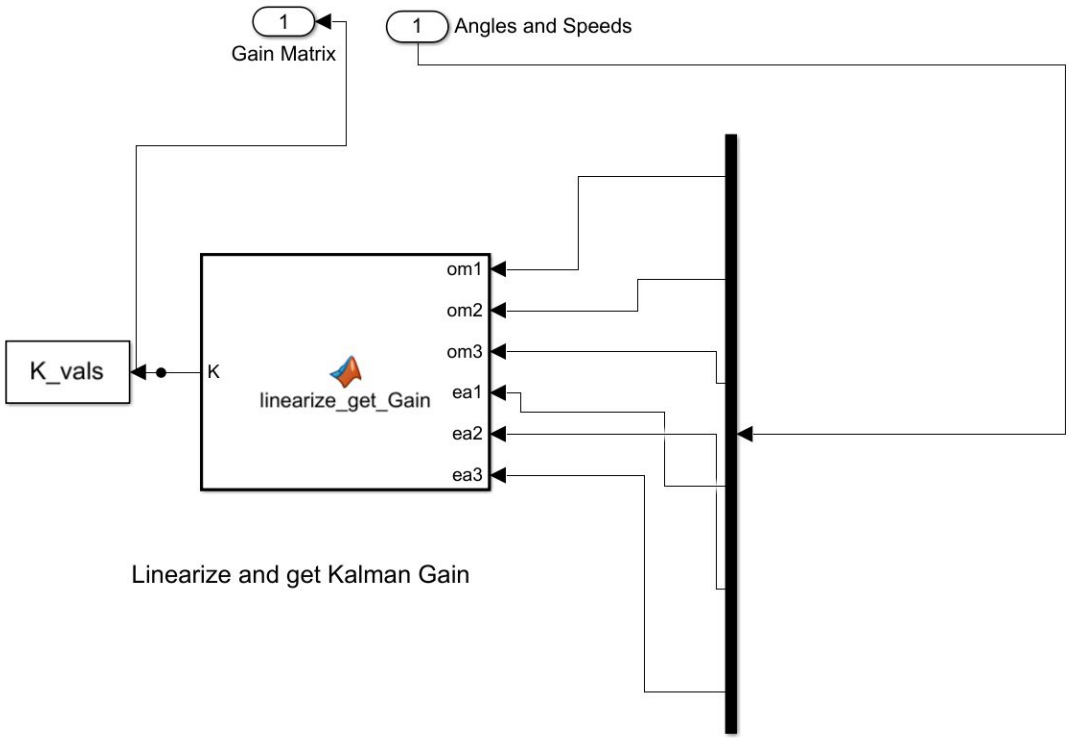

Figure 10.2.3.1.4: Linearize the Model, Find Kalman Gains

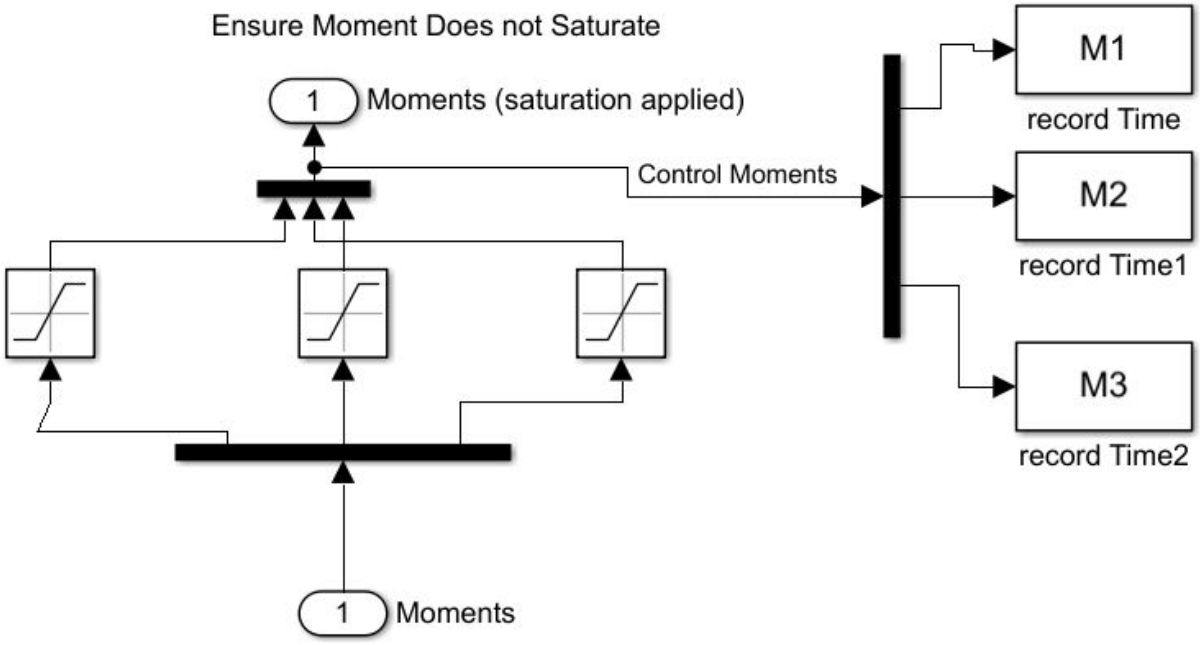

Figure 10.2.3.1.5: Ensure that the Control Moment is within the Bounds of the System

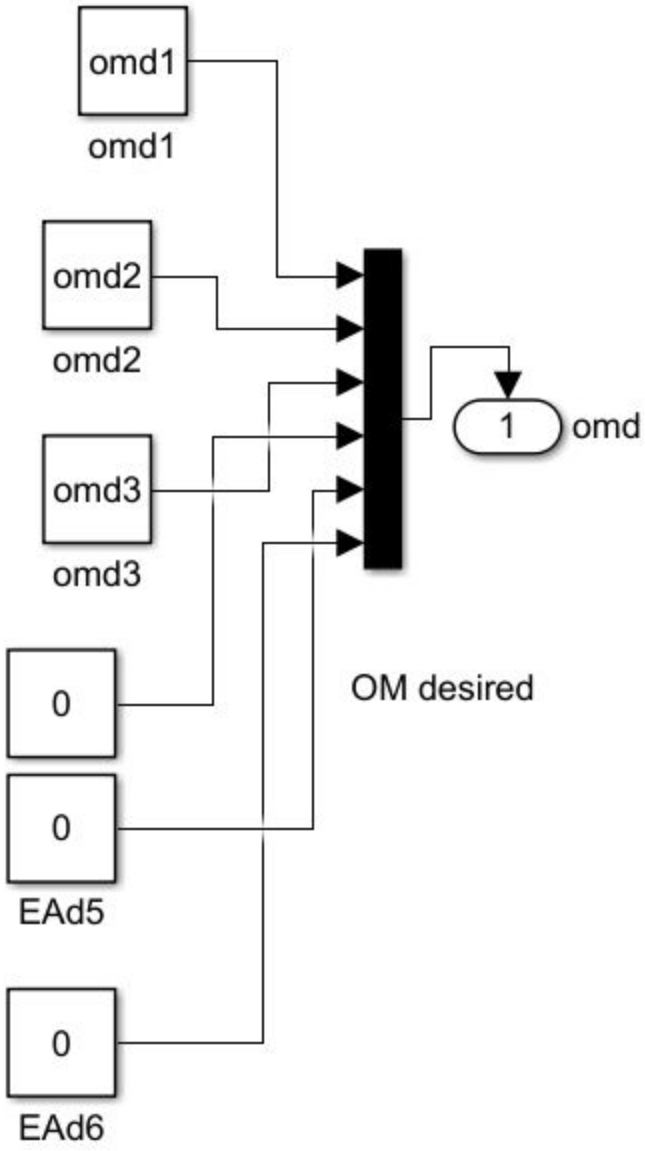

Figure 10.2.3.1.6: Apply Desired Direction and Velocity

10.2.3.1 Control system code

Spacecraft Nonlinear Model:

```
function dydt = fcn(om1,om2,om3,EA1,EA2,EA3,M1,M2,M3,EAd1,EAd2,EAd3,I1,I2,I3)
% Determine the derivative of the state

EA_desired = [EAd1;EAd2;EAd3;];
I = [I1;I2;I3;];
```

```
%% Update variables
om=[om1;om2;om3;];
EA = [EA1;EA2;EA3;];

%% Make Current SPACE123 DCM
EA1=EA(1);
EA2=EA(2);
EA3=EA(3);
C11=cos(EA2)*cos(EA3);
C12=cos(EA2)*sin(EA3);
C13=-sin(EA2);
C21=sin(EA1)*sin(EA2)*cos(EA3)-cos(EA1)*sin(EA3);
C22=sin(EA1)*sin(EA2)*sin(EA3)+cos(EA1)*cos(EA3);
C23=sin(EA1)*cos(EA2);
C31=cos(EA1)*sin(EA2)*cos(EA3)+sin(EA1)*sin(EA3);
C32=cos(EA1)*sin(EA2)*sin(EA3)-sin(EA1)*cos(EA3);
C33=cos(EA1)*cos(EA2);
DCM_actual=[C11 C12 C13; C21 C22 C23; C31 C32 C33];


%% Make Desiried orientation-SPACE123 DCM
EAd1=EA_desired(1);
EAd2=EA_desired(2);
EAd3=EA_desired(3);
C11d=cos(EAd2)*cos(EAd3);
C12d=cos(EAd2)*sin(EAd3);
C13d=-sin(EAd2);
C21d=sin(EAd1)*sin(EAd2)*cos(EAd3)-cos(EAd1)*sin(EAd3);
C22d=sin(EAd1)*sin(EAd2)*sin(EAd3)+cos(EAd1)*cos(EAd3);
C23d=sin(EAd1)*cos(EAd2);
C31d=cos(EAd1)*sin(EAd2)*cos(EAd3)+sin(EAd1)*sin(EAd3);
C32d=cos(EAd1)*sin(EAd2)*sin(EAd3)-sin(EAd1)*cos(EAd3);
C33d=cos(EAd1)*cos(EAd2);
DCM_desired=[C11d C12d C13d; C21d C22d C23d; C31d C32d C33d];

%% Get Derivatives
% Spacecraft Euler's Equations
I1 = I(1);
I2 = I(2);
```

```
I3 = I(3);

om1=om(1);
om2=om(2);
om3=om(3);
omdot1=(M1+(I2-I3)*om2*om3)/I1;
omdot2=(M2+(I3-I1)*om3*om1)/I2;
omdot3=(M3+(I1-I2)*om1*om2)/I3;
omdot=[omdot1; omdot2; omdot3];

%% kinematic differential equations of motion
EA1=EA(1);
EA2=EA(2);
EA3=EA(3);

EAdot1=(1/cos(EA2))*(om1*cos(EA2)+om2*sin(EA1)*sin(EA2)+om3*cos(EA1)*sin(EA2));
EAdot2=(1/cos(EA2))*(om2*cos(EA1)*cos(EA2)-om3*sin(EA1)*cos(EA2));
EAdot3=(1/cos(EA2))*(om2*sin(EA1)+om3*cos(EA1));
EAdot=[EAdot1; EAdot2; EAdot3];

% specify state derivative values
dydt= cat(1,omdot,EAdot);
End

Linearization and Kalman filter
function K = linearize_get_Gain(om1,om2,om3,ea1,ea2,ea3)
%This Code takes in the current states, linearizes about them,
% and returns the optimal gain matrix, K.

%create states:
om = [om1;om2;om3];
EA = [ea1; ea2; ea3];
Y0 = cat(1,om,EA);
T = [0;0;0]; % assume no moments

%get your A and B matricies
[A,B] = GetLinModFtxu_rolling(@model_no_moments_getlinmod,[],Y0,T);
C = eye(6);
D = zeros(6,3);
```

```
R = 1;
Q1 = 1;
Q = 100*[Q1 0 0 0 0 0;
   0 Q1 0 0 0 0;
   0 0 Q1 0 0 0;
   0 0 0 Q1 0 0;
   0 0 0 0 Q1 0;
   0 0 0 0 0 Q1];
R = eye(3);
%sym = issymmetric(R); % symm?
%[~,p] = chol(R);% pos def?

coder.extrinsic('lqr');
K = zeros(3,6);
K = lqr(A,B,Q,R);
End
```

Disturbance Torques:

```
%% Disturbance torque calculator
clear;close all;clc;

%% General Parameters
N = 10000; %number of samples to run
muSun = 1.3271244e11;
muEarth = 3.9860045e5;
muJupiter = 1.26686545e9;
muMars = 4.282837e4;
esc = 0.601470573561797;

ef= 0.655452978476002;

theta_intersect1 = 1.485638084937971;
theta_intersect2 = 1.287134158073098;
hsc =5.638717998683439e+09;
hf = 5.983015618347387e+09;
Ixx = 37648020.309663706;
Iyy = 10004089.107927233;
Izz = 38509783.135031499;
I = [Ixx,Iyy,Izz]./1e4;
```

```
I1 = I(1);
I2 = I(2);
I3 = I(3);

%% Find solar rad vs time
Theta1 = linspace(0,theta_intersect1,N);
Theta2 = linspace(theta_intersect2,pi,N);
Rt = hsc^2/muSun *1./(1 + esc*cos(Theta1));
Rf = hf^2/muSun *1./(1 + ef*cos(Theta2));
T1 = [];
T2 = [];
for i = 1:N
   T1(i) = TravelTime(hsc,esc,0,Theta1(i),muSun);
   T2(i) = TravelTime(hf,ef,theta_intersect2,Theta2(i),muSun);
end

T3 = T2+T1+8.058301e6;
time = [T1,T3];%,T3(end)+220752000];
dist = [Rt,Rf];

%% Find Jupiter rad vs time
hfinal = 3.920475810234752e+06;
efinal = 0.969669803104752;
Theta1 = linspace(0,pi,N);
RJup = hfinal^2/muJupiter *1./(1 + efinal*cos(Theta1));
TJup = [];
for i = 1:N
   TJup(i) = TravelTime(hfinal,efinal,0,Theta1(i),muJupiter);
end
TJextend = [];
adds = zeros(1,length(TJup));
for i = 1:length(TJup)-1
   adds(i+1) = TJup(i+1)-TJup(i);
end
RJ = [RJup,flip(RJup)];
TJ = [TJup,flip(flip(TJup)+adds)];%TJextend];
plot(TJup,RJup,'.');

%% Solar Torque transfer
```

```
distPlanets = [1;1.52;3;5.2];
distrs = distPlanets.*1.496e8;
press2 = @(r) 1.03e11/(r^2);
dishA = .392975; % m^2
thrusterA = .60544459;% m^2
A= thrusterA-dishA;
Torques_solar = [];%zeros(LOM);
t = 0;
for t = 1:length(time)
   disp(t);
   Fabs = press2(dist(t))*A*cosd(0);
   Fref = 2*press2(dist(t))*A*0.5*cosd(0);
   T = (Fref+Fabs)*2.3/2;
   Torques_solar = [Torques_solar,T];
end
figure(2)
plot(dist,Torques_solar)
title('Torque from Solar Pressure')
xlabel('Mission Time (Seconds)')
ylabel('Torque (N-M)')
trans_solar_T = trapz(time,Torques_solar);
fprintf('The total Solar angular momentum imparted during the transfer is %3f N-M-S
\n',trans_solar_T);
%% Solar torque in jupiters orbit
T3 = 8.058301e6;
time2 = [T3(end),T3(end)+220752000];
dist2 = [Rf(end),Rf(end)];
dishA = .392975; % m^2
thrusterA = .60544459;% m^2
A= thrusterA-dishA;
Torques_solar_juip = [];%zeros(LOM);
for t = 1:length(time2)
   Fabs = .5*press2(dist2(t))*A*cosd(0);
   Fref = 2*press2(dist2(t))*A*0.5*cosd(0);
   T = (Fref+Fabs)*2.3/2;
   Torques_solar_juip = [Torques_solar_juip,T];
end
solar_t_mission = trapz(time2,Torques_solar_juip);
```

```
fprintf('The total Solar angular momentum imparted during the Jupiter orbits is %3f
N-M-S\n',solar_t_mission);

%% Gravity gradient torques
Marscount = 0;
Jupcount = 0;
Earthcount =0;
Suncount = 0;
Torques_grav_Sun = [];
Torques_grav_Jup = [];
TimeJup = [];
Jup_dist = [];
Torques_grav_Mars = [];
TimeMars = [];
Mars_dist = [];
Torques_grav_Earth = [];
TimeEarth = [];
Earth_dist = [];
for t = 1:length(time)
   %if in jupiter SOI
   if (dist(t) < 777920000+48.2e6) &&  (dist(t) > 777920000-48.2e6)
      Mu = muJupiter*1e9;
      dist_local = (dist(t)-777920000)*1e3;
      if dist_local > 0
         Jup_dist = [Jup_dist,dist_local];
         T_grav = (3*Mu)/(2*(dist_local)^3)*abs(I(3)-I(2));
         %Ensure that we never accidientally calculate from
         %inside of jupiters radius
         if dist_local < 69.91*1e6
            if max(Torques_grav_Jup)>0
               T_grav = Torques_grav_Jup(end);
            else
               T_grav = 0;
            end
         end
         Torques_grav_Jup = [Torques_grav_Jup,T_grav];
         TimeJup = [TimeJup,time(t)];
      end
      %if in mars SOI
```

```
    elseif (dist(t) < 227392000+.576e6) &&  (dist(t) > 227392000-.576e6)
        Mu = muMars*1e9;
        dist_local = abs(dist(t)-227392000)*1e3;
        if dist_local > 0
            T_grav = max((3*Mu)/(2*(dist_local)^3)*abs(I(3)-I(2)));
            if dist_local < 3.389*1e6
                T_grav = Torques_grav_Mars(end);
            end
            Torques_grav_Mars = [Torques_grav_Mars,T_grav];
            TimeMars = [TimeMars,time(t)];
            Mars_dist = [Mars_dist,dist_local];
        end

    %if in earth SOI
    elseif (dist(t) < 149600000+.924e6) &&  (dist(t) > 149600000-.924e6)
        Mu = muEarth*1e9;
        dist_local = abs(dist(t)-149600000)*1e3;
        if dist_local > 0
            T_grav = max((3*Mu)/(2*(dist_local)^3)*abs(I(3)-I(2)));
            if dist_local < 6.378*1e6
                if t<5
                    T_grav = 0;
                else
                    T_grav = Torques_grav_Earth(end);
                end
            end
            Torques_grav_Earth = [Torques_grav_Earth,T_grav];
            TimeEarth = [TimeEarth,time(t)];
            Earth_dist = [Earth_dist,dist_local];
        end
    end
    % Else must be in sun SOI
    muSun_m = muSun*1e9;
    T_grav_sun = max((3*muSun_m)/(2*(dist(t)*1e3)^3)*abs(I(3)-I(2)));
    Torques_grav_Sun = [Torques_grav_Sun,T_grav_sun];
    %Mu = muSun*1e9;
    %T_grav = max(((3*Mu)/(2*(dist(t)*1e3)^3))*abs(I(2)-I(1))*sind(theta));

end
```

```
%TG = smooth(Torques_grav)
figure(3)
plot(dist,Torques_grav_Sun)
title('     Torque from Solar Gravity Gradient (Transfer Orbit)')
xlabel('Distance from Sun (Km)')
ylabel('Torque (N-M)')
xlim([1.496e8 8e8])
total_grav_sun = trapz(time,Torques_grav_Sun);

figure(4)
plot(Jup_dist./1000,Torques_grav_Jup)
title('   Torque from Jovian Gravity Gradient (Transfer Orbit)')
xlabel('Distance from jupiter (Km)')
ylabel('Torque (N-M)')
xlim([9.55e4 9e5])

total_grav_jup = 2*trapz(TimeJup,Torques_grav_Jup./100);

figure(5)
plot(Mars_dist./1000,Torques_grav_Mars)
title('Gravity Gradient from Mars (along approach)')
xlabel('Mars Distance (Km)')
ylabel('Torque (N-M)')
xlim([0 1e5])
total_grav_mars = 2*trapz(TimeMars,Torques_grav_Mars);

figure(6)
plot(Earth_dist./1000,Torques_grav_Earth)
title('Torque from Earth Gravity Gradient (Transfer Orbit)')
xlabel('Earth Distance (Km)')
ylabel('Torque (N-M)')
xlim([6500 .5e5])
total_grav_earth = 2*trapz(TimeEarth,Torques_grav_Earth./100);

total_transfer_ang_mom = total_grav_earth +
total_grav_jup+total_grav_earth+total_grav_sun+trans_solar_T;

fprintf('Total Gravity Gradient from the Sun is %3f N-M-S\n',total_grav_sun);
fprintf('Total Gravity Gradient from Jupiter (along approach) is %3f N-M-S\n',total_grav_jup);
```

```
fprintf('Total Gravity Gradient from the Mars (along approach) is %3f
N-M-S\n',total_grav_mars);
fprintf('Total Gravity Gradient from the Earth is %3f N-M-S \n\n',total_grav_earth);
fprintf('Total angular momentum imparted during the transfer is %3f
N-M-S\n',total_transfer_ang_mom);

%% Orbiting Jupiter Gravity Gradient
Mu = muJupiter*1e9;
Jup_dist = RJup.*1000 +69.91*1e6;
Torques_Jup_orbit = [];%zeros(length(Jup_dist),1);
for i = 1:length(Jup_dist)
   %The spacecraft will spend approximatly a 15% of its time in the
   %worst orientation for grav-grad
   T_grav1 = max((3*Mu)/(2*(Jup_dist(i))^3)*abs(I(3)-I(2)))*.15;
   T_grav2 = max((3*Mu)/(2*(Jup_dist(i))^3)*abs(I(3)-I(1)))*.85;
   T_grav = T_grav1+T_grav2;
   %Ensure that we never accidientally calculate from
   %inside of jupiters radius
   if Jup_dist(i) < 70*1e6
      if max(Torques_Jup_orbit)>0
         T_grav = Torques_Jup_orbit(end);
      else
         T_grav = 0;
      end
   end
   Torques_Jup_orbit = [Torques_Jup_orbit,T_grav];
end
figure(7)
plot(TJup,Torques_Jup_orbit)
title('Torque from Jovian Gravity Gradient (Per half orbit)')
xlabel('Distance from Jupiter (Km)')
ylabel('Torque (N-M)')
Grav_torque_per_orbit = 2*trapz(TJup,Torques_Jup_orbit);
ang_mom_per_orbit = (solar_t_mission/2.542336677777778e+04) + Grav_torque_per_orbit;
fprintf('Total angular momentum imparted per jovian orbit is %3f N_M_S per orbit
\n',ang_mom_per_orbit)

%% Fuel Calculations
Isp = 235; % isp in Sec
```

```
mdot = 10.4/1000; %mdot max n kg/sec
g0 = 9.81;
T = Isp*mdot*g0;
L_arm = 2.3;
T_motor = T*L_arm;
Time_burn_trans = total_transfer_ang_mom/T_motor;
Time_burn_orbit = ang_mom_per_orbit/T_motor;
M_trans = Time_burn_trans*mdot*1000;
M_orbit = Time_burn_orbit*mdot*1000*142*2;
fprintf('Total Fuel to desaturate for the tranfer is: %3f \n',M_trans)
fprintf('Total Fuel to desaturate during the duration of the orbiting is: %3f \n',M_orbit)

%% Desaturate with Mag Torque Tubes
B0 = 4.4e-4; %teslass
Turns = 1000;
current = 1;
r_tube = 7.25/100;
A = pi*r_tube^2;
R0 = 69.91*1e6; %Jupiter Radius in m
L = deg2rad(45);%orbit arount 45 degrees offset from upiter equator
BJup = @(r) ((B0*R0^3)/r^3)*sqrt(3*sin(L)+1);
Jup_dist = RJup.*1000 +69*1e6;
Torques_tube = [];%zeros(length(Jup_dist),1);
Blocals = [];
for i = 1:length(Jup_dist)
   Blocal = BJup(Jup_dist(i));
   Blocals = [Blocals,Blocal];
   T = Turns*current*A*Blocal*sind(45);
   Torques_tube = [Torques_tube,T];
end
figure(8)
plot(Jup_dist./1000,Blocals)
title('Jovian Magnetic Field Strength')
xlabel('Distance from Jupiter (Km)')
ylabel('Magnetic field (Teslas)')
xlim([7.4e4 5.7e5])
figure(9)
plot(RJup,Torques_tube)
title('Torque from Magnetic Torque Tube')
```

```
xlabel('Altitude (Km from Jupiter)')
ylabel('Avaliable Torque (N-M))')
Tot_mag_ang = 2*trapz(TJup,Torques_tube);
fprintf('Total angular momentum dissapated by torque tubes per orbit is %3f \n',Tot_mag_ang)

%% Calc power req by Torque Tubes;
revistivity = .05e-8; %revistivity Coppper at 20K
Rwire = .1/1000; %radius wire in M
Awire = pi*Rwire^2;
Lcoil = (Turns*2*pi*r_tube);
Rtube = revistivity*Lcoil/Awire;
V = current*Rtube;
P = V*current;
fprintf('This would require %3f Watts of power when fully on\n',P)
Power = P*1000/60; %Near Jupiter for approximatly 1000 seconds
P_desat = Power*(1.001177/Tot_mag_ang);
fprintf('or %3f KiloWatts-hours per orbit to desaturate \n',Power/1000)
vol = Awire*Lcoil;
mass_coil = vol*8960;
fprintf('This would require a coil of mass %3f Kg\n',mass_coil)
```

Linearize Model [35]. Used with Permission.

```
function  [A B]=GetLinModFtxu_rolling(ftxu,t,xs,us)
%% [A B]=GetLinModFtxu(ftxu,t,xs,us)
% ftxu if the function that evaluates xdot
% is must accept inputs t,x,u - this should be the
% same function you use with an ODE solver
%
% Numerical determination of state space matrices:
% If you have f(x,u) for xdot=f(x,u) for your function then you
% can numerically determine the values of the partial derivatives.
% To simulate the nonlinear equations you have to put the equations
% in this form (typically) so there is little
% work involved to numerically verify your expressions
% for the partial derivatives to get A and B:

% The A matrix is defined as the partial derivative of f with respect to x:
% A = pf/px.  Numerically we can approximate this derivative:
```

```
% A ~ [f(x+dx,u)-f(x-dx,u)]/2d
% Similarly
% B ~ [f(x,u+du)-f(x,u-du)]/2d
%
% time argument is typically not used, but this argument is passed in so
% you can determine A, B with the same function used with the ODE
% solver instead of writing a new one

%% numerically determine A:
n=length(xs); % the number of state variables
% a small change in x:
d=1e-6;  % "small" with respect to typically values of x or u.

% determine [pf/px1 pf/px2 - - - pf/pxn] by looping through
% each state variable x1, x2 - - -, xn
A = zeros(6);
for i=1:n % loop through a small change in each state:
   dx=zeros(n,1);
   dx(i,1)=d;
   A(:,i)=(ftxu(t,xs+dx,us)-ftxu(t,xs-dx,us))/(2*d);
end
B = zeros(6,3);
%% Numerically determine B:
m=length(us);% the number of inputs
if(m==0) % if ther are no inputs make B zero
   B=zeros(n,1);
else
   for i=1:m % loop through a small change in each input:
      du=zeros(m,1);
      du(i,1)=d;
      B(:,i)=(ftxu(t,xs,us+du)-ftxu(t,xs,us-du))/(2*d);
   end
end
```

10.3 Solar Panel Materials

10.3.1 Aluminum Honeycomb

Honeycomb data is provided by Toray [36]. The shear strength used in calculations is the minimum shear strength for a given honeycomb type.

Table 10.3.1.1: Properties of Aluminum Honeycomb

Honeycomb Type	Shear Strength (psi)	Density (lb/ft^3)
AAA-3.1-1/8-07N-5052	155	3.1
AAA-4.5-1/8-10N-5052	255	4.5
AAA-5.2-1/4-25N-5052	307	5.2
AAA-8.1-1/8-20N-5052	543	8.1
AAA-4.5-1/8-10N-5056	350	4.5
AAA-6.1-1/8-15N-5056	525	6.1
AAA-8.1-1/8-20N-5056	740	8.1

10.3.2 Carbon Fiber

The strengths and densities can vary from as low as 300MPa to 3000MPa depending on properties like the weave and fill material. For the purposes of the solar panels, it is assumed that the carbon fiber has a strength of 800MPa

10.4 Preliminary Design Report